Identifying Network Ties from Panel Data: Theory and an Application to Tax Competition[*]

Áureo de Paula   Imran Rasul   Pedro CL Souza[†]

January 2023

Abstract

Social interactions determine many economic behaviors, but information on social ties does not exist in most publicly available and widely used datasets. We present results on the identification of social networks from observational panel data that contains no information on social ties between agents. In the context of a canonical social interactions model, we provide sufficient conditions under which the social interactions matrix, endogenous and exogenous social effect parameters are all globally identified. While this result is relevant across different estimation strategies, we then describe how high-dimensional estimation techniques can be used to estimate the interactions model based on the Adaptive Elastic Net Generalized Method of Moments. We employ the method to study tax competition across US states. We find that the identified social interactions matrix implies tax competition differs markedly from the common assumption of competition between geographically neighboring states, providing further insights for the long-standing debate on the relative roles of factor mobility and yardstick competition in driving tax setting behavior across states. Most broadly, our identification and application show that the analysis of social interactions can be extended to economic realms where no network data exists. *JEL Codes: C31, D85, H71.*

1 Introduction

In many economic environments, behavior is shaped by social interactions between agents. In individual decision problems, social interactions have been key to understanding outcomes as diverse as educational test scores, the demand for financial assets, and technology adoption (Sacerdote, 2001; Bursztyn *et al.*, 2014; Conley and Udry, 2010). In macroeconomics, the structure of firm's production and credit networks propagate shocks, or help firms to learn (Acemoglu *et al.*, 2012; Chaney, 2014). In political economy, ties between jurisdictions are key to understanding tax setting behavior (Tiebout, 1956; Shleifer, 1985; Besley and Case, 1994).

Underpinning all these bodies of research is some measurement of the underlying social ties between agents. However, information on social ties does not exist in most publicly available and widely used datasets. To overcome this limitation, studies of social interaction either *postulate* ties based on common observables or homophily, or *elicit* data on networks. However, it is increasingly recognized that postulated and elicited networks remain imperfect solutions to the fundamental problem of missing data on social ties, because of econometric concerns that arise with either method, or simply because of the cost of collecting network data.[1]

Two consequences are that: (i) classes of problems in which social interactions occur are understudied, because social networks data is missing or too costly to collect; (ii) there is no way to validate social interactions analysis in contexts where ties are postulated. In this paper we tackle this challenge by deriving sufficient conditions under which global identification of the *entire structure* of social networks is obtained, using only observational panel data that itself contains *no* information on network ties. Our identification results allow the study of social interactions without data on social networks, and the validation of structures of social interaction where social ties have hitherto been postulated. The recovered networks are economically meaningful to explain the effects under study since they are entirely estimated from the data itself, and not driven by *ex ante* assumptions on how individuals interact.

A researcher is assumed to have panel data on individuals $i = 1, ..., N$ for instances $t = 1, ..., T$. An instance refers to a specific observation for i and need not correspond to a time period (for example if i refers to a firm, t could refer to market t). The outcome of interest for individual i in

---

[1]As detailed in de Paula (2017), elicited networks are often self-reported, and can introduce error for the outcome of interest. Network data can be censored if only a limited number of links can feasibly be reported. Incomplete survey coverage of nodes in a network may lead to biased aggregate network statistics. Chandrasekhar and Lewis (2016) show that even when nodes are randomly sampled from a network, partial sampling leads to non-classical measurement error, and biased estimation. Collecting social network data is also a time and resource intensive process. In response to these concerns, a nascent strand of literature explores cost-effective alternatives to full elicitation to recover aggregate network statistics (Breza *et al.*, 2020).

instance t is y_{it} and is generated according to a canonical structural model of social interactions:[2]

$$y_{it} = \rho_0 \sum_{j=1}^{N} W_{0,ij} y_{jt} + \beta_0 x_{it} + \gamma_0 \sum_{j=1}^{N} W_{0,ij} x_{jt} + \alpha_i + \alpha_t + \epsilon_{it} \qquad (1)$$

Outcome y_{it} depends on the outcome of other individuals to whom i is socially tied, y_{jt}, and x_{jt} includes characteristics of those individuals.[3] $W_{0,ij}$ measures how the outcome and characteristics of j causally impact the outcome for i. The network is initially assumed to be fixed over time, but we later provide an extension of the method for time-varying networks. As outcomes for all individuals obey equations analogous to (1), the system of equations can be written in matrix notation where the structure of interactions is captured by the adjacency matrix, denoted by W_0. Our approach allows for unobserved heterogeneity across individuals α_i and common shocks to all individuals α_t. This framework encompasses the classic linear-in-means specification of Manski (1993). In his terminology, ρ_0 and γ_0 capture endogenous and exogenous social effects, and α_t captures correlated effects. The distinction between endogenous and exogenous peer effects is critical, as only the former generates social multiplier effects.

Manski's seminal contribution set out the reflection problem of separately identifying endogenous, exogenous and correlated effects in linear models. However, it has been somewhat overlooked that he also set out another challenge on the identification of the social network in the first place.[4] This is the problem we tackle and so expand the scope of identification beyond ρ_0, β_0 and γ_0. Our point of departure from much of the literature is to therefore presume W_0 is *entirely unknown* to the researcher. We derive sufficient conditions under which all the entries in W_0, and the endogenous and exogenous social effect parameters, ρ_0 and γ_0, are globally identified. By identifying the social interactions matrix W_0, our results allow the recovery of aggregate network characteristics such as the degree distribution and patterns of homophily, as well as node-level statistics such as the strength of social interactions between nodes, and the centrality of nodes. This is useful because such aggregate and node-level statistics often map back to underlying models of social interaction (Ballester *et al.*, 2006; Jackson *et al.*, 2017; de Paula, 2017).

The mathematical strategy for our identification result is new and fundamentally different from those employed elsewhere in this nascent literature (and does not rely on requirements on network

---

[2]Blume *et al.* (2015), for example, present micro-foundations based on non-cooperative games of incomplete information for individual choice problems, that result in this estimating equation for a class of social interaction models.

[3]In the case in which t is considered to be a time period, x_{it} may also include lagged values of y_{it}.

[4]Manski (1993) highlights difficulties (and potential restrictions) for identifying ρ_0, β_0 and γ_0 when all individuals interact with each other, and when this is observed by the researcher. In (1), this corresponds to $W_{0,ij} = N^{-1}$, for $i, j = 1, \ldots, N$. At the same time, he states (p. 536), "I have presumed that researchers know how individuals form reference groups and that individuals correctly perceive the mean outcomes experienced by their supposed reference groups. There is substantial reason to question these assumptions (...) If researchers do not know how individuals form reference groups and perceive reference-group outcomes, then it is reasonable to ask whether observed behavior can be used to infer these unknowns (...) The conclusion to be drawn is that informed specification of reference groups is a necessary prelude to analysis of social effects."

sparsity). However it delivers sufficient conditions that are mild, and relate to existing results on the identification of social effects parameters when W_0 is known (Bramoullé *et al.*, 2009; De Giorgi *et al.*, 2010; Blume *et al.*, 2015). Our identification result is also useful in other estimation contexts, such as when a researcher has partial knowledge of W_0,[5] or in navigating between priors on reduced-form (later denoted Π) and structural (later denoted θ) parameters in a Bayesian framework, thus avoiding issues raised in Kline and Tamer (2016).

Global identification is a necessary requirement for consistency of extremum estimators such as those based on GMM (Hansen 1982; Newey and McFadden 1994). Our identification analysis thus provides primitives for this important condition. To estimate the model, we employ the Adaptive Elastic Net GMM method (Caner and Zhang, 2014) because this allows us to deal with a potentially high-dimensional parameter vector (in comparison to the time dimension in the data) including all the entries of the social interactions matrix W_0, although other estimation protocols may also be entertained (e.g. using Bayesian methods or *a priori* information). Our preferred method makes use of computationally efficient Least Angle Regression (LARS) algorithms (Efron *et al.*, 2004).[6]

We showcase the method using Monte Carlo simulations based on stylized random network structures as well as real world networks. In each case, we take a fixed network structure W_0, and simulate panel data as if the data generating process were given by (1). We then apply the method on the simulated panel data to recover estimates of all elements in W_0, as well as the endogenous and exogenous social effect parameters (ρ_0, γ_0). The networks considered vary in size, complexity, and their aggregate and node-level features. Despite this heterogeneity, we find the method to perform well in all simulations. In a reasonable dimension of panel data T and with varying node numbers across simulations (N), we find the true network structure W_0 is well recovered. For each simulated network, the majority of true links are correctly identified even for $T = 5$, and the proportion of true non-links (zeroes in W_0) captured correctly as zeros is over 85% even when $T = 5$. Both proportions rapidly increase with T. The endogenous and exogenous social effects are

---

[5]One such example is the nascent literature of Aggregate Relational Data (ARD) as in Breza *et al.* (2020). Another possibility is that individuals are known to belong to subgroups, so W_0 is block diagonal. We also interpret this situation generally as partial network knowledge. Partial information on the network is readily incorporated in this setup and may, in some circumstances, greatly reduce the number of parameters to be estimated. For example, Barrenho *et al.* (2019) study spillovers in the adoption of laparascopy using consultants in the UK health service. With a sample of $N = 1,500$ consultants and $T = 15$ years, they restrict links to occur between doctors who have worked in the same hospital.

[6]The elastic net was introduced by Zou and Hastie, 2005 in part to circumvent difficulties faced by alternative estimation protocols (e.g., LASSO) when the number of parameters, p, exceeds the number of observations, n (where p and n follow the notation in that paper). Whereas the theoretical results on the large sample properties of elastic net estimators usually have not exploited sparsity, several articles have demonstrated its performance in data scenarios where this occurs. For example, Zou and Hastie, 2005 consider an application to leukemia classification where $p = 7,129$ and $n = 72$ (see their Section 6) and Zou and Zhang, 2009 explore a scenario where $p = 1,000$ and $n = 200$. The favourable performance of the elastic net in these cases also relates to the literature on the 'effective number of parameters' (or 'effective degrees of freedom') in the estimation of sparse models (Tibshirani and Taylor, 2012). In Section 3 we provide an informal discussion on the minimum number of time periods such that penalized estimation is feasible in our context.

also correctly captured as T increases. Of course, small-T biases are as expected, being analogous to well-known results for autoregressive time series models. *A fortiori*, we estimate aggregate and node-level statistics of each network, demonstrating the accurate recovery of key players in networks for example. Furthermore, biases in the estimation of endogenous and exogenous effects parameters ($\hat{\rho}$, $\hat{\gamma}$) fall quickly with T and are close to zero for large sample sizes.

In the final part of our analysis, we apply the method to shed new light on a classic real world social interactions problem: tax competition between US states. The literatures in political economy and public economics have long recognized the behavior of state governors might be influenced by decisions made in 'neighboring' states. The typical empirical approach has been to postulate the relevant neighbors as being geographically contiguous states. Our approach allows us to infer the set of 'economic' neighbors determining social interactions in tax setting behavior from panel data on outcomes and covariates alone. In this application, the panel data dimensions cover mainland US states, $N = 48$, for years 1962-2015, $T = 53$.

The identified network structure of tax competition differs markedly from the common assumption of competition between geographic neighbors. The identified economic network has fewer edges than the geography-based network, and we identify non-adjacent states that influence tax setting behaviors. The marked differences in structure of the identified economic and geography-based networks gets reflected in the far lower clustering coefficient in the former (.042 versus .419). With the recovered social interactions matrix we establish, beyond geography, what covariates correlate to the existence of ties between states and so shed new light on the main hypotheses for social interactions in tax setting: factor mobility and yardstick competition (Tiebout, 1956; Shleifer, 1985; Besley and Case, 1994). The identified network highlights significant predictors of tax competition between states beyond just their distance: political homophily *reduces* the likelihood of a link, suggesting any yardstick competition driving social interactions occurs when voters compare their governor to those of the opposing party in other states. Tax haven states appear to be especially less influential in the tax setting behaviors of other states. The relatively weak influence of tax haven states eases concerns over a race-to-the-bottom in tax setting behaviors. Labor mobility between states does not robustly predict the existence of economic ties between states in tax setting behavior.

Given the relatively long study period in this application, at a final stage of analysis we extend our method to allow the strength of social interactions in tax competition (ρ_0, γ_0), and the structure of links in the economic network (W_0) to vary over time as we change the weight placed on observations from any given time period. We document the gradual increase in strength of social interactions over time, and the changing nature of the network of interactions. We utilize these findings to conduct counterfactual simulations of the general equilibrium propagation of tax shocks from a given state onto all other mainland US states, and how these general equilibrium effects of the same policy shock vary as we place weight on observations later in our study period.

Our paper contributes to the literature on the identification of social interactions models.

The first generation of papers studied the case where W_0 is known, so only the endogenous and exogenous social effects parameters need to be identified. It is now established that if the known W_0 differs from the linear-in-means example where all units are linked with equal weights, ρ_0 and γ_0 can be identified (Bramoullé *et al.*, 2009; De Giorgi *et al.*, 2010). Intuitively, identification in those cases can use peers-of-peers, that are not necessarily connected to individual i and can be used to leverage variation from exclusion restrictions in (1), or can use groups of different sizes within which all individuals interact among each other (Lee, 2007). Bramoullé *et al.* (2009) show these conditions are met if I, W_0 and W_0^2 are linearly independent, which is shown to hold generically by Blume *et al.* (2015). However, as made precise in Section 2, the linear algebraic arguments employed in Bramoullé *et al.* (2009) or Blume *et al.* (2015) do not apply when W_0 is unobserved and other arguments have to be used instead.[7]

Related to our work, Blume *et al.* (2015) investigate the case when W_0 is *partially* observed. Specifically, Blume *et al.* (2015, Theorem 6) show that if two individuals are *known* to not be directly connected, the parameters of interest in a model related to (1) can be identified. An alternative approach is taken in Blume *et al.* (2011, Theorem 7): they suggest a parameterization of W_0 according to a pre-specified distance between nodes. We do not impose such restrictions, but note that partial observability of W_0 (as in Blume *et al.*, 2015) or placing additional structure on W_0 (as in Blume *et al.*, 2011) is complementary to our approach as it reduces the number of parameters in W_0 to be retrieved. Bonaldi *et al.* (2015) and Manresa (2016) estimate models like (1) when W_0 is not observed, but where ρ_0 is restricted to be zero so there are no endogenous social effects. They use sparsity-inducing methods from the statistics literature, but the presence of ρ_0 in our case complicates identification non-trivially because it introduces issues of simultaneity that we address.[8]

Rose (2015) also presents related identification results for linear models like (1). Assuming sparsity of the neighborhood structure, Rose (2015) offers identification conditions under rank restrictions on sub-matrices of the reduced form coefficient matrix from a regression of outcomes (y_{it}) on covariates (x_{it}). Intuitively, given two observationally equivalent systems, sparsity guarantees the existence of pairs that are not connected in either. Since observationally equivalent systems are linked via the reduced-form coefficient matrix, this pair allows one to identify certain parameters in the model. Having identified those parameters, Rose (2015) shows that one can proceed to identify other aspects of the structure (see also Gautier and Rose, 2016). This is related to the ideas in Blume *et al.* (2015, Theorem 6), who show identification results can be leveraged if individuals are *known* not to be connected. Our main identification results do *not* rely on properties of sparse networks, and make use of plausible and intuitive conditions, whereas the auxiliary rank conditions

---

[7]Alternative identification approaches when W_0 is known focus on higher moments (variances and covariances across individuals) of outcomes (de Paula, 2017), and rely on additional restrictions on higher moments of ϵ_{it}. Note that (1) is a spatial autoregressive model. In that literature, W_0 is also typically assumed known (Anselin, 2010).

[8]Manresa (2016) allows for unit-specific β_0 parameters. While in many applications those are taken to be homogeneous, we also discuss extensions on how heterogeneity in those parameters can be handled when $\rho_0 \neq 0$.

necessary in Rose (2015) may be computationally complex to verify. More recently, Lewbel *et al.* (2022) propose an estimation strategy for the parameters ρ_0, β_0 and γ_0 of model (1) in the absence of network links if many different groups are able to be observed. Battaglini *et al.* (2022) estimate a structural model specifically for the case of unobserved social connections in the U.S. Congress.

Finally, in the statistics literature, Lam and Souza (2020) study the penalized estimation of model (1) when W_0 is not observed, assuming the model and social interactions are identified. The statistical literature on graphical models has investigated the estimation of neighborhoods defined by the covariance structure of the random variables at hand (Meinshausen and Buhlmann, 2006). This corresponds to a model where $y_t = (I - \rho_0 W_0)^{-1} \epsilon_t$ is jointly normal (abstracting from covariates). On a graph with N nodes corresponding to the variables in the model, an edge between two nodes (variables) i and j is absent when these two variables are conditionally independent given the other nodes. In this Gaussian model, this corresponds to a zero ij entry in the inverse covariance matrix for y_t (see, e.g., Yuan and Lin, 2007, p. 19). In the model above, the inverse covariance matrix is $(I - \rho_0 W_0)^\top \Sigma_\epsilon^{-1} (I - \rho_0 W_0)$, where Σ_ϵ is the variance covariance structure for ϵ_t. The discovery of zero entries in this matrix is not equivalent to the identification of W_0 as we study, and involves Σ_ϵ (as do identification strategies using higher moments when W_0 is known).[9] Related studies in the statistics literature also focus on higher moments and define neighborhoods differently (Diebold and Yilmaz, 2015; Rothenhäusler *et al.*, 2015).

We build on these papers by studying the problem where W_0 is potentially entirely unknown to the researcher. In so doing, we open up the study of social interactions to the many realms where complete social network data does not actually exist. In our case, we consider that the definition of the network as the one that mediates, together with the variables x_{it}, the outcome process y_{it} according to Equation (1). The identified network may be of a combination of elicited types of social interactions – such as friendship formation, lending and borrowing relations, links with relatives[10] –, or different from elicited data, as long as the links are relevant in determining the outcomes. In our case, and in line with the previous literature, the network ties W_{ij} are considered to be deterministic parameters or predetermined. Alternatively, the networks are assumed to be the outcome of a stochastic process, such as in Latent Distance model (Hoff *et al.*, 2002; Breza *et al.*, 2020) or Exponential Random Graphs models (Holland and Leinhardt, 1981).

Our conclusions discuss how our approach can be modified, and assumptions weakened, to integrate in partial knowledge of W_0. We discuss further applications and the steps required to simultaneously identify models of network formation and the structure of social interactions. The practical use of our proposed method has already been demonstrated in applications. For example, Fetzer *et al.* (2021) study the impact on conflict of the transition of security responsibilities between

---

[9]In fact, Meinshausen and Buhlmann (2006)'s neighborhood estimates (as also Lam and Souza (2020)'s) rely on (penalized) regressions of y_{it} on $y_{1t}, \ldots, y_{i-1,t}, y_{i+1,t}, \ldots, y_{N,t}$, which do not address the econometric endogeneity in estimating W_0.

[10]See Breza and Chandrasekhar (2019) for an empirical example that collects data on 12 types of social network interactions.

international and Afghan forces. Our proposed method is used to control for violation of SUTVA-type hypotheses that might occur because of spillover and displacement effects of insurgent forces across districts. Since the pattern of displacement is unobserved – and, in fact, insurgents have incentives to obfuscate their strategy – the current method is applied to fully recover the network and bound the effects of the end of the military occupation on conflict.[11]

Our paper proceeds as follows. Section 2 presents our core result: the sufficient conditions under which the social interactions matrix, endogenous and exogenous social effects are globally identified. Section 3 describes the high-dimensional estimation techniques used for estimation, based on the Adaptive Elastic Net GMM method and presents simulation results from stylized and real-world networks. Section 4 applies our methods to study tax competition between US states. Section 5 concludes. The Appendix provides proofs and further details on estimation and simulations.

2   Identification

2.1   Setup

Consider a researcher with panel data covering $i = 1, \ldots, N$ individuals repeatedly observed over $t = 1, \ldots, T$ instances. We consider that the number of individuals N in the network is fixed, but potentially large. The aim is to use this data to identify a social interactions model, with no data on actual social ties being available. For expositional ease, we first consider identification in a simpler version of the canonical model in (1), where we drop individual-specific (α_i) and time-constant fixed effects (α_t), and assume x_{it} is a one-dimensional regressor for individual i and instance t. Of course, we later extend the analysis to include individual-specific and time-constant fixed effects, and also allow for multidimensional covariates $x_{k,it}$, $k = 1, \ldots, K$. We adopt the subscript "0" to denote parameters generating the data, and non-subscripted parameters are generic values in the parameter space:

$$y_{it} = \rho_0 \sum_{j=1}^{N} W_{0,ij} y_{jt} + \beta_0 x_{it} + \gamma_0 \sum_{j=1}^{N} W_{0,ij} x_{jt} + \epsilon_{it}. \tag{2}$$

As outcomes for all individuals $i = 1, \ldots, N$ obey equations analogous to (2), the system of equations can be more compactly written in matrix notation as:

$$y_t = \rho_0 W_0 y_t + \beta_0 x_t + \gamma_0 W_0 x_t + \epsilon_t. \tag{3}$$

---

[11]Our identification results have also been applied, for instance, by Zhou (2019), who focusses on unobserved networks with grouped heterogeneity, and suggests a nonlinear least squares procedure for estimation on a single network observation. We believe our technical arguments may also be useful in related models (e.g., Vector Auto-Regressions).

The vector of outcomes $y_t = (y_{1t}, \ldots, y_{Nt})'$ assembles the individual outcomes in instance t; the vector x_t does the same with individual characteristics. y_t, x_t and ϵ_t have dimension $N \times 1$, the social interactions matrix W_0 is $N \times N$, and ρ_0, β_0, and γ_0 are scalar parameters. We do not make any distributional assumptions on ϵ_t beyond $\mathbb{E}(\epsilon_t|x_t) = 0$ (or $\mathbb{E}(\epsilon_t|z_t) = 0$ for an appropriate instrumental variable z_t if x_t is also endogenous). We assume the network structure is predetermined and constant, and that the number of individuals N is fixed. In reality and in empirical practice, networks may evolve over time especially when the applications consider long time spans. For this reason, we also expand the method for dynamic-network cases. The network structure W_0 is a parameter to be identified and estimated.[12]

The social interaction model (3) was widely studied in the literature – see, for instance, Manski (1993), Manresa (2016), Blume *et al.* (2015), among many others –, but it is also restrictive in at least two senses. First, we consider the W_{ij} to be fixed and predetermined, and not through models of strategic network formation (see, for example, Jackson and Wolinsky, 1996, de Paula *et al.*, 2018) or of stochastic nature, for example, the class of Exponential Random Graphs (Holland and Leinhardt, 1981) or Latent Distance models (Hoff *et al.*, 2002, Breza *et al.*, 2020). If there is feedback between outcome determination and link formation, and especially if this involves unobservables, it would be important the network formation more explicitly.

A regression of outcomes on covariates corresponds, then, to the reduced form for (3),

$$y_t = \Pi_0 x_t + \nu_t, \tag{4}$$

with $\Pi_0 = (I - \rho_0 W_0)^{-1}(\beta_0 I + \gamma_0 W_0)$ and $\nu_t \equiv (I - \rho_0 W_0)^{-1}\epsilon_t$.[13] If W_0 is observed, Bramoullé *et al.* (2009) note that a structure (ρ, β, γ) that is observationally equivalent to $(\rho_0, \beta_0, \gamma_0)$ is such that $(I - \rho_0 W_0)^{-1}(\beta_0 I + \gamma_0 W_0) = (I - \rho W_0)^{-1}(\beta I + \gamma W_0)$. This equation can be written as a linear equation in I, W_0 and W_0^2 and identification is established if those matrices are linearly independent. If W_0 is not observed, the putative unobserved structure now comprises W and an observationally equivalent parameter vector will instead satisfy $(I - \rho_0 W_0)^{-1}(\beta_0 I + \gamma_0 W_0) = (I - \rho W)^{-1}(\beta I + \gamma W)$. Following the strategy in Bramoullé *et al.* (2009) would lead to an equation in I, W, W_0 and WW_0, and the insights obtained in that paper then do *not* carry over for the case we study when W_0 is unknown.

We establish identification of the structural parameters of the model, including the social interactions matrix W_0, from the coefficients matrix Π_0. Without data on the network W_0, we treat it as an additional parameter in an otherwise standard model relating outcomes and covariates.

---

[12]A related set of papers instead focuses on the distribution of networks generating the pattern in data and aims to estimate aggregate network effects. Souza (2014) offers several identification and estimation results in this spirit. In particular, he infers the network distribution within a certain class of statistical network formation models from outcome data from many groups, such as classrooms, in few time periods. We instead concentrate on estimating the set of links for one group of size N followed over $t = 1, \ldots, T$ instances.

[13]This is also related to the identification in ARMA models, see for example Hamilton (1994, Ch. 3). This highlights potential applications for our identification strategy in other, related modelling frameworks.

Our identification strategy relies on how changes in covariates x_{it} reverberate through the system and impact y_{it}, as well as outcomes for other individuals. These are summarized by the entries of the coefficient matrix Π_0, which, in turn, encode information about W_0 and $(\rho_0, \beta_0, \gamma_0)$. A non-zero partial effect x_{it} of y_{jt} indicates the existence of direct *or* indirect links between i and j. When $\rho_0 = 0$ (and $\Pi_0 = \beta_0 I + \gamma_0 W_0$), only direct links would produce such a correlation. When $\rho \neq 0$, both direct and indirect connections may generate a non-zero response but distant connections will lead to a lower response. Our results formally determine sufficient conditions to precisely disentangle these forces.

We first set out six assumptions underpinning our main identification results. Three of these are entirely standard in the social interactions. A fourth is a normalization required to separately identify (ρ_0, γ_0) from W_0, and the fifth is closely related to known results on the identification of (ρ_0, γ_0) when W_0 is known (Bramoullé *et al.*, 2009). The sixth assumption pertains to relation between the nature of repeated multiple observations of the outcome and covariates and restrictions on the stability of W. These Assumptions (A1-A6) deliver an identified set of up to two points.

Our first assumption explicitly states that no individual affects himself and is a standard condition in social interaction models:

(A1) $(W_0)_{ii} = 0$, $i = 1, \ldots, N$.

Assumption (A1) rules out cases in which units affect themselves. This can rule out certain types of applications in which units affecting themselves is possible. For example, Input-Output matrices typically feature $(W_0)_{ii} > 0$ as firms tend to source from other firms in the same industry. With Assumption (A1), we can omit elements on the diagonal of W_0 from the parameter space. We thus can denote a generic parameter vector as $\theta = (W_{12}, \ldots, W_{N,N-1}, \rho, \gamma, \beta)' \in \mathbb{R}^m$, where $m = N(N-1) + 3$, and W_{ij} is the (i,j)-th element of W. Reduced-form parameters can be tied back to the structural model (3) by letting $\Pi : \mathbb{R}^m \to \mathbb{R}^{N^2}$ define the relation between structural and reduced-form parameters:

$$\Pi(\theta) = (I - \rho W)^{-1} (\beta I + \gamma W),$$

where $\theta \in \mathbb{R}^m$, and $\Pi_0 \equiv \Pi(\theta_0)$.

As ϵ_t (and, consequently, ν_t) is mean-independent from x_t, $\mathbb{E}[\epsilon_t | x_t] = 0$, the matrix Π_0 can be identified as the linear projection of y_t on x_t. We do not impose additional distributional assumptions on the disturbance term, except for conditions that allow us to identify the reduced-form parameters in (4). If x_t is endogenous, i.e. $\mathbb{E}[\epsilon_t | x_t] \neq 0$, a vector of instrumental variables z_t may still be used to identify Π_0. In either case, identification of Π_0 requires variation of the regressor across individuals i and through instances t. In other words, either $\mathbb{E}[x_t x_t']$ (if exogeneity holds) or $\mathbb{E}[x_t z_t']$ (otherwise) are full-rank.

Our next assumption controls the propagation of shocks and guarantees they die as they reverberate through the network. This provides adequate stability in the system, and is closely related to the concept of stationarity in network models. It implies the maximum eigenvalue norm of $\rho_0 W_0$ is less than one. It also ensures $(I - \rho_0 W_0)$ is a non-singular matrix, and so the variance of y_t exists, the transformation $\Pi(\theta_0)$ is well-defined, and the Neumann expansion $(I - \rho_0 W_0)^{-1} = \sum_{j=0}^{\infty} (\rho_0 W_0)^j$ is appropriate.

(A2) $\sum_{j=1}^{N} |\rho_0 (W_0)_{ij}| < 1$ for every $i = 1, \ldots, N$, $\|W_0\| < C$ for some positive $C \in \mathbb{R}$ and $|\rho_0| < 1$.

We next assume that network effects do not cancel out, another standard assumption. As we will show, this assumption rules out the pathological case in which endogenous and exogenous effects exactly cancel each other out:

(A3) $\beta_0 \rho_0 + \gamma_0 \neq 0$.

The need for this assumption can be shown by expanding the expression for $\Pi(\theta_0)$, which is possible by (A2):

$$\Pi(\theta_0) = \beta_0 I + (\rho_0 \beta_0 + \gamma_0) \sum_{k=1}^{\infty} \rho_0^{k-1} W_0^k. \tag{5}$$

If Assumption (A3) were violated, $\beta_0 \rho_0 + \gamma_0 = 0$ and $\Pi_0 = \beta_0 I$ so the endogenous and exogenous effects balance each other out, and network effects are altogether eliminated in the reduced form.[14]

Identification of the social effects parameters (ρ_0, γ_0) requires that at least one row of W_0 adds to a fixed and known number. Otherwise, ρ_0 and γ_0 cannot be separately identified from W_0. Clearly, no such condition would be required if W_0 was observed.

(A4) There is an i such that $\sum_{j=1,\ldots,N} (W_0)_{ij} = 1$.

Letting $W_y \equiv \rho_0 W_0$ and $W_x \equiv \gamma_0 W_0$ denote the matrices that summarize the influence of peers' outcomes (the endogenous social effects) and characteristics on one's outcome (the exogenous social effects), respectively, the assumption above can be seen as a normalization. In this case, ρ_0 and γ_0 represent the row-sum for individual i in W_y and W_x, respectively.[15] In line with the literature, we maintain that the same W_0 governs the structure of both endogenous (W_y) and exogenous (W_x) effects. This is a restrictive assumption as endogenous and exogenous social effects need not to

---

[14]One important case is when networks do not determine outcomes, which we interpret as $\rho_0 = \gamma_0 = 0$ or with W_0 representing the empty network. From equation (5), it is clear that if $\Pi(\theta_0)$ is *not* diagonal with constant entries, then it must be that $(\rho_0 \beta_0 + \gamma_0) \neq 0$, which implies that $\rho_0 \neq 0$ or $\gamma_0 \neq 0$, and also that W_0 is non-empty. Taken together, this suggests that the observation that $\Pi(\theta_0)$ is not diagonal is sufficient to ensure that network effects are present and Assumption (A3) is not violated.

[15]An alternative to Assumption (A4) is to impose the normalization on the parameters. For example, one could normalize $\rho^* = 1$ and allow the network to be rescaled accordingly. In this case, $W^* = \rho_0 W_0$ would be identified instead. Also $W_x = \frac{\gamma_0}{\rho_0} W^*$ so γ_0 would be identified relative to ρ_0. W_y and W_x are unchanged.

be driven by the same process. We later discuss relaxing this assumption when more than one regressor is used.

The fifth assumption provides for a specific kind of network asymmetry. We require the diagonal of W_0^2 not to be constant as one of our sufficient conditions for identification.

(A5) There exists l, k such that $(W_0^2)_{ll} \neq (W_0^2)_{kk}$, i.e. the diagonal of W_0^2 is not proportional to ι, where ι is the $N \times 1$ vector of ones.

In unweighted networks, the diagonal of the square of the social interactions matrix captures the number of reciprocated links for each individual or, in the case of undirected networks, the popularity of those individuals. Assumption (A5) hence intuitively suggests differential popularity across individuals in the social network.

This assumption is related to the network asymmetry condition proposed elsewhere, such as in Bramoullé *et al.* (2009). They show that when W_0 is known, the structural model (2) is identified if I, W_0, and W_0^2 are linearly independent. Given the remaining assumptions, this condition is satisfied if (A5) is satisfied, but the converse is *not* true: one can construct examples in which I, W_0, and W_0^2 are linearly independent when W_0^2 has a constant diagonal, so that Π_0 does not pin down θ_0. The strengthening of this hypothesis is the formal price to pay for the social interactions matrix W_0 being unknown to the researcher.[16]

Before proceeding to our formal results, we provide a very simple illustration to shed light on how the assumptions above come together to provide identification. Suppose the observed reduced-form matrix is,

$$
\Pi_0 = \frac{1}{455} \begin{bmatrix} 275 & 310 & 0 \\ 310 & 275 & 0 \\ 0 & 0 & 182 \end{bmatrix},
$$

and that, following (A4), the first row is normalized to one. From the third row and column of Π_0, we see there is no path of any length connecting the individual in row 3 to or from those in rows 1

---

[16]To see how the assumption of Bramoullé *et al.* (2009) grants identification when W_0 is known, choose constants c_1, c_2, and c_3 such that $c_1 I + c_2 W_0 + c_3 W_0^2 = 0$. Focusing on diagonal elements of this condition, we see that if the diagonal of W_0^2 is not proportional to the diagonal of I, then $c_1 = c_3 = 0$ because $\operatorname{diag}(W_0) = 0$. It follows that $c_2 = 0$ if at least one (off-diagonal) element of W_0 is non-zero. However, the converse is not true, so that if Assumptions A1-A6 do not hold, one can construct examples where Π_0 does not pin down θ_0. Take, for instance, $N = 5$ with θ_0 and θ where $\beta = \beta_0 = 1$, $\rho = 1.5$, $\rho_0 = 0.5$, $\gamma = -2.5$, $\gamma_0 = 0.5$,

$$
W_0 = \begin{bmatrix} 0 & 0.5 & 0 & 0 & 0.5 \\ 0.5 & 0 & 0.5 & 0 & 0 \\ 0 & 0.5 & 0 & 0.5 & 0 \\ 0 & 0 & 0.5 & 0 & 0.5 \\ 0.5 & 0 & 0 & 0.5 & 0 \end{bmatrix} \quad \text{and} \quad W = \begin{bmatrix} 0 & 0 & 0.5 & 0.5 & 0 \\ 0 & 0 & 0 & 0.5 & 0.5 \\ 0.5 & 0 & 0 & 0 & 0.5 \\ 0.5 & 0.5 & 0 & 0 & 0 \\ 0 & 0.5 & 0.5 & 0 & 0 \end{bmatrix}.
$$

Both W and W_0 violate (A5) ($(W^2)_{kk} = (W_0^2)_{kk} = 0.5$ for any k), and ρ violates (A2). Nonetheless, I, W_0 and W_0^2 are linearly independent and, likewise, so are I, W, and W^2. In this case, *both* parameter sets produce $\Pi = (I - \rho_0 W_0)^{-1}(\beta_0 I + \gamma_0 W_0) = (I - \rho W)^{-1}(\beta I + \gamma W)$. This arises even as W and W_0 represent very different network structures: any pair connected under W is not connected under W_0 and *vice-versa*.

or 2 since her outcome is not affected by their covariates and their outcomes are not affected by her covariates. In other words, individual 3 is isolated and $(W_0)_{13} = (W_0)_{23} = (W_0)_{31} = (W_0)_{32} = 0$. On the other hand, individuals 1 and 2 cannot be isolated as their covariates are correlated with the other individual's outcome, reflecting (A5).[17] Due to the row-sum normalization of the first row, $(W_0)_{12} = 1$. Using (A3), it can be seen that W_0 is symmetric if Π_0 is symmetric. We thus find that $(W_0)_{21} = 1$. This and (A1) map all elements of W_0, and thus,

$$W_0 = \begin{bmatrix} 0 & 1 & 0 \\ 1 & 0 & 0 \\ 0 & 0 & 0 \end{bmatrix}.$$

As the third individual is isolated, she will be only be affected by her exogenous x_i and not by endogenous or exogenous peer effects. Hence the $(3,3)$ element of Π_0 is equal to $\beta_0 = \frac{182}{455} = .4$. To find ρ_0, note that $(I - \rho_0 W_0)\Pi_0 = \beta_0 I + \gamma_0 W_0$. Hence focussing on the $(1,1)$ elements of the matrices above, we find that $\frac{275}{455} - \rho_0 \frac{310}{455} = .4$, implying $\rho_0 = .3$ (complying with (A2)). Finally, γ_0 is identified from entry $(1,2)$, giving $\gamma_0 = \frac{310}{455} - .3 \frac{275}{455} = .5$.

Our final assumption articulates the need for a constant network W_0 observed over multiple instances of y_t and x_t:

(A6) y_t and x_t are observed for individuals $i = 1, \ldots, N$, and instances $t = 1, \ldots, T$, and the network W_0 does not depend on t

Here, 'instances' can refer to time but also to settings in which the same units are observed over multiple episodes. For example, if i are firms, then t can be segmented markets in which they operate. For simplicity, we refer to an instance as a time period. Multiple observations are a requirement to be able to implement the estimator in practice, and to identify the reduced-form parameters. We expand on estimation requirements in Section 3.1.

Importantly, the main identification results that we articulate below could, in principle, be applied for each time period t. That is, one can write a version of Equation (3) as

$$y_t = \rho_0 W_{0t} y_t + \beta_0 x_t + \gamma_0 W_{0t} x_t + \epsilon_t,$$

where W_{0t} is time-varying and, consequently, the reduced-form interaction matrix $\Pi_t = (I - \rho W_t)^{-1}(I\beta + W_t\gamma)$ is also time-varying. The identification results we develop below could be applied for reduced-form matrix Π_t. This motivates an extension on the method, presented in Section 2.3.5, where Assumption (A6) is relaxed and allowed to vary with t.

---

[17]If on the other hand, $(W_0)_{ij} = 0.5, i \neq j$ in violation of (A5) and all agents were connected, the model would not be identified.

2.2 Main Identification Results

Under the relatively mild assumptions above, we can begin to identify parameters related to the network. These results are then useful for our main identification theorems. Let λ_{0j} denote an eigenvalue of W_0 with corresponding eigenvector $v_{0,j}$ for $j = 1, \ldots, N$. Assumptions (A2) and (A3) allow us to identify the eigenvectors of W_0 directly from the reduced form. As $|\rho_0| < 1$:

$$
\begin{aligned}
\Pi_0 v_{0,j} &= \beta_0 v_{0,j} + (\rho_0 \beta_0 + \gamma_0) \sum_{k=1}^{\infty} \rho_0^{k-1} W_0^k v_{0,j} \\
&= \left[\beta_0 + (\rho_0 \beta_0 + \gamma_0) \sum_{k=1}^{\infty} \rho_0^{k-1} \lambda_{0,j}^k \right] v_{0,j} \\
&= \frac{\beta_0 + \gamma_0 \lambda_{0,j}}{1 - \rho_0 \lambda_{0,j}} v_{0,j}.
\end{aligned}
\tag{6}
$$

The infinite sum converges as $|\rho_0 \lambda_{0,j}| < 1$ by (A2). The equation above implies that $v_{0,j}$ is also an eigenvector of Π_0 with associated eigenvalue $\lambda_{\Pi,j} = \frac{\beta_0 + \gamma_0 \lambda_{0,j}}{1 - \rho_0 \lambda_{0,j}}$. The fact that eigenvectors of Π_0 are also eigenvectors of W_0 has a useful implication: eigencentralities may be identified from the reduced form, even when W_0 is not identified. As detailed in de Paula (2017) and Jackson *et al.* (2017), such eigencentralities often play an important role in empirical work as they allow a mapping back to underlying models of social interaction.[18]

Now let $\Theta \equiv \{\theta \in \mathbb{R}^m : \text{Assumptions (A1)-(A6) are satisfied}\}$ be the structural parameter space of interest. Our identification argument are structured along the following steps: a) we first establish local identification of the mapping $\Pi(\theta)$ using classical results on the rank of gradient of Rothenberg, 1971 (Theorem 1); b) we then show that $\Pi(\theta)$ is proper (Corollary 1); c) and that it has a connected image (Lemma 2, in the Appendix); d) allowing us to state the cardinality of the pre-image $\Pi^{-1}(\bar{\Pi})$ is constant for any $\bar{\Pi}$ in the image of $\Pi(\cdot)$, and that the cardinality is at most 2 (Theorem 2). We then provide additional conditions to narrow the identified set to a singleton (Corrollary 2-4).

We now formally present our results. Our first theorem establishes local identification of the mapping. A parameter point θ_0 is locally identifiable if there exists a neighborhood of θ_0 containing no other θ which is observationally equivalent. Using classical results in Rothenberg (1971), we show that our assumptions are sufficient to ensure that the Jacobian of Π relative to θ is non-singular, which, in turn, suffices to establish local identification.

Theorem 1. *Assume (A1)-(A6). $\theta_0 \in \Theta$ is locally identified.*

An immediate consequence of local identification is that the set $\{\theta \in \Theta : \Pi(\theta) = \Pi(\theta_0)\}$ is discrete (i.e. its elements are isolated points). The following corollary establishes that Π is a

---

[18]To identify the eigencentralities, we identify the eigenvector that corresponds to the dominant eigenvalue. If W_0 is non-negative and irreducible, this is the (unique) eigenvector with strictly positive entries, by the Perron-Frobenius Theorem for non-negative matrices (see Horn and Johnson, 2013, p.534).

proper function, i.e. the inverse image $\Pi^{-1}(K)$ of any compact set $K \subset \mathbb{R}^{N^2}$ is also compact (Krantz and Parks, 2013, p. 124). Since it is discrete, the identified set must be finite.

Corollary 1. *Assume (A1)-(A6). Then $\Pi(\cdot)$ is a proper mapping. Moreover, the set $\{\theta : \Pi(\theta) = \Pi(\theta_0)\}$ is finite.*

Under additional assumptions, the identified set is at most a singleton in each of the partitioning sets $\Theta_- \equiv \Theta \cap \{\rho\beta + \gamma < 0\}$ and $\Theta_+ \equiv \Theta \cap \{\rho\beta + \gamma > 0\}$.[19] Since $\Theta = \Theta_- \cup \Theta_+$, if the sign of $\rho_0\beta_0 + \gamma_0$ is unknown, the identified set contains, at most, two elements. In the theorem that follows, we show global identification only for $\theta \in \Theta_+$, since arguments are mirrored for $\theta \in \Theta_-$.

Theorem 2. *Assume (A1)-(A6), then for every $\theta \in \Theta_+$ we have $\Pi(\theta) = \Pi(\theta_0) \Rightarrow \theta = \theta_0$. That is, θ_0 is globally identified with respect to the set Θ_+.*

Similar arguments apply if Theorem 2 instead were to be restricted to $\theta \in \Theta_-$. The proof of the corollary below is immediate and therefore omitted.

Corollary 2. *Assume (A1)-(A6). If $\rho_0\beta_0 + \gamma_0 > 0$, then the identified set contains at most one element, and similarly if $\rho_0\beta_0 + \gamma_0 < 0$. Hence, if the sign of $\rho_0\beta_0 + \gamma_0$ is unknown, the identified set contains, at most, two elements.[20]*

We now turn our attention to the problem of identifying the sign of $\rho_0\beta_0 + \gamma_0$ from the observation of Π_0. This would then allow us to establish global identification using Theorem 2. It is apparent from (5) that if $\rho_0 > 0$ and $(W_0)_{ij} \geq 0$, for all $i, j = \{1, \ldots, N\}$ the off-diagonal elements of Π_0 identify the sign of $\rho_0\beta_0 + \gamma_0$.

Corollary 3. *Assume (A1)-(A6). If $\rho_0 > 0$ and $(W_0)_{ij} \geq 0$, the model is globally identified.*

Real world applications often suggest endogenous social interactions are positive ($\rho_0 > 0$), in which case global identification is fully established by Corollary 3. On the other hand, if $\rho_0 < 0$ (e.g. if outcomes are strategic substitutes), ρ_0^k in (5) alternates signs with k, and the off-diagonal elements no longer carry the sign of $\rho_0\beta_0 + \gamma_0$. Nonetheless, if W_0 is non-negative and irreducible (i.e., not permutable into a block-triangular matrix or, equivalently, a strongly connected social network), the model is also identifiable without further restrictions on ρ_0:

Corollary 4. *Assume (A1)-(A6), $(W_0)_{ij} \geq 0$ and W_0 is irreducible. If W_0 has at least two real eigenvalues or $|\rho_0| < \sqrt{2}/2$, then the model is globally identified.*

---

[19]The global inversion results we use are related to, but different from, those used by Komunjer (2012), Lee and Lewbel (2013) and Chiappori *et al.* (2015). Those authors use variations on a classical inversion result of Hadamard. In contrast, we employ results on the cardinality of the pre-image of a function, relying on less stringent assumptions. Specifically, while the classical Hadamard result requires that the image of the function be simply-connected (Theorem 6.2.8 of Krantz and Parks, 2013), the results we rely on do not.

[20]Under some special conditions, the mirror image of θ_0 can be characterized from equation (5). If $-W_0$ satisfies Assumption (A4), we may set $\rho^* = -\rho_0$, $\beta^* = \beta_0$, $\gamma^* = -\gamma_0$ and $W^* = -W_0$. Then $\rho_0\beta_0 + \gamma_0 = -(\rho^*\beta^* + \gamma^*)$. Also note that $\sum_{k=1}^{\infty} \rho_0^{k-1}W_0^k = -\sum_{k=1}^{\infty}(\rho^*)^{k-1}(W^*)^k$, and so $(\rho_0\beta_0 + \gamma_0)\sum_{k=1}^{\infty} \rho_0^{k-1}W_0^k = (\rho^*\beta^* + \gamma^*)\sum_{k=1}^{\infty}(\rho^*)^{k-1}(W^*)^k$. It follows that $\Pi(\theta_0) = \Pi(\theta^*)$, where $\theta^* = (\rho^*, \beta^*, \gamma^*, W^*)$.

Corollary 4 requires that W_0 be irreducible, i.e., that it is not permutable into an upper-triangular matrix. In the context of directed graphs, this is similar to requiring that the matrix be strongly connected, that is, that any node can be reached from any other node. The corollary then rules out cases when the network is not connected, for example if there are two disjoint groups (with no connection across groups), or a star network pointing from the center towards the edges. The corollary holds if there are at least two real eigenvalues, or if ρ_0 is appropriately bounded. Since W_0 is non-negative, it has at least one real eigenvalue, by the Perron-Frobenius Theorem. If W_0 is symmetric, for example, its eigenvalues are all real, and Corollary 4 holds. It also holds if $(W_0)_{ij} \leq 0$, as we can re-write the model as $\rho W_0 = -\rho |W_0|$ where $|W_0|$, is the matrix whose entries are the absolute values of the entries in W_0. However, Corollary 4 rules out cases that mix positive $(W_0)_{ij} \geq 0$ and negative interactions $(W_0)_{ij} \leq 0$. In any case, the bound on $|\rho_0|$ is sufficient and holds in most (if not all) empirical estimates we are aware of obtained from either elicited or postulated networks, and in our application on tax competition.

2.3 Extensions

2.3.1 Individual Fixed Effects

We observe outcomes for $i = 1, \ldots, N$ individuals repeatedly through $t = 1, \ldots, T$ instances. If t corresponds to time, it is natural to think of there being unobserved heterogeneity across individuals, α_i, to be accounted for when estimating Π_0. The structural model (2) is then,

$$y_{it} = \rho_0 \sum_{j=1}^{N} W_{0,ij} y_{jt} + \beta_0 x_{it} + \gamma_0 \sum_{j=1}^{N} W_{0,ij} x_{jt} + \alpha_i + \epsilon_{it},$$

which can be written in matrix form as,

$$y_t = \rho_0 W_0 y_t + x_t \beta_0 + W_0 x_t \gamma_0 + \alpha^* + \epsilon_t,$$

where α^* is the vector of fixed effects. Individual-specific and time-constant fixed effects can be eliminated using the standard subtraction of individual time averages. Defining $\bar{y}_t = T^{-1} \sum_{t=1}^{T} y_t$, $\bar{x}_t = T^{-1} \sum_{t=1}^{T} x_t$ and $\bar{\epsilon}_t = T^{-1} \sum_{t=1}^{T} \epsilon_t$,

$$y_t - \bar{y}_t = \rho_0 W_0 (y_t - \bar{y}_t) + (x_t - \bar{x}_t) \beta_0 + W_0 (x_t - \bar{x}_t) \gamma_0 + \epsilon_t - \bar{\epsilon}_t,$$

if W_0 is does not change with time. Identification from the reduced form follows from previous theorems, since Π_0 is unchanged when regressing $y_t - \bar{y}_t$ on $x_t - \bar{x}_t$.[21]

---

[21] As is the case in panel data, this would require strict exogeneity ($\mathbb{E}[\epsilon_s | x_t] = 0$ for any s and t) or predetermined errors ($\mathbb{E}[\epsilon_s | x_t] = 0$ for $s \geq t$) so that the matrix Π_0 can be consistently estimated.

2.3.2 Common Shocks

We next allow for unobserved common shocks to all individuals in the network in the same instance t. Such correlated effects α_t can confound the identification of social interactions. As we have not placed any distributional assumption on the covariance matrix of the disturbance term, our analysis readily incorporates correlated effects that are orthogonal to x_t. When this is not the case, one possibility is to model the correlated effects α_t explicitly. The model then is,

$$y_t = \rho_0 W_0 y_t + x_t \beta_0 + \gamma_0 W_0 x_t + \alpha_t \iota + \epsilon_t,$$

where α_t is a scalar capturing shocks in the network common to all individuals. Let $\Pi_{01} = (I - \rho_0 W_0)^{-1}$ and $\Pi_{02} = (\beta_0 I + \gamma_0 W_0)$ such that $\Pi_0 = \Pi_{01} \Pi_{02}$. The reduced-form model is,

$$y_t = \Pi_0 x_t + \alpha_t \Pi_{01} \iota + v_t.$$

We propose a transformation to eliminate the correlated effects: exclude the individual-invariant α_t, subtracting the mean of the variables at a given period (global differencing). For this purpose, define $H = \frac{1}{n} \iota \iota'$. We note that in empirical and theoretical work it is customary to strengthen Assumption (A4) and require that *all* rows of W_0 sum to one if no individual is isolated (see for example Blume *et al.*, 2015). This strengthened assumption is usually referred to as row-sum normalization, and is stated below:

(A4') For all $i = 1, ...N$ we have that $\sum_{j=1,...,N} (W_0)_{ij} = 1$.

This can be written compactly as $W_0 \iota = \iota$. In this case, W_0 can be interpreted as the normalized adjacency matrix. Under row-sum normalization we have that,

$$
\begin{aligned}
(I - H) y_t &= (I - H)(I - \rho_0 W_0)^{-1} (\beta_0 I + \gamma_0 W_0) x_t + (I - H)(I - \rho_0 W_0)^{-1} \epsilon_t \\
&= (I - H) \Pi_0 x_t + (I - H) v_t,
\end{aligned}
$$

because $(I - H)(I - \rho_0 W_0)^{-1} \alpha_t \iota = 0$ if Assumption (A4') holds. It then follows that $\tilde{\Pi}_0 = (I - H)\Pi_0$ is identified. The next proposition shows that, under row-sum normalization of W_0, Π_0 is identified from $\tilde{\Pi}_0$ (and, as a consequence, the previous results immediately apply).

Proposition 1. *If W_0 is diagonalizable and row-sum normalized, Π_0 is identified from $\tilde{\Pi}_0$.*

Under row-sum normalization of W_0, a common group-level shock affects individuals homogeneously since $(I - \rho_0 W_0)^{-1} \alpha_t \iota = \alpha_t (I + \rho_0 W_0 + \rho_0^2 W_0^2 + \cdots) \iota = \frac{\alpha_t}{1 - \rho_0} \iota$, which is a vector with no variation across entries. Consequently, global differencing eliminates correlated effects and $(I - H)(I - \rho_0 W_0)^{-1} \alpha_t \iota = (I - \rho_0 W_0)^{-1} \alpha_t (I - H) \iota = 0$. In the absence of row-sum normalization, global differencing does not ensure that correlated effects are eliminated. To see this, note

that $(I - \rho_0 W_0)^{-1}$ is no longer row-sum normalized and, crucially, $\alpha_t (I - \rho_0 W_0)^{-1}\iota$ is not a vector with constant entries.

The next proposition makes this point formally, that the stronger Assumption (A4') is *necessary* to eliminate group-level shocks, by showing it is not possible to construct a data transformation that eliminates group effects in the absence of row-sum normalization.

Proposition 2. *Define* $r_{W_0} = (I - \rho_0 W_0)^{-1}\iota$. *If in space* $\Theta = \{\theta \in \mathbb{R}^m : Assumptions\ (A1)\text{-}(A6)$ *are satisfied} there are* N *matrices* $W_0^{(1)}, \ldots, W_0^{(N)}$ *such that* $[r_{W_0^{(1)}} \cdots r_{W_0^{(N)}}]$ *has rank* N, *then the only transformation such that* $(I - \tilde{H})(I - \rho_0 W_0)^{-1}\iota = 0$ *is* $\tilde{H} = I$.

It is useful to be able to test for row-sum normalization (A4') as it enables common shocks to be accounted for in the social interactions model. This is possible as,

$$
\begin{aligned}
\Pi_0 \iota &= \beta_0 \iota + (\rho_0 \beta_0 + \gamma_0) \sum_{k=1}^{\infty} \rho_0^{k-1} W_0^k \iota \\
&= \left[\beta_0 + (\rho_0 \beta_0 + \gamma_0) \sum_{k=1}^{\infty} \rho_0^{k-1} \right] \iota \\
&= \frac{\beta_0 + \gamma_0}{1 - \rho_0} \iota.
\end{aligned}
\tag{7}
$$

The last equality follows from the observation that, under row-normalization of W_0, $W_0^k \iota = W_0 \iota = \iota$, $k > 0$. This implies Π_0 has constant row-sums, which suggests row-sum normalization is testable. In the Appendix we derive a Wald test statistic to do so.[22]

2.3.3 Multivariate Covariates

Next, allowing for multivariate x_t of dimension $n \times k$, the reduced-form model (4) is,

$$
y_t = \sum_{k=1}^{K} \Pi_{0,k} x_{k,t} + \nu_t,
$$

where $\Pi_{0,k} = (I - \rho_0 W_0)^{-1}(\beta_{0,k} I + \gamma_{0,k} W_0)$, $x_{k,t}$ refers to the k-th column of x_t, and $\beta_{0,k}$ and $\gamma_{0,k}$ select the k-th element of K-dimensional β_0 and γ_0, respectively. The previous identification results then apply sequentially to each $\Pi_{0,k}$, $k = 1, \ldots, K$. In fact, we only then need to maintain $W_x = \gamma_0 W_0$ for one covariate. It is therefore possible to allow the structure of endogenous and exogenous social effects to differ for $K - 1$ of the covariates. With K covariates, equation (3) is,

$$
y_t = \rho_0 W_0 y_t + \sum_{k=1}^{K} \beta_{0,k} x_t + \sum_{k=1}^{K} \gamma_{0,k} W_{0,k} x_{k,t} + \epsilon_t.
$$

---

[22]For ease of explanation, in the Appendix we derive the test under the asymptotic distribution of the OLS estimator. The test generally holds with minor adjustments for estimators with known asymptotic distributions.

Let $W_{0,k} = W_0$ be the case for $k = 1$. Then, having identified ρ_0 and W_0 from $\Pi_{0,1}$,

$$(I - \rho_0 W_0)\Pi_{0,k} = \beta_{0,k}I + \gamma_{0,k}W_{0,k},$$

for $k = 2, \ldots, K$. The parameter $\beta_{0,k}$ then corresponds to the diagonal elements of $(I - \rho_0 W_0)\Pi_{0,k}$ and the off-diagonal entries correspond to the off-diagonal elements of $\gamma_{0,k}W_{0,k}$. If Assumption (A4) holds for every $k = 1, \ldots, K$, we can identify $\gamma_{0,k}$ and thus $W_{0,k}$ for every $k = 1, \ldots, K$.[23]

2.3.4 Heterogeneous β_0

While many applications assume β_0 to be homogeneous across individual units, we here consider possible avenues allowing for heterogeneous coefficients. In a slight abuse of notation, consider for this subsection β_0 in equation system (3) to be $diag(\beta_{01}, \ldots, \beta_{0N})_{N \times N}$. Instead of a homogeneous scalar, β_0 is a diagonal matrix with the individual-specific coefficients $\beta_{01}, \ldots, \beta_{0N}$ along its diagonal. When $\rho_0 = 0$ as in Manresa (2016), $\Pi_0 = \beta_0 + \gamma_0 W_0$. In this case, under Assumption (A1), β_0 is identified from the diagonal elements in Π_0 and $\gamma_0 W_0$ is identified from its off-diagonal elements.

With multiple covariates, as long as coefficients are homogeneous for one of the covariates, one can also identify heterogeneous coefficients on the remaining covariates as done in the previous Subsection. For example, let there be K covariates and $\beta_{0,k} = diag(\beta_{01,k}, \ldots, \beta_{0N,k})$ for $k = 1, \ldots, N$. Suppose $\beta_{01,k} = \cdots = \beta_{0N,k}$ for one of these covariates and let this $k = 1$ without loss of generality. Having identified ρ_0 and W_0 from $\Pi_{0,1}$,

$$(I - \rho_0 W_0)\Pi_{0,k} = \beta_{0,k} + \gamma_{0,k}W_{0,k},$$

for $k = 2, \ldots, K$. Then, under Assumption (A1) , $\beta_{0,k}$ is identified from the diagonal elements in $(I - \rho_0 W_0)\Pi_{0,k}$ and $\gamma_{0,k}W_{0,k}$ is identified from its off-diagonal elements for $k = 2, \ldots, K - 1$.

Alternatively, when $\gamma_0 = 0$ one can apply traditional simultaneous equation methods to attain identification. For example, let $B \equiv [(I - \rho_0 W_0)', \ -(\beta_0 + \gamma_0 W)']'_{2N \times N}$ and $R_{(N-1) \times 2N} = [0_{(N-1) \times (N+1)} \ I_{N-1}]$. The restriction that $\gamma_0 = 0$ in the first equation in equation system (3) can then be expressed as $RB_{\cdot,1} = 0_{(N-1) \times 1}$, where $B_{\cdot,1}$ is the first column in B. The rank condition for

---

[23]If x is a scalar, $\Pi = (I - W_y)^{-1}(\beta I + W_x)$, where we absorb ρ and γ into the neighborhood matrices for simplicity. Supposing both W_y and W_x have zero diagonals (Assumption (A1)) one has $2N(N - 1) + 1$ structural parameters against N^2 elements in Π. Since $2N(N - 1) + 1 > N^2$ for $N > 1$ one would not be able to identify the parameters of interest without further information. Blume *et al.* (2015) also study the case in which the social structure mediating endogenous and exogenous social effects might differ. When W_x is known and there is partial knowledge of the endogenous social interaction matrix W_0, they show that the parameters of the model can be identified (their Theorem 6). Analogously, when there are enough unconnected nodes in each of the social interaction matrices represented by W_x and W_0, and the identity of those nodes is known, identification is also (generically) possible (their Theorem 7).

the identification of the first equation is then given by,

$$RB = \begin{bmatrix} 0 & -\beta_{0,2} & \ldots & 0 \\ & \ldots & & \\ 0 & 0 & \ldots & -\beta_{0,N} \end{bmatrix}$$

having rank equal to $N - 1$ (see Theorem 9.2 in Wooldridge, 2002). This will be the case if $\beta_{0,2}, \ldots, \beta_{0,N} \neq 0$. Intuitively, this guarantees that individual specific covariates are valid instrumental variables for their outcomes. Hence, if $\beta_{0,1}, \ldots, \beta_{0,N}$ are each different from zero, identification from Π_0 is obtained.

More generally, because there are N^2 equations corresponding to the entries in Π_0 and, allowing for heterogeneity in β_0 and imposing assumptions (A1)-(A6), there are $N^2 + 1$ parameters, further restrictions (like row-sum normalization) would be necessary. We conjecture that adequate restrictions would deliver positive identification results, but focus in the more conventional setting with homogeneous β_0.

2.3.5   Time-varying W

We now relax Assumption (A6) which states that W_0 does not vary across the time periods $t = 1, \ldots, T$. The version of Equation (3) with time-varying network is

$$y_t = \rho_0 W_{0t} y_t + \beta_0 x_t + \gamma_0 W_{0t} x_t + \epsilon_t,$$

with reduced-form matrix $\Pi_{0t} = (I - \rho_0 W_{0t})^{-1}(I\beta_0 + W_{0t}\gamma_0)$. We note that identification results developed in Subsection 2.2 can, in principle, be applied sequentially to each Π_{0t}, leading to the identification of a time-varying W_{0t} (and, potentially, of the parameters ρ_0, β_0 and γ_0).

In practice, implementing any estimation strategy with a time-varying Π_{0t} (or W_{0t}) is not feasible using only observation from the single time period t. We instead adopt a kernel-weighted version. Define period-specific weights ω_t, and consider the transformed data $\tilde{y}_t = \omega_t y_t$ and $\tilde{x}_t = \omega_t x_t$. Evidently, uniform weights $\omega_t = 1$ are equivalent to the strategy not considering time-varying networks. Alternatively, one could estimate W_t in time windows by setting $\omega_t = 1[\underline{t} \leq t \leq \bar{t}]$, where $\underline{t}$ and $\bar{t}$ are the start and end of the time window for which W_t is estimated. In the context of DSGE models with time-varying parameters, Kapetanios *et al.* (2019) suggests a Gaussian kernel with positive weights throughout the entire sample. We further discuss this strategy in the estimation section, and it is implemented in the empirical application section below.

3 Implementation

We now transition from our core identification results to their practical implementation. In practice Ordinary Least Squares (OLS) can only be used to estimate θ if $T \gg N$, which is in practice unlikely to be met as this is a high-dimensional problem.[24] Our preferred approach makes use of penalized estimation techniques that can be used for any given T. More specifically, we make use of the Adaptive Elastic Net GMM (Caner and Zhang, 2014), that is based on the penalized GMM objective function. Given the identification results presented in Section 2, the population moments used in forming the GMM objective function will be satisfied at the true parameter vector.

After setting out the estimation procedure, we showcase the method using Monte Carlo simulations based both on stylized random network structures as well as real world networks. In each case, we take a fixed network structure W_0, and simulate panel data as if the data generating process were given by the model in Equation (1). We apply the method on the simulated panel data to recover estimates of all elements in W_0, as well as the endogenous and exogenous social effect parameters.

3.1 Estimation

The parameter vector to be estimated is high-dimensional: $\theta = (W_{12}, \ldots, W_{N,N-1}, \rho, \gamma, \beta)' \in \mathbb{R}^m$, where $m = N(N-1) + 3$ and W_{ij} is the (i, j)-th element of the $N \times N$ social interactions matrix W_0. To be clear, in a network with N individuals, there are $N(N-1)$ potential interactions because individuals could interact with everyone else but herself (which would violate Assumption A1). As a consequence, even with a modest N, there are many more parameters to estimate and m is large. For example, a network with $N = 50$ implies more than two thousand parameters to estimate. While we consider N (and thus m) is fixed, we still refer to θ as high-dimensional. OLS estimation requires $m \ll NT (\Rightarrow N \ll T)$, so many more time periods than individuals: a requirement often met in finance data sets (van Vliet, 2018) or in other fields (see, e.g., Section 4.2 in Rothenhäusler *et al.*, 2015). Instead, to estimate a large number of parameters with limited data we utilize high-dimensional estimation methods, that are the focus of a rapidly growing literature.

Sparsity is a key assumption underlying many high-dimensional estimation techniques. In the context of social interactions, we say that W_0 is sparse if $\tilde{m}$, the number of non-zero elements of W_0, is such that $\tilde{m} \ll NT$. The notion of sparsity thus depends on the number of time periods. Sparsity corresponds to assuming that individuals influence or are influenced by a small number of others, relative to the overall size of the potential network and the time horizon in the data. As such, sparsity is typically *not* a binding constraint in social networks analysis.[25]

---

[24]See Appendix B.3.

[25]For example, common stylized networks are sparse, such as: (i) star: all individuals receive spillovers from the same individual; (ii) lattice: each individual is a source of spillover only to one other individual; (iii) interactions in pairs or triads or small groups, such as those described by De Giorgi *et al.* (2010); and (iv) small world networks (Watts, 1999). Prominent real world economic networks are also sparse. For example, in individual-level elicited

In the estimation of sparse models, the "effective number of parameters" (or "effective degrees of freedom") relates to the number of variables with non-zero estimated coefficients (Tibshirani and Taylor, 2012). In the context of the current social network model (and the Elastic Net estimator on which the estimation strategy below builds on), this is approximately equivalent to the density of the network times the number of parameters m. We then require this number to be smaller than T. Implicitly, this calculation provides a rough assessment on the minimum required T. In particular, we employ the Adaptive Elastic Net GMM estimator presented in Caner and Zhang, 2014 which is shown to converge at rate $\sqrt{NT/\tilde{m}} = \sqrt{NT/[dN(N-1)+K]} = O(\sqrt{T/(dN)})$, where d is the density of the network (see remark 7 in Caner and Zhang, 2014). Hence the quality of the large sample results would rely on a comparison between T and dN. For example, if $N = 30$ and $d = 0.02$, $N \times d = 0.6$ and, assuming $K = 3$, $N(N-1) \times d + 3 = 20.4$.[26]

Finally, to reiterate, our identification results themselves do *not* depend on the sparsity of networks. In particular, Assumptions (A1) to (A6) *do not* impose restrictions on the number of links in W_0, or $\tilde{m}$.[27] The identification results presented in Section 2 apply more broadly and irrespective of the estimation procedure.

Our preferred approach estimates the interaction matrix in the reduced form while penalizing and imposing sparsity on the structural object W_0. We impose sparsity and penalization in the structural-form matrix W_0 because this is a weaker requirement than imposing sparsity and penalization in the reduced-form matrix Π_0.[28] To accomplish this, we make use of the Adaptive Elastic Net GMM (Caner and Zhang, 2014), that is based on the penalized GMM objective function,

$$G_{NT}(\theta, p) \equiv g_{NT}(\theta)' M_T g_{NT}(\theta) + p_1 \sum_{\substack{i,j=1 \\ i \neq j}}^{N} |W_{i,j}| + p_2 \sum_{\substack{i,j=1 \\ i \neq j}}^{N} |W_{i,j}|^2 \tag{8}$$

where $\theta = (W_{1,2}, \ldots, W_{N,N-1} \rho, \gamma, \beta)'$ with dimension $m = N(N-1)+3$, and p_1 and p_2 are the penalization terms. The term $g_{NT}(\theta)' M_T g_{NT}(\theta)$ is the unpenalized GMM objective function with moment conditions based on orthogonality between the structural disturbance term and the covariates: $g_{NT}(\theta) = \sum_{t=1}^{T} [x_{1t}e_t(\theta)' \cdots x_{Nt}e_t(\theta)']'$, $e_t(\theta) = y_t - \rho W y_t - \beta x_t - \gamma W x_t$. There are $q \equiv N^2$ moment conditions since x_{it} is orthogonal to e_{jt}, for each $i, j = 1, \ldots, N$. Hence

data from *AddHealth* on teenage friendships (defined as reciprocated nominations), the density of links is around 2% of all feasible links. In firm-level data, the density of production networks in the US is less than 1% of all feasible links (Atalay *et al.*, 2011).

[26] As pointed out by a referee, variation in x will also matter for estimation precision. This is reflected in the asymptotic distribution for this estimator, displayed later in this subsection.

[27] If $N \to \infty$, Assumption (A2) would imply vanishing $(W_0)_{ij}$ entries. As highlighted previously, we consider N to be fixed, in line with many practical applications. Furthermore, Assumption (A2) is used to represent inverse matrices as Neumann series in our identification results. What is necessary for this to hold is that a sub-multiplicative norm on ρW be less than one. Here we use a specific norm (i.e., the maximum row sum norm), but other (induced) norms are also possible (i.e., the 2-norm or the 1-norm) (see Horn and Johnson, 2013, Chapter 5.6).

[28] Note that even if W is sparse, Π may not be sparse. In Appendix B.1, we show that $[\Pi_0]_{ij} = 0$ if, and only if, there are no paths between i and j in W_0, and so the pair is not connected. So sparsity in Π_0 is understood as W_0 being 'sparsely connected', which is a stronger assumption than sparsity in W_0.

the GMM weight matrix M_T is of dimension $N^2 \times N^2$, symmetric, and positive definite. For simplicity, we use $M_T = I_{N^2 \times N^2}$. Note that if x_t is econometrically endogenous, one can also exploit moment conditions with respect to available instrumental variables.[29] Given the identification results presented in Section 2, if $\theta \neq \theta_0$ and does not belong to the identified set, then $\Pi(\theta) \neq \Pi(\theta_0)$. Consequently, the populational version of the GMM objective function is uniquely minimized at the true parameter vector θ_0.

The penalization terms in Equation (8) are what makes this different from a standard GMM problem. The first term, $p_1 \sum_{i,j=1,i\neq j}^{N} |W_{i,j}|$, penalizes the sum of the absolute values of W_{ij}, i.e. the sum of the strength of links, for all node-pairs. Depending on the choice of p_1, some $W_{i,j}$'s will be estimated as exact zeros. A larger share of parameters will be estimated as zeros if p_1 increases. The second term, $p_2 \sum_{i,j=1,i\neq j}^{N} |W_{i,j}|^2$, penalizes the sum of the square of the parameters. This term has been shown to provide better model-selection properties, especially when explanatory variables are correlated (Zou and Zhang, 2009). The first stage estimate is,

$$\tilde{\theta}(p) = (1 + p_2/T) \cdot \underset{\theta \in \mathbb{R}^m}{\arg\min} \ G_{NT}(\theta, p) \tag{9}$$

where $(1 + p_2/T)$ is a bias-correction term also used by Caner and Zhang (2014).

Implementing the numerical optimization embedded in Equation (9) is computationally challenging since $m = N(N-1) + 3$ may entail a large number of function arguments. We instead implement the following modification to make use of fast Least-Angle Regression (LARS) algorithms (Efron *et al.*, 2004). We note that, for any given ρ, β and γ, the expression for $e_t(\theta)$ is linear in W:

$$e_t(\theta) = y_t - x_t\beta - W(\rho y_t + x_t\gamma) \quad = \quad \tilde{y}_{it}(\beta) - W\tilde{x}_t(\rho,\gamma)$$

where $\tilde{y}_{it}(\beta) \equiv y_t - x_t\beta$ and $\tilde{x}_t(\rho,\gamma) \equiv \rho y_t + x_t\gamma$ and, following the strategy above, is instrumented with x_t. This motivates a two-step optimization routine:

$$\min_{\theta \in \mathbf{R}^m} G_{NT}(\theta, p) = \min_{(\rho,\beta,\gamma) \in \mathbf{R}^3} \left[\min_{W_{ij} \in \mathbf{R}^{N(N-1)}} G_{NT}(\theta, p) \right],$$

where the expression in brackets has a computationally efficient solution through the LARS algorithm. The numerical optimization is then subsequently conducted over the parameter space of (ρ, β, γ) only. Details of the implementation are expanded in Appendix Subsection B.2.

A second (adaptive) step provides improvements by re-weighting the penalization by the inverse

---

[29] For expositional ease, we describe estimation in the context of the reduced form model (4), thereby abstaining from individual fixed or correlated effects. As the GMM estimator uses moments between the structural disturbance terms and covariates, this endogeneity is built into the estimation procedure.

of the first-step estimates (Zou, 2006):

$$\tilde{\theta}^*(p) = (1 + p_2/T) \cdot \underset{\theta \in \mathbb{R}^m}{\arg\min} \left\{ g_{NT}(\theta)' M_T g_{NT}(\theta) + p_1^* \sum_{\substack{\{i,j:\tilde{W}_{ij} \neq 0, \\ i,j=1,\ldots,N, \\ i \neq j\}}} \frac{|W_{i,j}|}{|\tilde{W}_{i,j}|^c} + p_2 \sum_{\substack{\{i,j:\tilde{W}_{ij} \neq 0, \\ i,j=1,\ldots,N, \\ i \neq j\}}} |W_{i,j}|^2 \right\},$$

(10)

where $\tilde{W}_{i,j}$ is the (i,j)-th element of the first-step estimate of W. We follow Caner and Zhang (2014) to set $c = 2.5$. If $\tilde{W}_{i,j} < 0.05$, we set $\tilde{W}_{i,j} = 0.05$. This ensures that second-stage estimates can be non-zero even if first-stage estimates were zero or small. The computational improvement – described above for the first-stage estimator – is also applied at the adaptive stage.

As a third and final step, we fix the support of $\tilde{\theta}^*(p)$, $\mathcal{S} = \{\rho, \beta, \gamma\} \cup \{W_{ij} : \tilde{W}_{ij}^* \neq 0\}$ and estimate the final parameters without penalization. This takes as arguments only the elements of $\tilde{\theta}^*(p)$ that were estimated as non-zero in the adaptive step. In essence, this step turns down to a standard GMM approach,

$$\hat{\theta}_{\mathcal{S}}(p) = \underset{\theta \in \mathbb{R}^{|\mathcal{S}|}}{\arg\min} \left\{ g_{NT}(\theta)' M_T g_{NT}(\theta) \right\},$$

(11)

where $|\mathcal{S}|$ is the dimension of the support. Importantly, Caner and Zhang (2014) show that the third-step estimator is asymptotically normal, with a known and easy-to-compute distribution,

$$\delta' \left[\left(\hat{G}' M_T \hat{G} \right)^{-1} \cdot \left(\hat{G}' M_T \Omega M_T \hat{G} \right) \cdot \left(\hat{G}' M_T \hat{G} \right)^{-1} \right]^{1/2} \cdot \sqrt{NT/\tilde{m}} \cdot (\hat{\theta}_{\mathcal{S}} - \theta_0) \overset{d}{\longrightarrow} N(0,1),$$

where $\hat{G} \equiv \hat{G}(\hat{\theta}) = \nabla g_{NT}(\theta)$ and $\Omega \equiv E[g_{NT}(\theta) g_{NT}(\theta)'].$[30] This allows us to conduct hypothesis testing and inference on the ρ, β, γ and the non-zero elements of W.

We write $p = (p_1, p_1^*, p_2)$ as the final set of penalization parameters. Conditional on p, the estimate of the procedure is $\hat{\theta}(p)$. As in Caner and Zhang (2014, p. 35), the penalization parameters p are chosen by the BIC criterion. This balances model fit with the number of parameters included in the model.[31]

In Appendix B.2 we provide further implementation details, including the choice of initial conditions. Of course, other estimation methods are available and our identification results do not

---

[30]This applies for the case of small p_2. In the case of large p_2, the asymptotic distribution is pre-multiplied by $K_n = \frac{I + \lambda_2 \left[\hat{G}(\hat{\theta})' \hat{\Omega}^{-1} \hat{G}(\hat{\theta}) \right]^{-1}}{1 + \lambda_2/NT}$. See Theorem 4 of Caner and Zhang (2014).

[31]Following Caner and Zhang, 2014, the choice of p, which we denote as $\hat{p}$, is the one that minimizes

$$\text{BIC}(p) = \log \left[g_{NT}\left(\hat{\theta}(p)\right)' M_T g_{NT}\left(\hat{\theta}(p)\right) \right] + A\left(\hat{\theta}(p)\right) \cdot \frac{\log T}{T}$$

where $A\left(\hat{\theta}(p)\right)$ counts the number of non-zero coefficients among $\{W_{1,2}, \ldots, W_{N,N-1}\}$, and larger than a small numerical tolerance for numerical, which we set at 10^{-5}. See also Zou *et al.* (2007).

hinge on any particular estimator. Our aim is to demonstrate the practical feasibility of using the Adaptive Elastic Net estimator, rather than claim it is the optimal estimator.[32]

3.2 Simulations

We showcase the method using Monte Carlo simulations based both on stylized random network structures as well as real world networks. We describe the simulation procedures, results and robustness checks in more detail in the Appendix C.1. Here we just provide a brief overview to highlight how well the method works to recover social networks even in relatively short panels.

For each simulated network, we take a fixed network structure W_0, and simulate panel data as if the data generating process were given by (1). We then apply the method on the simulated panel data to recover estimates of all elements in W_0, as well as the endogenous and exogenous social effect parameters (ρ_0, γ_0). Our result identifies entries in W_0 and so naturally recovers links of varying strength. It is long recognized that link strength might play an important role in social interactions (Granovetter, 1973). Data limitations often force researchers to postulate some ties to be weaker than others (say, based on interaction frequency). In contrast, our approach identifies the continuous strength of ties, $W_{0,ij}$, where $W_{0,ij} > 0$ implies node j influences node i.

The stylized networks we consider are a random network, and a political party network in which two groups of nodes each cluster around a central node. The real world networks we consider are the high-school friendship network in Coleman (1964) from a small high school in Illinois, and one of the village networks elicited in Banerjee *et al.* (2013) from rural Karnataka, India.

Summary statistics for each network are presented in Panel A of Table A1.[33] The four networks differ in their size, complexity, and the relative importance of strong and weak ties. For example, the Erdos-Renyi network only has strong ties, the political party network has twice as many strong as weak ties. For the real world networks, the mean out-degree distributions are higher so the majority of ties are weak, with the high school network having around 80% of its edges being weak ties. All four networks are also sparse.

For the stylized networks, we assess the performance of the estimator for a fixed network size, $N = 30$. We simulate the real-world networks using non-isolated nodes in each (so $N = 70$ and 65 respectively).[34]

---

[32]For example, Manresa (2016) also relies on a Lasso-related methodology but restricts ρ_0 to be zero and so ignores endogenous social effects. If instrumental variables are available, Lam and Souza (2016) propose estimating (1) directly using the Adaptive Lasso and exploiting sparsity of the estimated W_0. Gautier and Rose (2016) extend the (identification-robust) Self-Tuning Instrumental Variable estimator in Gautier and Tsybakov (2014).

[33]Following Jackson *et al.* (2017), we consider the following network-wide statistics: number of edges, number of strong and weak edges, number of reciprocated edges, clustering coefficient, number of components, and the size of the maximal component. In addition, we report the standard deviation calculated across elements of the diagonal of W_0^2. If this is zero, then the diagonal of W_0^2 is either zero or proportional to the vector of ones, and Assumption A5 would not be satisfied. We can see that for each case this statistic is well above zero. Following Jackson *et al.* (2017), we consider the following node-level statistics: in- and out-degree distribution (mean and standard deviation), and the three most central individuals.

[34]As in Bramoullé *et al.*, 2009, we exclude isolated nodes because they do not conform with row-sum normalization.

We evaluate the procedure over varying panel lengths (starting from short panels with $T = 5$), using various metrics. Given our core contribution is to identify the social interactions matrix, we first examine the proportion of true zero entries in W_0 estimated as zeros, and the proportion of true non-zero entries estimated as non-zeros. A global perspective of the proximity between the true and estimated network can be inferred from their average absolute distance between elements. This is the mean absolute deviation of $\hat{W}$ and $\hat{\Pi}$ relative to their true values, defined as $MAD(\hat{W}) = \frac{1}{N(N-1)} \sum_{i,j,i \neq j} |\hat{W}_{ij} - W_{ij,0}|$ and $MAD(\hat{\Pi}) = \frac{1}{N(N-1)} \sum_{i,j,i \neq j} |\hat{\Pi}_{ij} - \Pi_{ij,0}|$. The closer these metrics are to zero, more of the elements in the true matrix are correctly estimated. Finally, we evaluate the performance of the procedure using averaged estimates of the endogenous and exogenous social effect parameters, $\hat{\rho}$ and $\hat{\gamma}$. In keeping with the estimation strategy in our empirical application, we report unpenalised GMM.

3.3 Results

Despite the heterogeneity across networks, the method performs well in all simulations: Figure A1 shows the simulation results as evaluated using the six metrics described above. Panel A shows that for each network, the proportion of zero entries in W_0 correctly estimated as zeros is above 95% even when $T = 5$. The proportion approaches 100% as T grows. Conversely, Panel B shows the proportion of non-zeros entries estimated as non-zeros is also high for small T. It is above 70% from $T = 5$ for the Erdos-Renyi network, being at least 85% across networks for $T = 25$, and increasing as T grows. As discussed above, the Adaptive Elastic Net estimator is better in recovering true zero entries because it is a well-known feature that shrinkage estimators tend to shrink small parameters to zero.

Panels C and D show that for each simulated network, the mean absolute deviation between estimated and true networks for $\hat{W}$ and $\hat{\Pi}$ falls quickly with T and is close zero for large sample sizes. Finally, Panels E and F show that biases in the endogenous and exogenous social effects parameters, $\hat{\rho}$ and $\hat{\gamma}$, also fall in T (we do not report the bias in $\hat{\beta}$ since it is close to zero for all T). The fact that biases are not zero is as expected for small T, being analogous to well-known results for autoregressive time series models.[35]

Figure A2 shows that, as T increases, weaker links are able to be detected by the procedure. This pattern is consistent with the well-known fact that small parameters are likely shrunk to zero due to the penalization (Belloni and Chernozhukov, 2011). In Panel A, we show the distribution of the estimates of $\hat{W}_{ij}$, with $T = 25$ and for the high-school network. We show the distribution for the five most common values of $W_{0,ij}$. We find that most edges weaker than .5 are not detected; edges with strength .75 are substantially more likely to be estimated as non-zeros. When we estimate W with $T = 150$, Panel B shows we observe virtually all edges with strength greater than .5 are

---

[35]The bias in spatial auto-regressive models with small number of observations *even when the network is observed* is similarly documented by Mizruchi and Neuman (2008), Farber *et al.* (2009), Smith (2009), Neuman and Mizruchi (2010), and Wang *et al.* (2014).

estimated as non-zeros, and most edges with strength .375 are also detected. Only edges smaller than .25 are not detected. Panels C and D show a similar conclusion for the village network.

Figure A3 visual represents the simulated and actual networks under $T = 100$ time periods. The network size is set to $N = 30$ in the two stylized networks, $N = 70$ for the high school network, and $N = 65$ for the village household network. In comparing the simulated and true network, Figure A3 distinguishes between three types of edges: kept edges, added edges and removed edges. Kept edges are depicted in blue: these links are estimated as non-zero in at least 5% of the iterations and are also non-zero in the true network. Added edges are depicted in green: these links are estimated as non-zero in at least 5% of the iterations but the edge is zero in the true network. Removed edges are depicted in red: these links are estimated as zero in at least 5% of the iterations but are non-zero in the true network. Figure A3 further distinguishes between strong and weak links: strong links are shown in solid edges ($W_{0,ij} > .3$), and weak links are shown as dashed edges.

Panel A of Figure A3 compares the simulated and true Erdos-Renyi network. All links are recovered. For the political party network, Panel B shows that all strong edges are correctly estimated. However, around half the weak edges are recovered (blue dashed edges) with the others being missed (red dashed edges). As discussed above, this is not surprising given that shrinkage estimators force small non-zero parameters to zero. Hence, larger T is needed to achieve similar performance as in the other simulated networks in terms of detecting weak links. For the more complex and larger real-world networks, Panel C shows that in the high school network, strong edges are all recovered. However, around half the weak edges are missing (red dashed edges) and there are a relatively small number of added edges (green edges): these amount to 87 edges, or approximately 1.9% of the 4,534 zero entries in the true high-school network. A similar pattern of results is seen in the village network in Panel D: strong edges are all recovered, and here the majority of weak edges are also recovered.

Panel B of Table A1 compares the network- and node-level statistics calculated from the recovered social interactions matrix $\hat{W}$ to those in Panel A from the true interactions matrix W_0. The random Erdos-Renyi network is perfectly recovered. For the political party network, the number of recovered edges is slightly lower than the true network (41 vs. 45). The mean of the in- and out-degree distributions are slightly lower in the recovered network, and all three nodes with the highest out-degree are correctly captured (nodes 1, 11 and 28), that includes both party leaders (individuals 1 and 11). Performance in the two real world networks is also encouraging. In the high school network, a third of strong edges are correctly recovered. However, as already noted in Figure A2, because weak edges are not well estimated in the high school network, the average in- and out- degrees are smaller in the recovered network relative to the true network. We recover all three individuals with the highest out-degree. Finally, in the village network, half the strong edges are recovered, and we again recover the three households with the highest out-degree (nodes 16, 35, and 57).

In the Appendix we show the robustness of the simulation results to: (i) varying network

sizes; (ii) alternative parameter choices and richening up the structure of shocks across nodes. We also demonstrate the gains from using the Adaptive Elastic Net GMM estimator over alternative estimators, such as the Adaptive Lasso estimator and OLS.

4   Application: Tax Competition Between US States

Our identification result can be used to shed new light on a classic social interactions problem: tax competition between US states (Wilson, 1999). Ever since the seminal empirical studies in tax competition between jurisdictions (Case *et al.*, 1989; Case *et al.*, 1993), it has been well-recognized that defining competing 'neighbors' still remains the central empirical challenge. Theory provides some guidance on the issue through two mechanisms driving the structure of interactions across jurisdictions: factor mobility and yardstick competition.

On factor mobility, Tiebout (1956) first argued that labor and capital can move in response to differential tax rates across jurisdictions. Factor mobility leads naturally to the postulated social interactions matrix being: (i) geographic neighbors given labor mobility; and (ii) jurisdictions with similar economic or demographic characteristics, given capital mobility (Case *et al.*, 1989).[36]

A second mechanism occurs through political economy channels (Shleifer, 1985). In particular, yardstick competition between jurisdictions is driven by voters making comparisons between states to learn about their own politician's quality. Besley and Case (1995) formalize the idea in a model where voters use taxes set by governors in other states to infer their own governor's quality. This generates informational externalities across jurisdictions, forcing incumbents into yardstick competition, where their tax setting behavior is determined by what other incumbents do. Yardstick competition leads naturally to the postulated interactions matrix corresponding to 'political neighbors': other states that voters make comparisons to.

This application shows the practical use of our approach to recover social interactions and help shed new light on this long-standing debate in economics. We do so in a setting in which the number of nodes and time periods is relatively low: the data covers mainland US states, $N = 48$, for years 1962-2015, $T = 53$. Our approach identifies the structure of social interactions among 'economic neighbors', that we denote W_{econ}. We contrast this against a null hypothesis that state taxes are only influenced by their geographic neighbors, W_{geo}, as postulated by Besley and Case, 1995 and shown in Figure 1A. With W_{econ} recovered, we can establish, beyond geography, what predicts the strength of ties between states, and thus provide fresh insights on the drivers of tax competition across jurisdictions.

---

[36]A body of evidence finds that tax bases are mobile in response to tax differentials (Hines, 1996; Devereux and Griffith, 1998; Kleven *et al.*, 2013, 2014)

4.1 Data and Empirical Specification

We denote state tax liabilities for state i in year t as τ_{it}, covering state taxes collected from real per capita income, sales and corporate taxes. We measure this using a series constructed from data published annually in the Statistical Abstract of the United States. As our series covers mainland states ($N = 48$) for years 1962-2015, ($T = 53$), we extend the sample used by Besley and Case (1995), that runs from 1962-1988 ($T = 26$).[37] The outcome considered, $\Delta \tau_{it}$, is the change in tax liabilities between years t and $(t-2)$ because it might take a governor more than a year to implement a tax program. Their model implies a standard social interactions specification for the tax setting behavior of state governors:

$$\Delta \tau_{it} = \rho \sum_{j=1}^{N} W_{0,ij} \Delta \tau_{jt} + \sum_{k=1}^{K} \sum_{j=1}^{N} W_{0,ij} x_{jkt} \gamma_{0,k} + \sum_{k=1}^{K} \beta_{0,k} x_{ikt} + \alpha_i + \alpha_t + \epsilon_{it}. \quad (12)$$

where $k = 1, \ldots, K$ are the covariates, for state i at time period t. The model above mimics the specification discussed in Section 2.3.3. Tax setting behavior is thus determined by (i) endogenous social effects arising through neighbors' tax changes ($\sum_{j=1}^{N} W_{0,ij} \Delta \tau_{jt}$); (ii) exogenous social effects arising through the economic/demographic characteristics of neighbors ($\sum_{j=1}^{N} W_{0,ij} x_{jkt}$); (iii) state i's characteristics (x_{ikt}), that include income per capita, the unemployment rate, and the proportions of young and elderly in the state's population. All specifications include state and time effects (α_i, α_t), so allowing for time-invariant unobserved heterogeneity across states, and for common (macroeconomic) shocks. Due to the inclusion of the time effects α_t, we normalize the rows of W_{econ} to one. Table A6 presents descriptive statistics for the Besley and Case (1995) sample and our extended sample.

Much of the earlier literature on tax competition has focused on endogenous social effects and ignored exogenous social effects by setting $\gamma = 0$. Our identification result allows us to relax this restriction and estimate the full typology of social effects described by Manski (1993). This is important because only endogenous social effects lead to social multipliers from tax competition, and are crucial to identify as they can lead to a race-to-the-bottom or sub-optimal public goods provision (Brennan and Buchanan, 1980; Wilson, 1986; Oates and Schwab, 1988).

4.2 Preliminary Findings

Table 1 presents our preliminary findings and comparison to Besley and Case (1995). Column 1 shows OLS estimates of (12) where the postulated social interactions matrix is based on geographic

---

[37]Besley and Case (1995) test their political agency model using a two equation set-up: (i) on gubernatorial re-election probabilities; and (ii) on tax setting. Our application focuses on the latter because this represents a social interaction problem. They use two tax series: (i) TAXSIM data (from the NBER) which runs from 1977-88; and (ii) state tax liabilities series constructed from data published annually in the Statistical Abstract of the US that runs from 1962-1988. All their results are robust to either series. We extend the second series.

neighbors, exogenous social effects are ignored so $\gamma = 0$ and the panel includes all 48 mainland states but runs only from 1962-1988 as in Besley and Case (1995). Social interactions influence gubernatorial tax setting behavior: $\widehat{\rho}_{OLS} = .375$. Column 2 shows this to be robust to instrumenting neighbors' tax changes using the instrument set proposed by Besley and Case (1995): namely, instrumenting for $\Delta\tau_{jt}$ using geographic neighbors' lagged change in income per capita, and neighbors' lagged change in unemployment rate. These instruments are in the spirit of using exogenous social effects to instrument for neighbor's tax changes. $\widehat{\rho}_{2SLS}$ is more than double the magnitude of $\widehat{\rho}_{OLS}$ suggesting tax setting behaviors across jurisdictions are strategic complements, and OLS estimates are downward-biased.

Columns 3 and 4 replicate both specifications over the longer sample period, and confirm Besley and Case's (1995) finding on social interactions to be robust. We again note that $\widehat{\rho}_{2SLS}$ is more than double the magnitude of $\widehat{\rho}_{OLS}$. The result in Column 4 implies that for every dollar increase in the average tax rates among geographic neighbors, a state increases its own taxes by 64 cents. This is similar to the headline estimate of Besley and Case (1995).[38]

4.3 Endogenous and Exogenous Social Interactions (ρ and γ)

We now move beyond much of the earlier political economy and public economics literature to first establish whether there are endogenous and exogenous social interactions in tax setting behavior. We first focus on the endogenous and exogenous social interaction parameters, and in the next subsection we detail the identified social interactions matrix, $\hat{W}_{econ}$. To do so we need to modify slightly how we instrument for neighbors' tax changes: the instrument set proposed by Besley and Case (1995) based on geographic neighbor's characteristics will generally be weaker when estimating the full specification in (12) because the instruments are now directly controlled for in (12). We use an Adaptive Elastic Net GMM approach which instruments neighbors' tax changes with the characteristics of all other states. With the inclusion of endogenous and exogenous social effects, this represents our preferred approach.

Columns 1 and 2 of Table 2 shows OLS and GMM estimates for ρ obtained from the Adaptive Elastic Net procedure where we still set $\gamma = 0$ but use our preferred instrument set based on all other state's characteristics: $\widehat{\rho}_{GMM} = .709 > \widehat{\rho}_{OLS} = .649$. Columns 3 and 4 estimate the full model in (12). Relative to when exogenous social effects are assumed away ($\gamma = 0$), the OLS and GMM estimates of ρ are smaller, but we continue to find robust evidence of endogenous social interactions in tax setting behavior across states. The specification in Column 4 represents our preferred one: $\widehat{\rho}_{GMM} = .452$ (with a standard error of .132). This value meets the requirements

---

[38]Nor is the magnitude very different from earlier work examining fiscal expenditure spillovers. For example, Case *et al.* (1989) find that US state government levels of per-capita expenditures are significantly impacted by the expenditures of their neighbors, with the size of the impact being that a one dollar increase in neighbors' expenditures leads to an increase in own-state expenditures by seventy cents.

on ρ in Corollaries 3 and 4 for global identification.[39]

4.4 Identified Social Interactions Matrix ($\hat{W}_{econ}$)

Figure 1B shows how the structure of economic ($\hat{W}_{econ}$) and geographic networks (W_{geo}) differ, where connected edges imply that two states are linked in at least one direction (either state i causally impacts state taxes in j, and/or *vice versa*). This comparison makes it clear whether all states geographically adjacent to i matter for its tax setting behavior and whether there are non-adjacent states that influence its tax rate.

The left-hand panel of Figure 1B shows the network of geographic neighbors (whose edges are colored blue), onto which we have superimposed the edges that are *not* identified as links in W_{econ}; these dropped edges are indicated in red. The vast majority of geographically adjacent states are irrelevant for tax setting behavior. The right-hand panel of Figure 1B adds new edges identified in $\hat{W}_{econ}$ that are *not* part of W_{geo}; these added edges are indicated in green. These represent non-geographically adjacent states through which social interactions occur. For tax-setting behavior, economic distance is imperfectly measured if we simply assume that interactions depend only on geographical distance. The existence of spatially disperse social interactions between states hints against the role of labor mobility driving social interactions in tax setting behavior across states.

Table 3 summarizes the comparison between W_{geo} and $\hat{W}_{econ}$. W_{geo} has 214 edges, while $\hat{W}_{econ}$ has only 49 edges. Economic networks for tax competition are sparser than is implied by simply postulating geographic networks. $\hat{W}_{econ}$ and W_{geo} have 9 edges in common. Hence, the vast majority of geographical neighbors ($205/214 = 96\%$) are not relevant for tax setting. $\hat{W}_{econ}$ has 40 edges that are absent in W_{geo}, and the identified social interactions are more spatially dispersed than under the assumption of geographic networks. This is reflected in the far lower clustering coefficient in $\hat{W}_{econ}$ than in W_{geo} (.042 versus .419).[40]

4.5 Links and Reciprocity

Our estimation strategy identifies the continuous strength of links, $W_{0,ij}$, where $W_{0,ij} > 0$ is interpreted as state j influencing outcomes in state i. This is useful because recent developments in tax competition theory, using insights from the social networks literature, suggest links need not be reciprocal (Janeba and Osterleh, 2013).

Table 3 reveals that only 12.2% of edges in $\hat{W}_{econ}$ are reciprocal (all edges in W_{geo} are reciprocal

---

[39]Table A7 shows the full set of exogenous social effects (so Columns 1 and 2 refer to the same specifications as Columns 3 and 4 in Table 2). Exogenous social effects operate through economic neighbors' unemployment rate, demographic characteristics, and their governor's age. Income per capita of neighbors to state i do not impact its tax rate.

[40]The clustering coefficient is the frequency of the number of fully connected triplets over the total number of triplets. Other metrics can also be used to provide a scalar comparison of W_{geo} and $\hat{W}_{econ}$. One way to do so is to reshape both matrices as vectors of length (48×47) and to compute their correlation.

by definition). Hence, tax competition is both spatially disperse and asymmetric. In most cases where tax setting in state i is influenced by taxes in state j, the opposite is not true.

Given common time shocks α_t in (12), row-sum normalization is required and ensures $\sum_j W_{0,ij} = 1$. Hence, for every state i there will be at least one economic neighbor state j^* impacts it, so that $W_{0,ij^*} > 0$. This just reiterates that social interactions matter. On the other hand, our procedure imposes no restriction on the derived columns of $\hat{W}_{econ}$. It could be that a state does not affect any other state. To see this in more detail, the final rows of Table 3 report the degree distribution across all nodes (states), splitting for in-networks and out-networks. In W_{geo}, the in-degree is by construction equal to the out-degree, as all ties are reciprocal. The greater sparsity of the network of economic neighbors is again reflected in the degree distribution being lower for $\hat{W}_{econ}$ than for W_{geo}. In $\hat{W}_{econ}$, the dispersion of in- and out-degree networks is very different (as measured by the standard deviation), being near nine times higher for the in-degree. Hence one reason for such few reciprocal ties being in the economic network is that out-degree network ties are rarely also in-degree ties.

This asymmetry in $\hat{W}_{econ}$ further suggests that some highly influential states drive tax setting behavior in other states. To make clear which states these are, Figure 2 shows a histogram for the number of out-degree links from states. Twenty states have an out-degree of zero and so their tax rates have no direct impact on any other state's tax setting behavior. The most influential states in terms of the highest out-degree are Alabama (that directly impacts tax setting behavior in five other states), and South Carolina, Pennsylvania and Montana (all of which directly impact tax setting behavior in four other states). Taking South Carolina as an example, the four states that are directly impacted by it include its geographic neighbor, Georgia, as well as non-geographic neighbors Missouri, Montana and Virginia.

4.6 Factor Mobility or Yardstick Competition?

We can use the identified social interactions matrix $\hat{W}_{econ}$ to shed light on the roles of factor mobility and yardstick competition in driving social interactions across states. To do so we estimate the factors correlated with the existence of links between states i and j in $\hat{W}_{econ}$ relative to $\hat{W}_{geo}$ For state pairs with non-zero links in either $\hat{W}_{econ}$ or $\hat{W}_{geo}$, we define a dummy outcome $\hat{W}_{econ,ij} = 1$ if a link between states i and j is estimated under $\hat{W}_{econ}$ and $\hat{W}_{econ,ij} = 0$ if a link between states i and j exists under $\hat{W}_{geo}$ but not under $\hat{W}_{econ}$ Hence we essentially examine the correlates of links described across columns in Table 3 using the following dyadic regression:

$$\hat{W}_{econ,ij} = \lambda_0 + \lambda_1 X_{ij} + \lambda_2 X_i + \lambda_3 X_j + u_{ij}, \tag{13}$$

We estimate this using a linear probability model. The elements X_{ij}, X_i, and X_j correspond to characteristics of the pair of states (i, j), of state i, and state j, respectively. Covariates are

time-averaged over the sample period, and robust standard errors are reported.

Table 4 presents the dyadic regression results. Column 1 controls only for the distance between states i and j: this is highly predictive of an economic link between them. This reflects that the economic network of state i often comprises states are in the same region, but not necessarily contiguous to state i. The next set of specifications use the insight that economic neighbors are likely to be based on a mixture of similarity in geography, income per capita, and demography (Case *et al.*, 1989). Column 2 thus adds two X_{ij} covariates to capture the economic and demographic homophily between states i and j. GDP homophily is the absolute difference in the states GDP per capita. Demographic homophily is the absolute difference of the share of young people (aged 5-17) plus the absolute difference of the share of elderly people (aged 65+) across the states. GDP homophily does not predict economic ties, whereas demographic homophily does.

Columns 3 to 5 then sequentially add in several sets of controls. For labor mobility, we use net state-to-state migration data to control for the net migration flow of individuals from state i to state i (defined as the flow from i to j minus the flow from j to i).[41] We then add a political homophily variable between states. For any given year, this is set to one if a pair of states have governors of the same political party. As this is time averaged over our sample, this element captures the share of the sample period in which the states have governors of the same party. Lastly, we include whether state j is considered a tax haven (and so might have disproportionate influence on other states). Based on Findley *et al.* (2012), the following states are coded as tax havens: Nevada, Delaware, Montana, South Dakota, Wyoming and New York.

The specification in Column 5 shows that with this full set of controls, distance remains a robust predictor of the existence of economic links between states. However, the identified economic network highlights additional significant predictors of tax competition between states: political homophily *reduces* the likelihood of a link, suggesting any yardstick competition driving social interactions occurs when voters compare their governor to those of the opposing party in other states. Tax haven states appear to be especially less influential in the tax setting behaviors of other states. This mirrors what was observed in Figure 2 where some of the prominent tax havens – Nevada, Delaware and New York – where all identified to have zero out-degree links. The relatively weak influence of tax haven states eases concerns over a race-to-the-bottom in tax setting behaviors.

The final Column in Table 4 controls for state i and state j fixed effects. This reinforces the idea that distance and political homophily robustly correlate to the strength of influence states tax setting has on others (the tax haven dummy cannot be separately identified in this specification). Labor mobility between states does not robustly predict the existence of economic ties.

---

[41]We also experimented with alternative measures of labor migration, and results were qualitatively the same. State-to-state migration data are based on year-to-year address changes reported on individual income tax returns filed with the IRS. The data cover filing years 1991 through 2015, and include the number of returns filed, which approximates the number of households that migrated, the number of personal exemptions claimed, which approximates the number of individuals who migrated. The data are available at https://www.irs.gov/statistics/soi-tax-stats-migration-data (accessed September 2017).

4.7 Dynamics

As in our identification result, our empirical approach so far has taken the network structure as fixed over the entire sample period. The strength of this assumption depends on the specific application: with high frequency panel data over a short span of time, this might be reasonable to maintain. To understand tax competition between states over our study period, this is less likely to be true. We can examine the issue in more detail by allowing the estimated W_{econ} matrix to vary over time by changing the weight placed on observations from any given time period. More precisely, for any given time period t, we weight observations using a Gaussian kernel with its center varying period-by-period from 1962 to 2015. The variance of the kernel is set such that 75% of the weight is given to the first half of the data (i.e. pre-1988) when the kernel is centered at 1962. Figure A4 shows the kernel employed as we vary its centre: the solid kernel is that centred on 1962, the start of our sample – when we place most weight on observations from 1962. The earlier static case considered previously is akin to using a uniform kernel over the sample period.

This kernel weighting approach is outlined on Section 2.3.5 and, importantly, builds on the fact that our identification results do not depend on time. We fully describe the algorithm in Appendix Section B.2.

We begin by considering time varying estimates of the endogenous and exogenous social interaction parameters from the full model in (12). The results for the endogenous social interactions parameter are shown in Figure 3 where the shaded areas are the 95% confidence intervals of the period-by-period estimates. Panel A shows OLS estimates of $\widehat{\rho}$. These drift up over time, so that the strength of endogenous social interactions in tax setting behavior steadily increases over time from around .35 in the late 1960s to .50 by the 2010s. In all time periods we can reject the null that the endogenous social effect is zero. Recall the earlier static estimate was $\widehat{\rho}_{OLS} = .375$.

Panel B shows the estimated endogenous social effect when we use GMM based on characteristics of all other states as IVs. This also drifts up over time from around .35 in the late 1960s to .50 by the 2010s. In the majority of time periods we can reject the null of no endogenous social effect, despite these estimates being noisier than the OLS estimates.

Figure 4 shows the evolution of $\hat{W}_{econ}$ over time as we centre the kernel on different time periods. This follows the same color coding as in Figure 1. In all time periods, geography-based edges play little role, and over time the economic network becomes denser. This highlights not only that economic networks for tax competition always differ starkly from geography-based networks, but that the nature of economic networks relevant for tax competition has changed steadily over time.

To characterize the evolution of $\hat{W}_{econ}$ in more detail, Figure 5 shows how key features of $\hat{W}_{econ}$ evolve as we place greater weight from early to later time periods. For each statistic, we plot the period by period estimate when we centre the kernel on any given time period $t = 1962, ..., 2015$. The resulting smoothed estimates are then shown. To ease exposition, in all networks edges with $W_{0,ij} < 1/47$ are removed. This cutoff is chosen as, in theory, states can only link at maximum

with 47 other states. Panel A details the stability of estimates of $\hat{W}_{econ}$ by showing the share of edges that are kept from the previous estimate (that is centred on the previous time period). We see relatively high levels of stability in $\hat{W}_{econ}$ with the smoothed estimate suggesting more than 60% of edges always being kept from one estimate to the next, with this stability increasing from the late 1980s until the end of the sample period.

Panel B shows how the overlap between $\hat{W}_{econ}$ and W_{geo} varies over time, as measured by the share of edges that are only present in $\hat{W}_{econ}$. There is little overlap between the two networks over the entire sample. The smoothed estimate suggests that at least 80% of identified edges in $\hat{W}_{econ}$ are never in W_{geo}. The divergence between economic and geographic neighbors becomes starker from the mid 1980s onwards – the period over which we extend the Besley and Case (1995) sample.

Panels C and D then show how clustering and reciprocity of links in $\hat{W}_{econ}$ vary as we gradually increase the weight given to later observations. Clustering of $\hat{W}_{econ}$ increases from the 1960s through to the early 2000s. Thereafter the estimates suggest social interactions in tax competition between US states have become sparser. We also observe a reversal in the extent to which social interactions across states are reciprocal: with reciprocity rising to a peak in the early 1980s – when 20% of ties were reciprocal – and slowly falling thereafter.

Taken together, the results suggest the nature of tax competition between US states has changed over time through two mechanisms: (i) the strength of endogenous social interactions ($\hat{\rho}$) has increased over time; (ii) and the network of states interacted with ($\hat{W}_{econ}$) varies over time. This has important implications for policy evaluation: the same intervention might have different spillover effects if implemented at different moments in time due to the evolution of $\hat{\rho}$ and $\hat{W}_{econ}$. We consider this point next using counterfactual simulations.

4.8 Counterfactuals

We use a counterfactual exercise to contrasts how shocks to tax setting in a given state propagate under the identified interactions matrix $\hat{W}_{econ}$, relative to what would have been predicted under a postulated network structure based on W_{geo}. We do so both for the static and dynamic estimates of $\hat{W}_{econ}$. We focus on South Carolina, a state with among the highest out-degree as shown in Figure 2 (or as implied through the dynamic estimates of $\hat{W}_{econ}$). We consider a scenario in which South Carolina exogenously increases its taxes per capita, so $\Delta\tau_{it}$ increases by 10%. We measure the differential change in equilibrium state taxes in state j under the two network structures using the following statistic:

$$\Upsilon_j = \log(\Delta\tau_{jt}|\hat{W}_{econ}) - \log(\Delta\tau_{jt}|W_{geo}), \tag{14}$$

so that positive (negative) values imply equilibrium taxes being higher (lower) under $\hat{W}_{econ}$.[42]

Starting with the static case, Panel A of Figure 6 shows for each mainland US state (including

---

[42]For W_{geo}, we calculate the counterfactual at $\hat{\rho}_{GMM} = .452$, the endogenous effect parameter estimated in our preferred specification, Column 4 of Table 2.

South Carolina, the origin of the shock), the spillover effects through the economic network of tax competition. This highlights positive spillovers on tax rates in many states that are not geographic neighbors of South Carolina. Panel B then graphs Υ_j to make precise how spillovers derived from $\hat{W}_{econ}$ diverge from those predicted under W_{geo}. In 26 states, Υ_j is smaller than .01% because both networks predict negligible spillovers to those states. In the remaining 22 mainland states, there is a wide discrepancy between the equilibrium state tax rates predicted under $\hat{W}_{econ}$ relative to W_{geo}: Υ_j varies from -1 to 4.03. The long run effect in South Carolina itself is also higher under $\hat{W}_{econ}$ than under W_{geo}. The former states that given feedback effects, the long run increase in tax rates in South Carolina from a 10% increase is 11.4%, while the geographic based network does not capture such strong feedback effects and only implies an equilibrium increase of 10.3%.

As $\hat{W}_{econ}$ is spatially more dispersed than W_{geo}, the general equilibrium effects are different under the two network structures. Table 5 summarizes the general equilibrium implications for tax inequality under $\hat{W}_{econ}$ and the W_{geo} counterfactual. The average tax rate increase under $\hat{W}_{econ}$ is three times that estimated under W_{geo}. Moreover, the dispersion of tax rates across states increases under $\hat{W}_{econ}$ relative to that predicted under W_{geo}. Finally, assuming interactions across states are based solely on geographic rather than economic neighbors, we miss the fact that many states have relatively small tax increases.

Finally, we can repeat the simulation exercise using the dynamically estimated economic network, as we vary the weight placed on different time periods. Throughout, we calculate the general equilibrium effects of the *same* policy experiment: South Carolina increasing its taxes per capita by 10%. These general equilibrium effects vary over the sample period because the strength of social interactions in tax competition vary ($\hat{\rho}_{GMM}$) as shown in Figure 3 and identified economic neighbors vary over time ($\hat{W}_{econ}$) as shown in Figure 4. The results are summarized in Figure 7. This shows that placing weight on the early or later part of the sample generates similar changes in average tax rates and their variance in general equilibrium – with both being lower than simulated under the static model. Placing more weight on the middle of the sample period generates higher changes in average tax rates and their variance in general equilibrium.

The differential general equilibrium impacts found as we place different weight across sample observations, links to recent discussions on external validity of internally valid causal impacts based on micro evidence. While the earlier literature has emphasized the potential interaction of treatment effects with aggregate shocks (Rosenzweig and Udry, 2020) or how behavioral responses to social insurance policies vary over thee business cycle (Kroft and Notowidigdo, 2016), our analysis provides another explanation for changing impacts of policies where social interactions determine behavior: changes in the strength of social interactions and changes in the network of economic interactions.

5 Discussion

In a canonical social interactions model, we provide sufficient conditions under which the social interactions matrix, and endogenous and exogenous social effects are all globally identified, even absent information on social links. Our identification strategy is novel, and may bear fruit in other areas. We describe how high-dimensional estimation techniques can be used to estimate the model based on the Adaptive Elastic Net GMM method. We showcase the method in Monte Carlo simulations using two stylized and two real world networks: these highlight that even in panels as short as $T = 5$, the majority of social ties can be correctly identified. Finally, we employ this estimation strategy to provide novel insights in a classic social interactions problem: tax competition across US states.

The method is immediately applicable to other classic social interactions problems, but where data on social links is either missing or partial. In fields such as macroeconomics, political economy and trade, there are core areas of research where social interactions across jurisdictions/countries etc. could drive key outcomes, panel data exist over many periods, and the number of nodes is relatively fixed. Moreover, while our discussion and application have focused on a continuous policy response (state taxes), our methods can also be applied to the extensive margin of policy adoption and diffusion. Such diffusion models might generate network interactions where some states influence the later adoption of economic and social policies in other jurisdictions. This issue is studied in DellaVigna and Kim (2022) in the context of US state policies – they examine the diffusion of over 700 policies for the past 70 years. Their work also suggests the nature of interactions across states has changed over time: while geographic proximity is a good predictor of policy diffusion, they also find that since 2000 political alignment across states has become the strongest predictor of diffusion.

In other areas of economics, such as finance, high frequency panel data is readily available and relevant for the study of core research questions. For example, a long-standing question has been whether CEOs are subject to relative performance evaluation, and if so, what is the comparison set of firms/CEOs used (Edmans and Gabaix, 2016).[43] More generally, our method can be readily applied to a large class of economic questions around contagion, risk and the fragility of economic systems. Since the financial crisis of 2008 it has become clear that linkages between actors such as firms or banks are complex and often hidden, yet because endogenous network interactions cause feedback loops and have multiplier effects, they can have enormous implications for the evolution

---

[43]Edmans and Gabaix (2016) overview the theory and empirics of executive compensation. Applying the informativeness principle in contract theory to CEO pay suggests peer performance is informative about the degree to which firm value is due to high CEO effort or luck. In a first generation of studies, Aggarwal and Samwick (1999) and Murphy (1999) showed that CEO pay is determined by absolute, rather than relative performance. However, this conclusion has been challenged by others such as Gong *et al.* (2011) who argue these conclusions arise from identifying relative performance evaluation (RPE) based on an implicit approach, assuming a peer group (e.g. based on industry and/or size). Indeed, when Gong *et al.* (2011) study the explicit use of RPE, based on the disclosure of peer firms and performance measures mandated by the SEC in 2006, they actually find that 25% of S&P 1500 firms explicitly using RPE. We are currently working on using our method to provide novel evidence on the matter.

of financial crisis or propagation of supply shocks in aggregate. Identifying such synchronicity is a critical first step to putting in place policies to reduce the fragility of economic systems (Elliott and Golub, 2022; Goldstein *et al.*, 2022).van Vliet (2018) studies the interconnectedness between the largest financial institutions in during the 2008 financial crisis using readlily available market data, in which $N = 13$ and $T = 500$.

Advances in the availability of administrative data, data from social media, mobile technologies, and online economic transactions, all offer new possibilities to identify social interactions with long panels or high frequency data collections where data on social ties will typically be missing.

Three further directions for future research are of note. First, under partial observability of W_0 (as in Blume *et al.*, 2015), the number of parameters in W_0 to be retrieved falls quickly. Our approach can then still be applied to complete knowledge of W_0, such as if Aggregate Relational Data is available, and this could be achieved with potentially weaker assumptions for identification, and in even shorter panels. To illustrate possibilities, Figure 4 shows results from a final simulation exercise in which we assume the researcher starts with partial knowledge of W_0. We do so for the Banerjee *et al.* (2013) village family network, showing simulation results for scenarios in which the researcher knows the social ties of the three (five, ten) households with the highest out-degree. For comparison we also show the earlier simulation results when W_0 is entirely unknown. This clearly illustrates that with partial knowledge of the social network, performance on all metrics improves rapidly for any given T.

Second, we have developed our approach in the context of the canonical linear social interactions model (1). This builds on Manski (1993) when W_0 is known to the researcher, and the reflection problem is the main challenge in identifying endogenous and exogenous social effects. However, as established in Blume *et al.* (2011) and Blume *et al.* (2015), the reflection problem is functional-form dependent and may not apply to many non-linear models. An important topic for future research is thus to extend the insights gathered here to non-linear social interaction settings.

Finally, our approach has largely taken the network structure as predetermined and fixed. Clearly, an important part of the social networks literature examines endogenous network formation (Jackson *et al.*, 2017; de Paula, 2017). Our analysis allows us to begin probing the issue in two ways. First, the kind of dyadic regression analysis in Section 4 on the correlates of entries in $W_{0,ij}$ suggests factors driving link formation and dissolution. Second, this leads naturally to a broad agenda going forward, to address the challenge of simultaneously identifying and estimating time varying models of network formation and social interaction, all in cases where data on social networks is not required.

References

ACEMOGLU, D., V. CARVALHO, A. OZDAGLAR, AND A. TAHBAZ-SALEHI (2012). The Network Origins of Aggregate Fluctuations. *Econometrica*, 80, 1977–2016.

AGGARWAL, R. K. AND A. A. SAMWICK (1999). Executive Compensation, Strategic Competition, and Relative Performance Evaluation: theory and evidence. *The Journal of Finance*, 54.

AMBROSETTI, A. AND G. PRODI (1972). On the Inversion of Some Differentiable Mappings with Singularities between Banach Spaces. *Annali di Matematica Pura ed Applicata*, 93, 231–46.

——— (1995). *A Primer of Nonlinear Analysis*, Cambridge University Press.

ANSELIN, L. (2010). Thirty Years of Spatial Econometrics. *Papers in Regional Science*, 89, 3–25.

ATALAY, E., A. HORTACSU, J. ROBERTS, AND C. SYVERSON (2011). Network Structure of Production. *Proceedings of the American Mathematical Society*, 108, 5199–202.

BALLESTER, C., A. CALVO-ARMENDOL, AND Y. ZENOU (2006). Who's Who in Networks. Wanted: The Key Player. *Econometrica*, 74, 1403–17.

BANERJEE, A., A. G. CHANDRASEKHAR, E. DUFLO, AND M. O. JACKSON (2013). The Diffusion of Microfinance. *Science*, 341, 1236498.

BARRENHO, E., M. MIRALDO, C. PROPPER, AND C. ROSE (2019). Peer and Network Effects in Medical Innovation: The Case of Laparoscopic Surgery in the English NHS. University of York Working Paper.

BATTAGLINI, M., E. PATACCHINI, AND E. RAINONE (2022). Endogenous social interactions with unobserved networks. *The Review of Economic Studies*, 89, 1694–1747.

BELLONI, A. AND V. CHERNOZHUKOV (2011). High Dimensional Sparse Models: an Introduction. Tech. Rep. 1106.5242, arXiv.org Collection, http://arxiv.org/abs/1106.5242.

BESLEY, T. AND A. CASE (1994). Unnatural Experiments? Estimating the Incidence of Endogenous Policies. *NBER Working Paper 4956*.

——— (1995). Incumbent Behavior: Vote-seeking, Tax-setting, and Yardstick Competition. *American Economic Review*, 85, 25–45.

BLUME, L., W. A. BROCK, S. N. DURLAUF, AND Y. IOANNIDES (2011). Identification of Social Interactions. in *Handbook of Social Economics*, ed. by J. Behabib, A. Bisin, and M. O. Jackson, Noth-Holland, vol. 1B.

BLUME, L. E., W. A. BROCK, S. N. DURLAUF, AND R. JAYARAMAN (2015). Linear Social Interactions Models. *Journal of Political Economy*, 123, 444–96.

BONALDI, P., A. HORTACSU, AND J. KASTL (2015). An Empirical Analysis of Funding Costs Spillovers in the EURO-zone with Application to Systemic Risk. Princeton University Working Paper.

BRAMOULLÉ, Y., H. DJEBBARI, AND B. FORTIN (2009). Identification of Peer Effects Through Social Networks. *Journal of Econometrics*, 150, 41–55.

BRENNAN, G. AND J. BUCHANAN (1980). *The Power to Tax: Analytical Foundations of a Fiscal Constitution*, Cambridge University Press.

BREZA, E. AND A. G. CHANDRASEKHAR (2019). Social networks, reputation, and commitment: evidence from a savings monitors experiment. *Econometrica*, 87, 175–216.

BREZA, E., A. G. CHANDRASEKHAR, T. H. McCORMICK, AND M. PAN (2020). Using aggregated relational data to feasibly identify network structure without network data. *American Economic Review*, 110, 2454–84.

BURSZTYN, L., F. EDERER, B. FERMAN, AND N. YUCHTMAN (2014). Understanding Mechanisms Underlying Peer Effects: Evidence From a Field Experiment on Financial Decisions. *Econometrica*, 82, 1273–301.

CANER, M., X. HAN, AND Y. LEE (2018). Adaptive Elastic Net GMM Estimation With Many Invalid Moment Conditions: Simultaneous Model and Moment Selection. *Journal of Business and Economic Statistics*, 36, 24–46.

CANER, M. AND H. H. ZHANG (2014). Adaptive Elastic Net for Generalized Method of Moments. *Journal of Business and Economic Statistics*, 32, 30–47.

CASE, A., J. R. HINES, AND H. S. ROSEN (1989). Copycatting: Fiscal Policies of States and Their Neighborrs. *NBER Working Paper 3032*.

CASE, A., H. ROSEN, AND J. HINES (1993). Budget Spillovers and Fiscal Policy Interdependence: Evidence from the States. *Journal of Public Economics*, 52, 285–307.

CHANDRASEKHAR, A. AND R. LEWIS (2016). Econometrics of Sampled Networks. Working Paper.

CHANEY, T. (2014). The Network Structure of International Trade. *American Economic Review*, 104, 3600–34.

CHIAPPORI, P.-A., I. KOMUNJER, AND D. KRISTENSEN (2015). Nonparametric Identification and Estimation of Transformation Models. *Journal of Econometrics*, 188, 22–39.

COLEMAN, J. S. (1964). *Introduction to Mathematical Sociology*, London Free Press Glencoe.

CONLEY, T. G. AND C. R. UDRY (2010). Learning About a New Technology: Pineapple in Ghana. *American Economic Review*, 100, 35–69.

DE GIORGI, G., M. PELLIZZARI, AND S. REDAELLI (2010). Identification of Social Interactions through Partially Overlapping Peer Groups. *American Economic Journal: Applied Economics*, 2, 241–75.

DE MARCO, G., G. GORNI, AND G. ZAMPIERI (2014). Global Inversion of Functions: an Introduction. *ArXiv:1410.7902v1*.

DE PAULA, A. (2017). Econometrics of Network Models. in *Advances in Economics and Econometrics: Theory and Applications*, ed. by B. Honore, A. Pakes, M. Piazzesi, and L. Samuelson, Cambridge University Press.

DE PAULA, A., E. TAMER, AND S. RICHARDS-SHUBIK (2018). Identifying Preferences in Networks with Bounded Degree. *Econometrica*, 86, 263–288.

DELLAVIGNA, S. AND W. KIM (2022). Policy Diffusion and Polarization across US States. *National Bureau of Economic Research*.

DEVEREUX, M. AND R. GRIFFITH (1998). Taxes and the Location of Production: Evidence from a Panel of US Multinationals. *Journal of Public Economics*, 68, 335–67.

DIEBOLD, F. X. AND K. YILMAZ (2015). *Financial and Macroeconomic Connectedness: A Network Approach to Measurement and Monitoring*, Oxford University Press.

EDMANS, A. AND X. GABAIX (2016). Executive Compensation: a modern primer. *Journal of Economic literature*, 54, 1232–87.

EFRON, B., T. HASTIE, I. JOHNSTONE, AND R. TIBSHIRANI (2004). Least angle regression. *The Annals of statistics*, 32, 407–499.

ELLIOTT, M. AND B. GOLUB (2022). Networks and Economic Fragility. *Annual Review of Economics*, 14, 665–696.

ERDOS, P. AND A. RENYI (1960). On the Evolution of Random Graphs. *Publ. Math. Inst. Hung. Acad. Sci*, 5, 17–60.

FARBER, S., A. PÁEZ, AND E. VOLZ (2009). Topology and dependency tests in spatial and network autoregressive models. *Geographical Analysis*, 41, 158–180.

FETZER, T., P. C. SOUZA, O. VANDEN EYNDE, AND A. L. WRIGHT (2021). Security transitions. *American Economic Review*, 111, 2275–2308.

FINDLEY, M., D. NIELSON, AND J. SHARMAN (2012). Global Shell Games: Testing Money Launderers' and Terrorist Financiers' Access to Shell Companies. Griffith University Working Paper.

GAUTIER, E. AND C. ROSE (2016). Inference in Social Effects when the Network is Sparse and Unknown. (in preparation).

GAUTIER, E. AND A. TSYBAKOV (2014). High-Dimensional Instrumental Variables Regression and Confidence Sets. Working Paper CREST.

GOLDSTEIN, I., A. KOPYTOV, L. SHEN, AND H. XIANG (2022). Synchronicity and Fragility. *Manuscript*.

GONG, G., L. Y. LI, AND J. Y. SHIN (2011). Relative Performance Evaluation and Related Peer Groups in Executive Compensation Contracts. *The Accounting Review*, 86, 1007–43.

GRANOVETTER, M. (1973). The Strength of Weak Ties. *American Journal of Sociology*, 6, 1360–80.

HAMILTON, J. D. (1994). *Time Series Analysis*, Princeton University Press.

HINES, J. (1996). Altered States: Taxes and the Location of Foreign Direct Investment in America. *American Economic Review*, 86, 1076–94.

HOFF, P. D., A. E. RAFTERY, AND M. S. HANDCOCK (2002). Latent space approaches to social network analysis. *Journal of the american Statistical association*, 97, 1090–1098.

HOLLAND, P. W. AND S. LEINHARDT (1981). An Exponential Family of Probability Distributions for Directed Graphs. *Journal of the American Statistical Association*, 76, 33–50.

HORN, R. A. AND C. R. JOHNSON (2013). *Matrix Analysis*, Cambridge University Press.

JACKSON, M., B. ROGERS, AND Y. ZENOU (2017). The Economic Consequences of Social Network Structure. *Journal of Economic Literature*, 55, 49–95.

JACKSON, M. AND A. WOLINSKY (1996). A Strategic Model of Social and Economic Networks. *Journal of Economic Theory*, 71, 44–74.

JANEBA, E. AND S. OSTERLEH (2013). Tax and the City – A Theory of Local Tax Competition. *Journal of Public Economics*, 106, 89–100.

KAPETANIOS, G., R. M. MASOLO, K. PETROVA, AND M. WALDRON (2019). A time-varying parameter structural model of the UK economy. *Journal of Economic Dynamics and Control*, 106, 103705.

KLEVEN, H., C. LANDAIS, AND E. SAEZ (2013). Taxation and International Mobility of Superstars: Evidence from the European Football Market. *American Economic Review*, 103, 1892–924.

——— (2014). Migration and Wage Effects of Taxing Top Earners: Evidence from the Foreigners' Tax Scheme in Denmark. *Quarterly Journal of Economics*, 129, 333–78.

KLINE, B. AND E. TAMER (2016). Bayesian Inference in a Class of Partially Identified Models. *Quantitative Economics*, 7, 329–366.

KOMUNJER, I. (2012). Global Identification in Nonlinear Models with Moment Restrictions. *Econometric Theory*, 28, 719–29.

KRANTZ, S. G. AND H. R. PARKS (2013). *The Implicit Function Theorem*, Birkhauser.

KROFT, K. AND M. J. NOTOWIDIGDO (2016). Should unemployment insurance vary with the unemployment rate? Theory and evidence. *The Review of Economic Studies*, 83, 1092–1124.

LAM, C. AND P. C. SOUZA (2016). Detection and Estimation of Block Structure in Spatial Weight Matrix. *Econometric Reviews*, 35, 1347–1376.

——— (2020). Estimation and selection of spatial weight matrix in a spatial lag model. *Journal of Business & Economic Statistics*, 38, 693–710.

LEE, L.-F. (2004). Asumptotic Distributions of Quasi-Maximum Likelihood Estimators for Spatial Autoregressive Models. *Econometrica*, 72, 25.

——— (2007). Identification and Estimation of Econometric Models with Group Interactions, Contextual Factors and Fixed Effects. *Journal of Econometrics*, 60, 531–42.

LEE, S. AND A. LEWBEL (2013). Nonparametric Identification of Accelerated Failure Time Competing Risks Models. *Econometric Theory*, 29, 905–19.

LEWBEL, A., X. QU, AND X. TAN (2022). Social Networks with Unobserved Links. *Journal of Political Economy (forthcoming)*.

MANRESA, E. (2016). Estimating the Structure of Social Interactions Using Panel Data. Manuscript.

MANSKI, C. F. (1993). Identification of Endogenous Social Effects: the reflection problem. *The Review of Economic Studies*, 60, 531–42.

MEINSHAUSEN, N. AND P. BUHLMANN (2006). High-Dimensional Graphs and Variable Selection with the Lasso. *The Annals of Statistics*, 34, 1436–1462.

MIZRUCHI, M. S. AND E. J. NEUMAN (2008). The effect of density on the level of bias in the network autocorrelation model. *Social Networks*, 30, 190–200.

MURPHY, K. J. (1999). Executive Compensation. *Handbook of Labor Economics*, 3, 2485–563.

NEUMAN, E. J. AND M. S. MIZRUCHI (2010). Structure and bias in the network autocorrelation model. *Social Networks*, 32, 290–300.

OATES, W. AND R. SCHWAB (1988). Economic Competition Among Jurisdictions: Efficiency-enhancing or Distortion-inducing?. *Journal of Public Economics*, 35, 333–54.

ROSE, C. (2015). Essays in Applied Microeconometrics. Ph.D. thesis, University of Bristol.

ROSENZWEIG, M. R. AND C. UDRY (2020). External validity in a stochastic world: Evidence from low-income countries. *The Review of Economic Studies*, 87, 343–381.

ROTHENBERG, T. (1971). Identification in Parametric Models. *Econometrica*, 39, 577–91.

ROTHENHÄUSLER, D., C. HEINZE, J. PETERS, AND N. MEINSHAUSEN (2015). BACKSHIFT: Learning causal cyclic graphs from unknown shift interventions. in *Advances in Neural Information Processing Systems*, 1513–1521.

SACERDOTE, B. (2001). Peer Effects with Random Assingment: Results for Dartmouth Roommates. *The Quarterly Journal of Economics*, 116, 681–704.

SHLEIFER, A. (1985). A Theory of Yardstick Competition. *Rand Journal of Economics*, 16.

SMITH, T. E. (2009). Estimation bias in spatial models with strongly connected weight matrices. *Geographical Analysis*, 41, 307–332.

SOUZA, P. C. (2014). Estimating Network Effects without Network Data. PUC-Rio Working Paper.

TIBSHIRANI, R. J. AND J. TAYLOR (2012). Degrees of freedom in lasso problems. *The Annals of Statistics*, 40, 1198–1232.

TIEBOUT, C. (1956). A Pure Theory of Local Expenditures. *Journal of Political Economy*, 64, 416–24.

VAN VLIET, W. (2018). Connections as Jumps: Estimating Financial Interconnectedness from Market Data. Manuscript.

WANG, W., E. J. NEUMAN, AND D. A. NEWMAN (2014). Statistical power of the social network autocorrelation model. *Social Networks*, 38, 88–99.

WATTS, D. J. (1999). Networks, Dynamics, and the Small-World Phenomenon. *American Journal of Sociology*, 105, 493–527.

WILSON, J. (1986). A Theory of Interregional Tax Competition. *Journal of Urban Economics*, 19, 296–315.

——— (1999). Theories of Tax Competition. *National Tax Journal*, 52, 269–304.

WOOLDRIDGE, J. (2002). *Econometric Analysis of Cross Section and Panel Data*, The MIT Press.

YUAN, M. AND Y. LIN (2007). Model Selection and Estimation in the Gaussian Graphical Model. *Biometrika*, 94, 19–35.

ZHOU, W. (2019). A Network Social Interaction Model with Heterogeneous Links. *Economics Letters*, 180, 50–53.

ZOU, H. (2006). The Adaptive Lasso and Its Oracle Properties. *Journal of the American Statistical Association*, 101, 1418–29.

ZOU, H. AND T. HASTIE (2005). Regularization and Variable Selection via the Elastic Net. *Journal of the Royal Statistical Society: Series B (Statistical Methodology)*, 67, 301–320.

ZOU, H., T. HASTIE, AND R. TIBSHIRANI (2007). On the "Degrees of Freedom" of the LASSO. *The Annals of Statistics*, 35, 2173–2192.

ZOU, H. AND H. H. ZHANG (2009). On the Adaptive Elastic-net with a Diverging Number of Parameters. *Ann. Statist.*, 37, 1733–51.

A   Proofs

Theorem 1

Proof. The local identification result follows Rothenberg (1971). Under the assumptions in our model, the parameter space $\Theta \subset \mathbb{R}^m$ is an open set (recall that $m = N(N-1) + 3$.) This corresponds to Assumption I in Rothenberg (1971).

We have that,

$$
\begin{aligned}
\frac{\partial \Pi}{\partial W_{ij}} &= \rho \left(I - \rho W\right)^{-1} \Delta_{ij} \left(I - \rho W\right)^{-1} \left(\beta I + \gamma W\right) + \left(I - \rho W\right)^{-1} \gamma \Delta_{ij} \\
\frac{\partial \Pi}{\partial \rho} &= \left(I - \rho W\right)^{-1} W \left(I - \rho W\right)^{-1} \left(\beta I + \gamma W\right) \\
\frac{\partial \Pi}{\partial \gamma} &= \left(I - \rho W\right)^{-1} W \\
\frac{\partial \Pi}{\partial \beta} &= \left(I - \rho W\right)^{-1},
\end{aligned}
$$

where Δ_{ij} is the $N \times N$ matrix with 1 in the (i,j)-th position and zero elsewhere. Write the $N^2 \times m$ derivative matrix $\nabla_\Pi \equiv \frac{\partial \mathrm{vec}(\Pi)}{\partial \theta'}$. By assumption, row i in matrix W sums up to one, incorporated through the restriction that $\varphi \equiv \sum_{j=1, j \neq i}^{N} W_{ij} - 1 = 0$, for the unit-normalised row i. The derivative of the restriction φ is the m-dimensional vector $\nabla_W' \equiv \frac{\partial \varphi}{\partial \theta'} = \begin{bmatrix} e_i' \otimes \iota_{N-1}' & 0_{1 \times 3} \end{bmatrix}$ (where e_i is an N-dimensional vector with 1 in the ith component and zero, otherwise). Following Theorem 6 of Rothenberg (1971), the structural parameters $\theta \in \Theta$ are locally identified if, and only if, the matrix $\nabla \equiv [\nabla_\Pi' \ \nabla_W']'$ has rank m.[44]

If ∇ is does not have rank m, there is a nonzero vector $\mathbf{c} \equiv \left(c_{W_{12}}, \ldots, c_{W_{N,N-1}}, c_\rho, c_\gamma, c_\beta\right)'$ such that $\nabla \cdot \mathbf{c} = 0$. This implies that

$$
c_{W_{12}} \frac{\partial \Pi}{\partial W_{12}} + \cdots + c_{W_{N,N-1}} \frac{\partial \Pi}{\partial W_{N,N-1}} + c_\rho \frac{\partial \Pi}{\partial \rho} + c_\gamma \frac{\partial \Pi}{\partial \gamma} + c_\beta \frac{\partial \Pi}{\partial \beta} = 0 \tag{15}
$$

and, for the unit-normalized row i (see A4),

$$
\sum_{j \neq i, j = 1, \ldots, n} c_{W_{ij}} = 0. \tag{16}
$$

---

[44]For a parameter vector to be locally identified, Rothenberg (1971) requires that the derivative matrix ∇ have rank m at that point and that this vector be (rank-)regular. A (rank-)regular point of the parameter space is one for which there is a neighborhood where the rank of ∇ is constant (see Definition 4 in Rothenberg, 1971). Because we show that the derivative matrix has rank m at every point in the parameter space, this also guarantees that every point in the parameter space is (rank-)regular.

Premultiplying equation (15) by $(I - \rho W)$ and substituting the derivatives,

$$\sum_{i,j=1,i\neq j}^{N} c_{W_{ij}} \left[\rho \Delta_{ij} (I - \rho W)^{-1} (\beta I + \gamma W) + \gamma \Delta_{ij} \right] +$$
$$+ c_\rho W (I - \rho W)^{-1} (\beta I + \gamma W) + c_\gamma W + c_\beta I = 0.$$

Define $C \equiv \sum_{i,j=1,i\neq j}^{N} c_{W_{ij}} \Delta_{ij}$. Since the spectral radius of ρW is strictly less than one by A2, one can show (by representing $(I - \rho W)^{-1}$ as a Neumann series, for instance) that $(\beta I + \gamma W)$ and $(I - \rho W)^{-1}$ commute. Then, the expression above is equivalent to

$$\rho C (\beta I + \gamma W) (I - \rho W)^{-1} + \gamma C + c_\rho W (\beta I + \gamma W) (I - \rho W)^{-1} + c_\gamma W + c_\beta I = 0.$$

Post-multiplying by $(I - \rho W)$, we obtain

$$\rho C (\beta I + \gamma W) + \gamma C (I - \rho W) + c_\rho W (\beta I + \gamma W) + c_\gamma W (I - \rho W) + c_\beta (I - \rho W) = 0$$

which, upon rearrangement, yields

$$(\gamma + \rho \beta) C + c_\beta I + (\beta c_\rho - c_\beta \rho + c_\gamma) W + (c_\rho \gamma - \rho c_\gamma) W^2 = 0. \tag{17}$$

Because $C_{ii} = 0$ and $W_{ii} = 0$ (by A1), we have that $c_\beta + (c_\rho \gamma - \rho c_\gamma)(W^2)_{ii} = 0$ for all $i = 1, \ldots, N$. Since by assumption A5 there isn't a constant κ such that $\text{diag}(W_0^2) = \kappa \iota$, then $c_\beta = c_\rho \gamma - \rho c_\gamma = 0$. Plugging back in (17), we obtain

$$(\gamma + \rho \beta) C + (\beta c_\rho + c_\gamma) W = 0.$$

which implies that $C = -\frac{\beta c_\rho + c_\gamma}{\gamma + \rho \beta} W$ since $\gamma + \rho \beta \neq 0$ by assumption A3. Taking the sum of the elements in row i, we get

$$(\gamma + \rho \beta) \sum_{j \neq i, j=1,\ldots,n} c_{W_{ij}} + (\beta c_\rho + c_\gamma) = 0.$$

Note that, by equation (16), $\sum_{j \neq i, j=1,\ldots,n} c_{W_{ij}} = 0$. So $\beta c_\rho + c_\gamma = 0$ and $C = -\frac{\beta c_\rho + c_\gamma}{\gamma + \rho \beta} W = 0$. This implies that $c_{W_{ij}} = 0$ for any i and j. Combining $\beta c_\rho + c_\gamma = 0$ with $c_\rho \gamma - \rho c_\gamma = 0$ obtained above, we get that $c_\rho (\rho \beta + \gamma) = 0$. Since $\rho \beta + \gamma \neq 0$, then $c_\rho = 0$. Given that $\beta c_\rho + c_\gamma = 0$, it follows that $c_\gamma = 0$. This shows that $\theta \in \Theta$ is locally identified. $\qquad \square$

Corollary 1

Proof. The parameter θ_0 being locally identified (see Theorem 1) implies that the set $\{\theta : \Pi(\theta) = \Pi(\theta_0)\}$ is discrete. If it is also compact, then the set is finite. To establish that we now show that

Π is a proper function: the inverse image $\Pi^{-1}(K)$ of any compact set $K \subset \mathbb{R}^m$ is also compact (see Krantz and Parks, 2013, p.124).

Let $\mathcal{A}$ be a compact set in the space of $N \times N$ real matrices. Since it is a compact set in a finite dimensional space, it is closed and bounded. Since Π is a continuous function of θ, the pre-image of a compact set, which is closed, is also closed. Because $\|W\|$ is bounded and $\rho \in (-1, 1)$, their corresponding coordinates in $\theta \in \Pi^{-1}(\mathcal{A})$ are bounded. Suppose the coordinates for β or γ in $\theta \in \Pi^{-1}(\mathcal{A})$ are not bounded. So one can find a sequence $(\theta_k)_{k=1}^\infty$ such that $|\beta_k| \to \infty$ or $|\gamma_k| \to \infty$.

Denote the Frobenius norm of the matrix A as $\|A\|$. By the submultiplicative property $\|AB\| \leq \|A\| \cdot \|B\|$,

$$\|\beta I + \gamma W\| \leq \|I - \rho W\| \cdot \left\|(I - \rho W)^{-1}(\beta I + \gamma W)\right\| = \|I - \rho W\| \cdot \|\Pi\|.$$

It follows that

$$\frac{\|\beta I + \gamma W\|}{\|I - \rho W\|} \leq \|\Pi\|.$$

Given W has zero main diagonal,

$$\|\beta I + \gamma W\|^2 = \beta^2 \|I\|^2 + \gamma^2 \|W\|^2 = \beta^2 N + \gamma^2 \|W\|^2.$$

Also, $\|I - \rho W\|^2 = N + \rho^2 \|W\|^2 \leq N + \rho^2 C$, for some constant $C \in \mathbb{R}$ by Assumption (A2). We then have that

$$\frac{\sqrt{\beta^2 N + \gamma^2 \|W\|^2}}{\sqrt{N + \rho^2 C}} \leq \|\Pi\|.$$

By Assumption (A2) the denominator above is bounded. Hence $|\beta_k| \to \infty \Rightarrow \|\Pi(\theta_k)\| \to \infty$. We now use the fact that $\sum_j W_{ij} = 1$ to show that there is a lower bound on $\|W\|^2$, and so $|\gamma_k| \to \infty \Rightarrow \|\Pi(\theta_k)\| \to \infty$. To see this, note that

$$\min_{\text{s.t. } \sum_j W_{ij}=1} \|W\|^2 \geq \min_{\text{s.t. } \sum_j W_{ij}=1} \sum_{j=1}^N W_{ij}^2.$$

Since the objective function in above is convex, it can be shown that it is minimized at $W_{ij} = \frac{1}{N-1}, j \neq i$ and, consequently, $\|W\|^2 \geq (N-1)\frac{1}{(N-1)^2} = \frac{1}{N-1}$. Hence, if $|\gamma_k| \to \infty$, the numerator in the lower bound for $\|\Pi\|$ above also goes to infinity. Consequently, $\mathcal{A}$ would not be compact.

Therefore, if $\mathcal{A}$ is compact the coordinates in $\theta \in \Pi^{-1}(\mathcal{A})$ corresponding to β and γ are also bounded. Hence, $\Pi^{-1}(\mathcal{A})$ is bounded (and closed). Consequently it is compact.

For a given reduced form parameter matrix Π, the set $\{\theta : \Pi(\theta) = \Pi(\theta_0)\}$ is then compact. Since it is also discrete, it is finite. $\qquad\square$

The following lemmas are used in proving Theorem 2.

Lemma 1. *Assume (A1)-(A6). If $\gamma_0 = 0$, W_0 is such that $(W_0)_{1,2} = (W_0)_{2,1} = 1$ and $(W_0)_{ij} = 0$ otherwise, with $\rho_0 \neq 0$ and $\beta_0 \neq 0$, then $\theta_0 \in \Theta$ is identified.*

Proof. Take $\theta = (W_{12}, \ldots, W_{N,N-1}, \rho, \gamma, \beta) \in \Theta$ possibily different from θ_0 such that the models are observationally equivalent, so $\Pi_0 = \Pi$. Then

$$(I - \rho_0 W_0)^{-1}(\beta_0 I + \gamma_0 W_0) \quad = \quad (I - \rho W)^{-1}(\beta I + \gamma W).$$

Since $\gamma_0 = 0$ and $(I - \rho W)^{-1}$ and $(\beta I + \gamma W)$ commute (see the proof for Theorem 1), it follows that

$$\Pi_0 = \Pi \quad \Leftrightarrow \quad \beta_0(I - \rho_0 W_0)^{-1} = (\beta I + \gamma W)(I - \rho W)^{-1}$$

or, equivalently,

$$\beta_0(I - \rho W) \quad = \quad (I - \rho_0 W_0)(\beta I + \gamma W).$$

This last equation implies that

$$(\beta_0 - \beta)I - (\gamma + \beta_0 \rho)W + \rho_0 \beta W_0 + \rho_0 \gamma W_0 W \quad = \quad 0. \tag{18}$$

We first note that $(W_0 W)_{N,N} = 0$ since $(W_0)_{N,i} = 0$ for any $1 \leq i \leq N$ and, by Assumption (A1), $(W)_{N,N} = (W_0)_{N,N} = 0$. So $\beta_0 = \beta$. Taking elements (i, j) such that $i \geq 3$ and $i \neq j$ in equation (18), and using the fact that $\beta_0 = \beta$, we find that $-(\gamma + \beta_0 \rho)(W)_{ij} = -(\gamma + \beta \rho)(W)_{ij} = 0$ for any (i, j) such that $i \geq 3$ and $i \neq j$. By Assumption (A3), $\gamma + \beta \rho \neq 0$ and it follows that $(W)_{ij} = 0$ for any (i, j) such that $i \geq 3$ and $i \neq j$. In fact, since $(W)_{i,i} = 0$ by Assumption (A1), we get that $(W)_{ij} = 0$ for any (i, j) such that $i \geq 3$.

Using Assumption (A1) and since $\beta_0 = \beta$, elements $(1, 1)$ and $(2, 2)$ in equation (18) imply that $\rho_0 \gamma(W)_{2,1} = \rho_0 \gamma(W)_{1,2} = 0$. Given that $\rho_0 \neq 0$, we get that $\gamma(W)_{2,1} = \gamma(W)_{1,2} = 0$. From element $(1, 2)$ in equation (18) we find that $-(\gamma + \beta_0 \rho)(W)_{1,2} + \rho_0 \beta = 0$ or, equivalently, $(\rho_0 - \rho(W)_{1,2})\beta_0 - \gamma(W)_{1,2} = 0$. Given that $\gamma(W)_{1,2} = 0$ and $\beta_0 \neq 0$, it must be that $\rho_0 - \rho(W)_{1,2} = 0$. Making the analogous argument for element $(2, 1)$, we would also obtain that $\rho_0 - \rho(W)_{2,1} = 0$.

If both $(W)_{1,2}$ and $(W)_{2,1}$ are equal to zero, using the fact that $W_{ij} = 0$ for any (i, j) such that

$i \geq 3$, we would then obtain that W^2 is equal to

$$
\begin{bmatrix}
0 & 0 & (W)_{1,3} & \cdots & (W)_{1,N} \\
0 & 0 & (W)_{2,3} & \cdots & (W)_{2,N} \\
0 & 0 & 0 & \cdots & 0 \\
\vdots & \vdots & \vdots & \ddots & \vdots \\
0 & 0 & 0 & \cdots & 0
\end{bmatrix}^2
=
\begin{bmatrix}
0 & 0 & 0 & \cdots & 0 \\
0 & 0 & 0 & \cdots & 0 \\
0 & 0 & 0 & \cdots & 0 \\
\vdots & \vdots & \vdots & \ddots & \vdots \\
0 & 0 & 0 & \cdots & 0
\end{bmatrix},
$$

which contradicts Assumption (A5). Hence $(W)_{1,2} \neq 0$ or $(W)_{2,1} \neq 0$. If $(W)_{1,2} \neq 0$, using the fact that $\gamma(W)_{1,2} = 0$, we get that $\gamma = 0$. Equivalently, if $(W)_{2,1} \neq 0$, and using the fact that $\gamma(W)_{2,1} = 0$, we again get that $\gamma = 0$. So, in either case, $\gamma = \gamma_0 = 0$.

Taking element $(1,j)$ in equation (18), with $j \geq 3$, we get that $-(\gamma + \rho\beta_0)W_{1,j} + \gamma\rho_0(W)_{2,j} = -\rho\beta_0 W_{1,j} = 0$. Similarly, element $(2,j)$, with $j \geq 3$ implies that $-(\gamma + \rho\beta_0)W_{2,j} + \gamma\rho_0(W)_{1,j} = -\rho\beta_0 W_{2,j} = 0$. Then, from $-\rho\beta_0(W)_{1,j} = -\rho\beta_0(W)_{2,j} = 0$ for $j \geq 3$, it follows that $-\rho(W)_{1,j} = -\rho(W)_{2,j} = 0$ since $\beta_0 \neq 0$.

From $\rho_0 - \rho(W)_{1,2} = 0$, if $(W)_{1,2} \neq 0$, we get that $\rho = \rho_0/(W)_{1,2} \neq 0$. Equivalently, if $(W)_{2,1} \neq 0$, we get that $\rho = \rho_0/(W)_{2,1} \neq 0$. Since $(W)_{1,2} \neq 0$ or $(W)_{2,1} \neq 0$, we obtain that $\rho \neq 0$. Then, because $-\rho(W)_{1j} = \rho(W)_{2j} = 0$ for $j \geq 3$, we have that $(W)_{1j} = (W)_{2j} = 0$ for $j \geq 3$.

Given that $\rho_0 - \rho(W)_{1,2} = 0$, $\rho_0 - \rho(W)_{2,1} = 0$ and $\rho \neq 0$, we obtain that $(W)_{1,2} = (W)_{2,1} = \frac{\rho_0}{\rho}$. Since $(W)_{1,j} = 0$ for $j \neq 2$, $(W)_{2,j} = 0$ for $j \neq 1$ and $(W)_{ij} = 0$ for $i \geq 3$, by Assumption (A5) we get that $(W)_{1,2} = (W)_{2,1} = 1$ and $\rho = \rho_0$. Hence, $((W)_{1,2}, \ldots, (W)_{N,N-1}, \rho, \gamma, \beta) = ((W_0)_{1,2}, \ldots, (W_0)_{N,N-1}, \rho_0, \gamma_0, \beta_0)$. □

Lemma 2. *Assume (A1)-(A2) and (A4)-(A6). The image of $\Pi(\cdot)$, for $\theta \in \Theta_+$, is path-connected and, therefore, connected.*

Proof. Take θ and $\theta^* \in \Theta_+$. Consider first the subvectors corresponding to the adjacency matrices W and W^*. Without loss of generality, let $1, \ldots, N$ be ordered such that $(W^2)_{11} > (W^2)_{22}$. Consider the adjacency matrix W_* corresponding to the network of directed connections $\{(1,2),(2,1)\}$ and $\{(3,4),(4,5),\ldots,(N-1,N),(N,3)\}$:

$$
W_* =
\begin{bmatrix}
0 & 1 & 0 & 0 & \cdots & 0 \\
1 & 0 & 0 & 0 & \cdots & 0 \\
0 & 0 & 0 & 1 & \cdots & 0 \\
\vdots & \vdots & \vdots & \ddots & \ddots & \vdots \\
0 & 0 & 1 & 0 & \cdots & 0
\end{bmatrix}.
$$

Note that $\mathrm{diag}(W_*^2) = (1,1,0,\ldots,0)$ and this is an admissible adjacency matrix under assumptions (A1)-(A2) and (A4)-(A6). We first show that W is path-connected to W_*.

Consider the path given by

$$W(t) = tW_* + (1-t)W$$

which implies that

$$(W(t)^2)_{11} = (1-t)^2(W^2)_{11} + t^2 + (1-t)t(W_{12} + W_{21})$$
$$(W(t)^2)_{22} = (1-t)^2(W^2)_{22} + t^2 + (1-t)t(W_{12} + W_{21}).$$

Since $(W(t)^2)_{11} - (W(t)^2)_{22} = (1-t)^2[(W^2)_{11} - (W^2)_{22}] > 0$ for $t \in [0,1)$ and $W(1) = W_*$, (A5) is satisfied for any matrix $W(t)$ such that $t \in [0,1]$. Since all rows in W_* sum to one and $(W_*)_{ii} = 0$ for any i, it is straightforward to see that $W(t)$ also satisfies (A1) and (A4). Finally, $\sum_{j=1}^{N} |W_{ij}(t)| \leq t \sum_{j=1}^{N} |(W_*)_{ij}| + (1-t) \sum_{j=1}^{N} |W_{ij}| \leq 1$ for every $i = 1, \ldots, N$ and $W(t)$ satisfies Assumption (A2).

If W^* is such that $(W^{*2})_{11} \neq (W^{*2})_{22}$, the convex combination of W^* and W_* is also seen to satisfy (A1)-(A2) and (A4)-(A6) and a path between W and W^* can be constructed via W_*. If, on the other hand $(W^{*2})_{11} = (W^{*2})_{22}$, suppose without loss of generality that $(W^{*2})_{11} \neq (W^{*2})_{33}$. In this case, one can construct a path between W^* and W_{**} where W_{**} represents the network of directed connections $\{(1,3),(3,1)\}$ and $\{(2,4),(4,5),\ldots,(N-1,N),(N,2)\}$:

$$W_{**} = \begin{bmatrix} 0 & 0 & 1 & 0 & \cdots & 0 \\ 0 & 0 & 0 & 1 & \cdots & 0 \\ 1 & 0 & 0 & 0 & \cdots & 0 \\ \vdots & \vdots & \vdots & \ddots & \ddots & \vdots \\ 0 & 1 & 0 & 0 & \cdots & 0 \end{bmatrix}.$$

Like $W(t)$ above, this path can be seen to satisfy assumptions (A1)-(A2) and (A4)-(A6). Now note that a path can also be constructed between W_* and W_{**} as their convex combination also satisfies (A1)-(A2) and (A4)-(A6). For example, note that $\hat{W}(t) = tW_* + (1-t)W_{**}$ is such that $(\hat{W}(t)^2)_{11} = t^2 + (1-t)^2$ and $(\hat{W}(t)^2)_{NN} = 0$ so $(\hat{W}(t)^2)_{11} - (\hat{W}(t)^2)_{NN} > 0$ for any $t \in (0,1)$ and both $\hat{W}(0)$ and $\hat{W}(1)$ satisfy (A5). Hence, we can construct a path $W(t)$ between W and W^* through W_* and W_{**}.

Furthermore, $\rho(t) = t\rho^* + (1-t)\rho$, $\beta(t) = (t\rho^*\beta^* + (1-t)\rho\beta)/(t\rho^* + (1-t)\rho)$, $\gamma(t) = t\gamma^* + (1-t)\gamma$ are such that

$$f(t) \equiv \rho(t)\beta(t) + \gamma(t) = t(\rho^*\beta^* + \gamma^*) + (1-t)(\rho\beta + \gamma) > 0,$$

since θ^* and $\theta \in \Theta_+$. (Note also that $|\rho(t)| < 1$ so Assumption (A2) is satisfied.) These facts taken

together imply that

$$\theta(t) \equiv (W(t)_{12}, \ldots, W(t)_{N,N-1}, \rho(t), \gamma(t), \beta(t)) \in \Theta_+.$$

That is, Θ_+ is path-connected and therefore connected. Since $\Pi(\cdot)$ is continuous on Θ_+, $\Pi(\Theta_+)$ is connected. $\qquad\square$

Theorem 2

Proof. The proof uses Corollary 1.4 in Ambrosetti and Prodi (1995, p. 46),[45] which we reproduce here with our notation for convenience: *Suppose the function $\Pi(\cdot)$ is continuous, proper and locally invertible with a connected image. Then the cardinality of $\Pi^{-1}(\overline{\overline{\Pi}})$ is constant for any $\overline{\overline{\Pi}}$ in the image of $\Pi(\cdot)$.*

The mapping $\Pi(\theta)$ is continuous and proper (by Corollary 1), with connected image (Lemma 2), and non-singular Jacobian at any point (as per the proof for Theorem 1) which guarantees local invertibility. Following Corollary 1.4 in Ambrosetti and Prodi (1995, p.46) reproduced above, we obtain that the cardinality of the pre-image of $\Pi(\theta)$ is finite and constant. Take $\theta \in \Theta_+$ such that $\gamma = 0$, $(W)_{1,2} = (W)_{2,1} = 1$ and $(W)_{i,j} = 0$ otherwise, with $\rho \neq 0$ and $\beta \neq 0$. By Lemma 1, that cardinality is one. $\qquad\square$

Corollary 3

Proof. Since $\rho \in (0,1)$ and $W_{ij} \geq 0$, $\sum_{k=1}^{\infty} \rho^{k-1} W^k$ is a non-negative matrix. By (5), the off-diagonal elements of $\Pi(\theta)$ are equal to the off-diagonal elements of $(\rho\beta + \gamma)\sum_{k=1}^{\infty} \rho^{k-1} W^k$, the sign of those elements identifies the sign of $\rho\beta + \gamma$. By Theorem 2, the model is identified. $\qquad\square$

Corollary 4

Proof. Since W_0 is non-negative and irreducible, there is a real eigenvalue equal to the spectral radius of W_0 corresponding to the unique eigenvector whose entries can be chosen to be strictly positive (i.e., all the entries share the same sign). A generic eigenvalue of W_0, λ_0, corresponds to an eigenvalue of Π_0 according to:

$$\lambda_{\Pi_0} = \beta_0 + (\rho_0\beta_0 + \gamma_0)\frac{\lambda_0}{1 - \rho_0\lambda_0}$$

If $\lambda_0 = a_0 + b_0 i$ where $a_0, b_0 \in \mathbb{R}$ and $i = \sqrt{-1}$, then

$$\lambda_{\Pi_0} = \beta_0 + (\rho_0\beta_0 + \gamma_0)\frac{a_0(1 - \rho_0 a_0) - \rho_0 b_0^2}{(1 - \rho_0 a_0)^2 + \rho_0^2 b_0^2} + (\rho_0\beta_0 + \gamma_0)\frac{b_0}{(1 - \rho_0 a_0)^2 + \rho_0^2 b_0^2}i.$$

---

[45]Related results can be found in Ambrosetti and Prodi (1972) and de Marco *et al.* (2014)

If the eigenvalue λ_0 is real, $b_0 = 0$ and the corresponding λ_{Π_0} eigenvalue is also real. Differentiating $Re(\lambda_{\Pi_0})$, the real part of λ_{Π_0}, with respect to $Re(\lambda_0) = a_0$, we get:

$$\frac{\partial Re(\lambda_{\Pi_0})}{\partial a_0} = \frac{(1 - \rho_0 a_0)^2 - \rho_0^2 b_0^2}{[(1 - \rho_0 a_0)^2 + \rho_0^2 b_0^2]^2} \times (\rho_0 \beta_0 + \gamma_0). \tag{19}$$

If the eigenvalue λ_0 is real, the expression (19) becomes:

$$\frac{\partial Re(\lambda_{\Pi_0})}{\partial a_0} = \frac{\partial \lambda_{\Pi_0}}{\partial a_0} = \frac{1}{(1 - \rho_0 a_0)^2} \times (\rho_0 \beta_0 + \gamma_0).$$

The fraction multiplying $\rho_0 \beta_0 + \gamma_0$ is positive. If $\rho_0 \beta_0 + \gamma_0 < 0$, the real eigenvalues of Π_0 are decreasing on the real eigenvalues of W_0. Consequently, the eigenvector corresponding to the largest (real) eigenvalue of W_0 will be associated with smallest real eigenvalue of Π_0. If, on the other hand, $\rho_0 \beta_0 + \gamma_0 > 0$ the eigenvector corresponding to the largest real eigenvalue of W_0 will correspond to the largest real eigenvalue of Π_0. Since that eigenvector is the unique eigenvector that can be chosen to have strictly positive entries, the sign of $\rho_0 \beta_0 + \gamma_0$ is identified by the λ_{Π_0} eigenvalue it is associated with and whether it is the largest or smallest real eigenvalue. By Theorem 2, the model is identified.

If there is only one real eigenvalue, note that the denominator in the fraction in (19) is positive. The minimum value of the numerator subject to $|\lambda_0|^2 = a_0^2 + b_0^2 \le 1$ is given by

$$\min_{a_0, b_0} (1 - \rho_0 a_0)^2 - \rho^2 b_0^2 \text{ s.t. } a_0^2 + b_0^2 \le 1.$$

The Lagrangean for this minimization problem is given by:

$$\mathcal{L}(a_0, b_0; \mu) = (1 - \rho_0 a_0)^2 - \rho^2 b_0^2 + \mu(a_0^2 + b_0^2 - 1).$$

where μ is the Lagrange multiplier associated with the constraint $a_0^2 + b_0^2 \le 1$. The Kuhn-Tucker necessary conditions for the solution (a_0^*, b_0^*, μ^*) of this problem are given by:

$$
\begin{aligned}
(\partial a_0 :) \quad & \rho_0(1 - \rho_0 a_0^*) - \mu^* a_0^* = 0 \\
(\partial b_0 :) \quad & (\rho_0^2 - \mu^*) b_0^* = 0 \\
& \mu^*(a_0^{*2} + b_0^{*2} - 1) = 0 \\
& a_0^{*2} + b_0^{*2} \le 1 \text{ and } \mu^* \ge 0,
\end{aligned}
$$

Let $\rho_0 \ne 0$. (Otherwise, the objective function above is equal to one irrespective of a_0 or b_0 and the partial derivative is $\rho_0 \beta_0 + \gamma_0$.) If $\mu^* = 0$, ∂b_0 implies that $b_0^* = 0$. Then ∂a_0 would have $a_0^* = \rho_0^{-1}$ which violates $a_0^{*2} + b_0^{*2} \le 1$.

Hence, a solution should have $\mu^* > 0$. In this case, there are two possibilities: $b_0^* = 0$ or

$b_0^* \neq 0$. If $b_0^* \neq 0$, condition ∂b_0 implies that $\mu^* = \rho_0^2$ and ∂a_0 then gives $a_0^* = (2\rho_0)^{-1}$. Because the constraint is binding, $b_0^{*2} = 1 - (4\rho_0^2)^{-1}$. In this case, $a_0^{*2} \leq 1$ and $b_0^{*2} \geq 0$ requires that $|\rho_0| \geq 1/2$. The value of the minimised objective function in this case $1/2 - \rho_0^2$. This is positive if $|\rho_0| < \sqrt{2}/2$.

The other possibility is to have $b_0 = 0$. Because the constraint is binding, $a_0 = 1$ and the objective function takes the value $(1 - \rho_0)^2 > 0$. Since $(1 - \rho_0)^2 - 1/2 + \rho_0^2 = 2\rho_0^2 - 2\rho_0 + 1/2 \geq 0$, this solution is dominated by the previous one when $|\rho_0| \geq 1/2$.

Consequently, the fraction multiplying $\rho_0\beta_0 + \gamma_0$ is non-negative and it can be ascertained that

$$\text{sgn}\left[\frac{\partial Re(\lambda_{\Pi_0})}{\partial a_0}\right] = \text{sgn}[\rho_0\beta_0 + \gamma_0]$$

as long as $|\rho_0| < \sqrt{2}/2$.

If $\rho_0\beta_0 + \gamma_0 < 0$, the real part of the eigenvalues of Π_0 is decreasing on the real part of the eigenvalues of W_0. Since the dominant eigenvalue for W_0 will be real and thus the one with the largest real part, we only need to focus on the real part of the eigenvalues. Consequently, the eigenvector corresponding to the eigenvalue of W_0 with the largest real part will correspond to the eigenvalue of Π_0 with the smallest real part. If, on the other hand, $\rho_0\beta_0 + \gamma_0 > 0$ the eigenvector corresponding to the eigenvalue of W_0 with the largest real part will correspond to the eigenvalue of Π_0 with the largest real part. Since that eigenvector is the unique eigenvector that can be chosen to have strictly positive entries, the sign of $\rho_0\beta_0 + \gamma_0$ is identified by the λ_{Π_0} eigenvalue it is associated with.

By Theorem 2, the model is identified. $\qquad\square$

Proposition 1

Proof. From equation (6) we observed that $\Pi_0 v_j = \lambda_{\Pi_0,j} v_j$, where v_j is an eigenvector of both W_0 and Π_0 with corresponding eigenvalue $\lambda_{\Pi_0,j} = \frac{\beta_0 + \gamma_0\lambda_{0,j}}{1 - \rho_0\lambda_{0,j}}$. Defining c as the row-sum of Π_0, we also have that

$$
\begin{aligned}
\tilde{\Pi}_0(I - H)v_j &= (I - H)\Pi_0(I - H)v_j &= (I - H)\Pi_0 v_j - (I - H)\Pi_0 H v_j \\
&= \lambda_{\Pi_0,j}(I - H)v_j - (I - H)cH v_j &= \lambda_{\Pi_0,j}(I - H)v_j - (H - H^2)c v_j \\
&= \lambda_{\Pi_0,j}(I - H)v_j - (H - H)c v_j &= \lambda_{\Pi_0,j}(I - H)v_j,
\end{aligned}
$$

where the third equality obtains from $\Pi_0 H = cH$ and the fifth equality holds since H is idempotent. So $\tilde{\Pi}_0$ and Π_0 have common eigenvalues, with corresponding eigenvector $\tilde{v}_j = v_j - \bar{v}_j\iota$ for $\tilde{\Pi}_0$, where $\bar{v}_j = \frac{1}{N}\iota' v_j$, $j = 1, \ldots, N$. Since $\lambda_{\Pi_0,j}$ and $\tilde{v}_j$ are observed from $\tilde{\Pi}_0$, identification of Π_0 is equivalent to identification of $\bar{v}_j$ (given diagonilizability).

To establish identification of $\bar{v}_j$, note that $W_0(\tilde{v}_j + \bar{v}_j\iota) = \lambda_{0,j}(\tilde{v}_j + \bar{v}_j\iota)$ since v_j is an eigenvector

of W_0. Consider an alternative constant $\bar{v}_j^* \neq \bar{v}_j$ that satisfies the previous equation. Then

$$W_0 \iota (\bar{v}_j - \bar{v}_j^*) = \lambda_{0,j} (\bar{v}_j - \bar{v}_j^*).$$

Since $W_0 \iota = \iota$, v_j must satisfy $(1 - \lambda_{0,j})(\bar{v}_j - \bar{v}_j^*) = 0$. For $j = 2, \ldots, N$, $|\lambda_{0,j}| < 1$. So $\bar{v}_j = \bar{v}_j^*$ and therefore identified. For $j = 1$, it is known that $\lambda_1 = 1$ with eigenvector $v_1 = \iota$. $\qquad\square$

Proposition 2

Proof. Under row-sum normalization and $|\rho_0| < 1$, $(I - \rho_0 W_0)^{-1} \iota = \iota + \rho_0 W_0 \iota + \rho_0^2 W_0^2 \iota + \cdots = \iota + \rho_0 \iota + \rho_0^2 \iota + \cdots = \iota \frac{1}{1 - \rho_0}$, so $\Pi_{01} \equiv (I - \rho_0 W)^{-1}$ has constant row-sums. If row-sum normalization fails, Π_{01} may not have constant row-sums. Define h_{ij} as the (ij)-th element of $\tilde{H}$. The first row of the system $(I - \tilde{H})(I - \rho_0 W)^{-1} \iota = (I - \tilde{H}) r_{W_0} = 0$ is $h_{11}^* r_{W_0,1} - h_{12} r_{W_0,2} - \cdots - h_{1N} r_{W_0,N} = 0$ where $h_{11}^* = 1 - h_{11}$ and $r_{W_0,l}$ is the l-th element of r_{W_0}. If there are N possible $W_0, W_0^{(1)}, \ldots, W_0^{(n)}$, such that $[r_{W_0^{(1)}} \cdots r_{W_0^{(N)}}]$ has rank N, then $h_{11}^* = h_{12} = \cdots = h_{1N} = 0$. Since the same reasoning applies to all rows, $\tilde{H}$ is the trivial transformation $\tilde{H} = I$. $\qquad\square$

B Estimation

B.1 Sparsity of W_0 and Π_0

Define $\tilde{M}$ as the number of non-zero elements of Π_0. We say that Π_0 is sparse if $\tilde{M} \ll NT$. Denote the number of connected pairs in W_0 via paths of any length as $\tilde{m}_c$. We equivalently say that W_0 is "sparse connected" if $\tilde{m}_c \ll NT$. We show that sparsity of Π_0 is related to sparse connectedness of W_0.

Proposition 3. Π_0 *is sparse if, and only if, the number of unconnected pairs W_0 is large.*

Proof. For $|\rho_0| < 1$, we have that

$$\Pi_0 = \beta_0 I + (\rho_0 \beta_0 + \gamma_0) \sum_{k=1}^{\infty} \rho_0^{k-1} W_0^k.$$

Given that $\rho_0 \beta_0 + \gamma_0 \neq 0$, it follows directly that $[\Pi_0]_{ij} = 0$ if, and only if, there are no paths between i and j in W_0. Therefore, sparsity of Π_0 translates into a large number of (i,j) unconnected pairs in W_0. $\qquad\square$

On the one hand, sparsity does not imply sparse connectedness. A circular graph is clearly sparse, but all nodes connect with all other nodes through a path of length at most $\frac{N}{2}$. On the other hand, the sparse connectedness implies sparsity and therefore is a stronger requirement. To see this, take any arbitrary network G with $\tilde{m}(G)$ non-zero elements and $\tilde{m}_c(G)$ connected

pairs. Now consider the operation of "completing" G: for every connected (i,j) pair, add a direct link between (i,j) if non-existent in G and denote the resulting matrix as $\mathcal{C}(G)$. It is clear that $\tilde{m}(G) \leq \tilde{m}(\mathcal{C}(G))$. Yet, $\tilde{m}(\mathcal{C}(G)) = \tilde{m}_c(G)$.

B.2 Adaptive Elastic Net

In this section, we detail the algorithm, the computational steps, and the property of the estimator as derived in Caner and Zhang (2014). For any given choice of $p = (p_1, p_1^*, p_2)$, the algorithm is composed of three main steps pertaining to the estimation of the Elastic Net (step 5 below), the Adaptive Elastic Net version (step 6), and the Unpenalised Post-GMM estimator (step 7). Other steps deal with the selection of the initial conditions, and other details of the implementation. R codes are available upon request. Running time for a given set of penalization parameters (that is, steps 1-7 below) is expected to be around 2-3 mins for $N = 30$ and 15-20 mins for $N = 70$. The increase in the computational time is due to the fact that the number of parameters to estimate grows at a N^2 rate.[46]

1. For any choice of penalization parameters $p = (p_1, p_1^*, p_2)$, run steps 2-7 below.

2. Data is standardised (subtracing the mean and dividing by the standard error) and removed of individual and time effects.

   a. For the dynamic versions, use time weights ω_t which are chosen by the practitioner and applied after standardization.

3. Initial conditions are set at $(\rho, \beta, \gamma) = (0.5, \hat{\beta}_{ols}, 0)$, where $\hat{\beta}_{ols}$ is the OLS regression of y_{it} on x_{it} after demeaning.

4. The derivatives of the objective function with respect to all w_{ij} are computed, and set to $w_{ij} = 0$ for the derivatives that are smaller than a small number η. This number can be chosen to be equal to p_1 following Caner and Zhang (2014). To be conservative, we choose $\eta = \min(p_1, 0.01)$. Those w_{ij} are set at zero for all the algorithm that follows.

5. *Elastic Net.* We devise an algorithm in the following manner.

   a. For any given (ρ, β, γ), we write

   $$\underbrace{y_t - x_t\beta}_{\equiv \tilde{y}_{it}} = W \underbrace{(\rho y_t + x_t\gamma)}_{\equiv \tilde{x}_t} + \epsilon_t$$

   which is endogenous due to the mechanical dependence of $\tilde{x}_t$ on y_t, and so it is instrumented with x_t. This expression is implemented through a fast Least-Angle Regression

---

[46]Benchmarked on 2020 Macbook Pro with M1 processor and 16gm RAM.

algorithm (LARS) from Caner *et al.* (2018) (Section 4.2) that extends the original LARS algorithm to the GMM case. We obtain $\hat{W}$ for any given (ρ, β, γ). At this stage, only impose that $|w_{ij}| \leq 1$ and, in particular, do not impose row-sum normalization.

    b. Use L-BFGS-B algorithm to minimize the objective function and obtain $(\tilde{\rho}, \tilde{\beta}, \tilde{\gamma})$, and then compute $\tilde{W}$ from step 5a.

6. *Adaptive Elastic Net.* Use $\tilde{W}$ to compute the adaptive weights. Following Caner and Zhang (2014), we select the adaptive weight penalty as $w_{ij}^{-\kappa}$ if $w_{ij} > 0.05$ where $\kappa = 2.5$. If $w_{ij} < 0.05$, we set $0.05^{-\kappa}$. This ensures that second-stage estimates can be non-zero even if first-stage estimates were zero or small.

    a. We then run a version of the algorithm described in step 5a, which the difference that we impose row-sum normalization. Due to this, we can no longer use restriction-free LARS algorithm. We instead use CVXR, a convex optimization routine package in R.

    b. Similar to step 5b, we use L-BFGS-B package to solve for $(\hat{\rho}, \hat{\beta}, \hat{\gamma})$, and compute the associated $\widehat{W}$.

7. *Unpenalised Post-GMM.* Re-estimate (ρ, β, γ) and W, on the support estimated at the previous step. In other words, the zero elements of $\widehat{W}$ are set to zero, i.e., the GMM objective function is estimated under the restriction that $\{W_{ij} = 0 : \widehat{W}_{ij} = 0\}$ and setting the penalization to zero. Asymptotic standard errors are also computed at this step.

8. Re-compute steps 1-6 on a grid for (p_1, p_1^*, p_2) and choose the penalization parameter by BIC.

We implement the following modifications and adjustments of the algorithm for the empirical analysis presented in Section 4. Steps 4' and 8' provide more stability to the period-by-period estimates by avoiding small-sample biases in the estimation of the derivative and of the information criteria.

2a'. We use uniform weights $\omega_t = 1$ and a Gaussian kernel with center varying period-by-period from $t = 1963$ to 2015, i.e. ranging from the beginning to the end of the sample. The variance of the kernel is set such that 75% of the weight is given to the first half of the data (pre-1988) when the center of the kernel is at the beginning of the sample at $t = 1963$.

4'. We compute the derivative under uniform weights, store it, and input the derivate for each dynamic-network version. This is computationally efficient (given that the numerical approximation of the derivative is intensive) and ensures that the derivative is computed from the full sample.

8'. The grid for the dynamic-network versions is set around the penalization parameters chosen under uniform kernel. More specifically, we run the procedure for the penalization parameters one point in all directions in the grid, and select the dynamic-network penalization parameters by BIC.

B.3 OLS

For the purpose of estimation, it is convenient to write the model in the stacked form. Let $x = [x_1, \ldots, x_T]'$ be the $T \times N$ matrix of explanatory variables, $y_i = [y_{i1}, \ldots, y_{iT}]'$ be the $T \times 1$ vector of response variables for individual i and $\pi_i^0 = [\pi_{i1}^0, \ldots, \pi_{iN}^0]'$ where π_{ij}^0 is a short notation for the (i,j)-th element of Π_0. The concise model is then,

$$y_i = x\pi_i^0 + v_i \tag{20}$$

for each $i = 1, \ldots, N$, where also $v_i = [v_{i1}, \ldots, v_{iT}]'$. Model (20) can then be estimated equation-by-equation. Denote $\pi^0 = [\pi_1^{0'}, \ldots, \pi_N^{0'}]'$. Stacking the full set of N equations,

$$y = X\pi^0 + v \tag{21}$$

where $y = [y_1, \ldots, y_N]$, $X = I_N \otimes x$, $\pi^0 = \text{vec}(\Pi_0')$, and $v = [v_1, \ldots, v_N]$. If the number of individuals in the network N is fixed and much smaller than data points available, $N^2 \ll NT$, equation (21) can be estimated via ordinary least squares (OLS). Under suitable regularity conditions, the OLS estimator $\hat{\pi} = (X'X)^{-1} X'y$ is asymptotically distributed,

$$\sqrt{NT}(\hat{\pi} - \pi^0) \xrightarrow{d} \mathcal{N}\left(0, Q^{-1}\Sigma Q^{-1}\right)$$

where $Q_T \equiv \frac{1}{NT}X'X$, $Q \equiv p\lim_{T\to\infty} Q_T$, $\Sigma_T \equiv \frac{1}{NT}X'vv'X$ and $\Sigma \equiv p\lim_{T\to\infty} \Sigma_T$. The proof is standard and omitted here. As noted above, in typical applications it is customary to row-sum normalize matrix W. If no individual is isolated, one obtains that, by equation (5),

$$
\begin{aligned}
\Pi_0 \iota_N &= \beta_0 \iota + (\rho_0\beta_0 + \gamma_0) \sum_{k=1}^{\infty} \rho_0^{k-1} W_0^k \iota \\
&= \frac{\beta_0 + \gamma_0}{1 - \rho_0} \iota \tag{22}
\end{aligned}
$$

where ι_N is the N-length vector of ones. The last equality follows from the observation that, under row-normalization of W_0, $W^k\iota = W\iota = \iota$, $k > 0$. Equation (22) implies that Π_0 has constant row-sums, which implies that row-sum normalization is, in principle, testable. This suggests a

simple Wald statistic applied to the estimates of π^0. Under the null hypothesis,

$$\sqrt{NT}R\hat{\pi} \xrightarrow{d} \mathcal{N}\left(0, RQ^{-1}\Sigma Q^{-1}R'\right)$$

where $R = [I_{N-1} \otimes \iota'_N; -\iota_{N-1} \otimes \iota'_N]$. The Wald statistic is $W = NT\left(R\hat{\pi}\right)'\left(Q^{-1}\Sigma Q^{-1}\right)^{-1}\left(R\hat{\pi}\right) \sim \chi^2_{N-1}$ which is a convenient expression for testing row-sum normalization of W_0. We also note that the asymptotic distribution of $\hat{\theta}$ can be immediately obtained by the Delta Method,

$$\sqrt{T}(\hat{\theta} - \theta_0) \xrightarrow{d} \mathcal{N}\left(0, \nabla'^{-1}_\theta Q^{-1}\Sigma Q^{-1}\nabla_\theta\right)$$

where ∇_θ is the gradient of $\hat{\theta}$ with respect to $\hat{\pi}$. We note that the derivation of the Wald statistic for testing the row-sum normalization and the asymptotic distribution of $\hat{\theta}$ does not depend on the OLS implementation, and can be easily adjusted for any estimator for which the asymptotic distribution is known.

C   Simulations

C.1   Set-Up

The simulations are based on two stylized random network structures, and two real world networks. These networks vary in their size, complexity, and aggregate and node-level features. All four networks are also sparse. The two stylized networks considered are:

(i) Erdos-Renyi network: we randomly pick exactly one element in each row of W_0 and set that element to 1. This is a random graph with in-degree equal to 1 for every individual (Erdos and Renyi, 1960). Such a network could be observed in practice if connections are formed independently of one another. With $N = 30$, the resulting density of links is 3.45%.

(ii) Political party network: there are two parties, each with a party leader. The leader directly affects the behavior of half the party members. We assume that one party has twice the number of members as the other. More specifically, we assume individuals $i = 1, \ldots, \frac{N}{3}$ are affiliated to Party A and are led by individual 1; individuals $i = \frac{N}{3} + 1, \ldots, N$ are affiliated to Party B and are led by individual $\frac{N}{3} + 1$. This difference in party size allows us to evaluate our ability to recover and identify central leaders, even in the smaller party. To test the procedure further, we add one random link per row to represent ties that are not determined by links to the Party leader. We simulate this network for various choices of N. If N is not a multiple of three, we round $\frac{N}{3}$ to the nearest integer. With $N = 30$, this network has a density of 5.17%.

(iii) Coleman's (1964) high school friendship network survey: in 1957/8, students in a small high

school in Illinois were asked to name, "fellows that they go around with most often." A link was considered if the student nominated a peer in either survey wave. The full network has $N = 73$ nodes, of which 70 are non-isolated and so have at least one link to another student. On average, students named just over five friendship peers. This network has density 7.58%. Furthermore, the in-degree distribution shows that most individuals received a small number of links, while a small number received many peer nominations.

(*iv*) Banerjee *et al.*'s (2013) village network survey: these authors conducted a census of households in 75 villages in rural Karnataka, India, and survey questions include several about relationships with other households in the village. To begin with, we use social ties based on family relations (later examining insurance networks). We focus on village 10 that is comprised of $N = 77$ households, and so similar in size to network *(iii)*. In this village there are 65 non-isolated households, with at least one family link to another household. This network has density 5.07%.

We simulate the real-world networks *(iii)* and *(iv)* using non-isolated nodes in each (so $N = 70$ and 65 respectively). We proceed as follows for each network. First, for each node we randomly assign one of their links to have strength three times compared to other links. As the underlying data generating process is assumed to allow for common time effects (α_t), we then set the weight on all other links from the node to be equal and such that row-sum normalization (A4') is complied with. For example, if in a given row of W_0 there are two links, one will be randomly selected to be set to .75, and the other set to .25. If there are three links, one is set to .6 and the other two set to each have weight .2 to maintain row-sum normalization, and so on. For the Erdos-Renyi network, there are thus only strong ties as each node has only one link to another node.

As we consider larger networks, we typically expect them to have more non-zero entries in each row of W_0, but row-sum normalization means that each weaker link will be of lower value. This works *against* the detection of weaker links using estimation methods involving penalization, because they impose small parameter estimates shrink to zero.[47] Finally, to aid exposition, we set a threshold value for link strength to distinguish 'strong' and 'weak' links. A strong (weak) link is defined as one for which $W_{0,ij} > (\leq)$ .3.

Panel data for each of the four simulations is generated as,

$$y_t = (I - \rho_0 W_0)^{-1}(x_t \beta + W_0 x_t \gamma + \alpha_t \iota + \alpha^* + \epsilon_t),$$

where α_t is a (scalar) time effect and α^* is a $N \times 1$ vector of fixed effects, drawn respectively from $N(1, 1)$ and $N(\iota, I_{N \times N})$ distributions. We consider $T = \{5, 10, 15, 25, 50, 75, 100, 125, 150\}$. The true parameters are set to $\rho_0 = .3$, $\beta_0 = .4$ and $\gamma_0 = .5$ (thus satisfying Assumption A3). The

---

[47]Caner and Zhang (2014) state that "local to zero coefficients should be larger than $T^{-\frac{1}{2}}$ to be differentiated from zero."

exogenous variable (x_t) and error term (ϵ_t) are simulated as standard Gaussian, both generated from $N(0_N, I_{N \times N})$ distributions. This is similar to variance terms set in other papers, e.g., Lee (2004). We later conduct a series of robustness checks to evaluate the sensitivity of the simulations to alternative parameters choices, and the presence of common- and individual-level shocks. For each combination of parameters, we conduct $1,000$ simulation runs.

C.2 Robustness

Table A2 presents results for the recovered stylized networks under varying network sizes, $N = \{15, 30, 50\}$. Differences between the true and estimated networks are fairly constant as N increases: even for small $N = 15$ a large proportion of zeros and non-zeros are correctly estimated. In all cases, biases in $\hat{\rho}$ and $\hat{\gamma}$ decrease with larger T.

Table A3 conducts robustness checks on the sensitivity of the estimates to parameters choices for the stylized networks. We consider true parameters $\rho_0 = \{.1, .3, .7, .9\}$, $\gamma_0 = \{.3, .7\}$, $\beta_0 = \{.2, .6\}$. We also introduce a common shock in the disturbance variance-covariance matrix by varying q in,

$$
\epsilon_t \sim N \left(0, \begin{bmatrix} 1 & q & \cdots & q \\ q & 1 & \cdots & q \\ \vdots & \vdots & \ddots & \vdots \\ q & q & \cdots & 1 \end{bmatrix} \right)
$$

where we consider $q = \{.3, .5, .8, 1\}$. We find the procedure to be robust to the true values of ρ_0, β_0, γ_0, and q. The method performs well in all scenarios.

The next set of robustness checks demonstrate the gains from using the Adaptive Elastic Net GMM estimator over alternative estimators. Table A4 shows simulation results using Adaptive Lasso estimates of the interaction matrix Π_0, so estimating and penalizing the reduced-form. The Adaptive Lasso estimator performs relatively worse, and increased sample sizes are necessary to achieve similar performance compared to the Adaptive Elastic Net GMM. Table A5 then shows the performance of the procedure based on OLS estimates of Π_0. Given OLS requires $m \ll NT$, we use a time dimension ten times larger, $T = \{500, 1000, 1500\}$, and still find a deterioration in performance compared to the Adaptive Elastic Net GMM estimator.[48]

Taken together, these robustness checks suggest the Adaptive Elastic Net GMM estimator is preferred over Adaptive Lasso and OLS estimators. This procedure does well in recovering true network structures, and *a fortiori*, network- and node-level statistics. It does so in networks that vary in size and complexity, and as the underlying social interactions model varies in the strength of endogenous and exogenous social effects, and the structure of shocks.

---

[48]As opposed to the penalized estimates, all OLS estimates are different from zero. We compute the "% True Zeroes" as the proportion of true zero elements in the social interaction matrix that are estimated as smaller than .05.

Figure 1A: Network Graph of US States, Geographic Neighbors
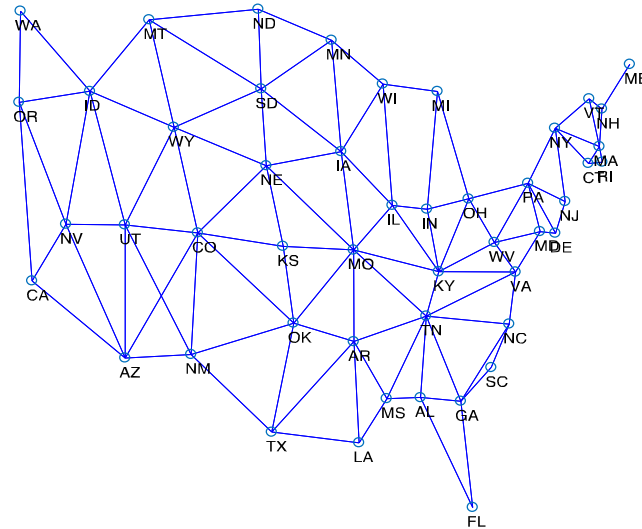
Notes: Figure 1A represents the continental US states (N=48). An edge is drawn between a pair of states if they share a geographic border. State abbreviations are as used by US Post Office (http://about.usps.com/who-we-are/postal-history/state-abbreviations.pdf).

Figure 1B: Network Graph of US States, Identified Economic Neighbors

Geographic network edges
Removed (geographic) edges in economic network
New edges added in economic networks
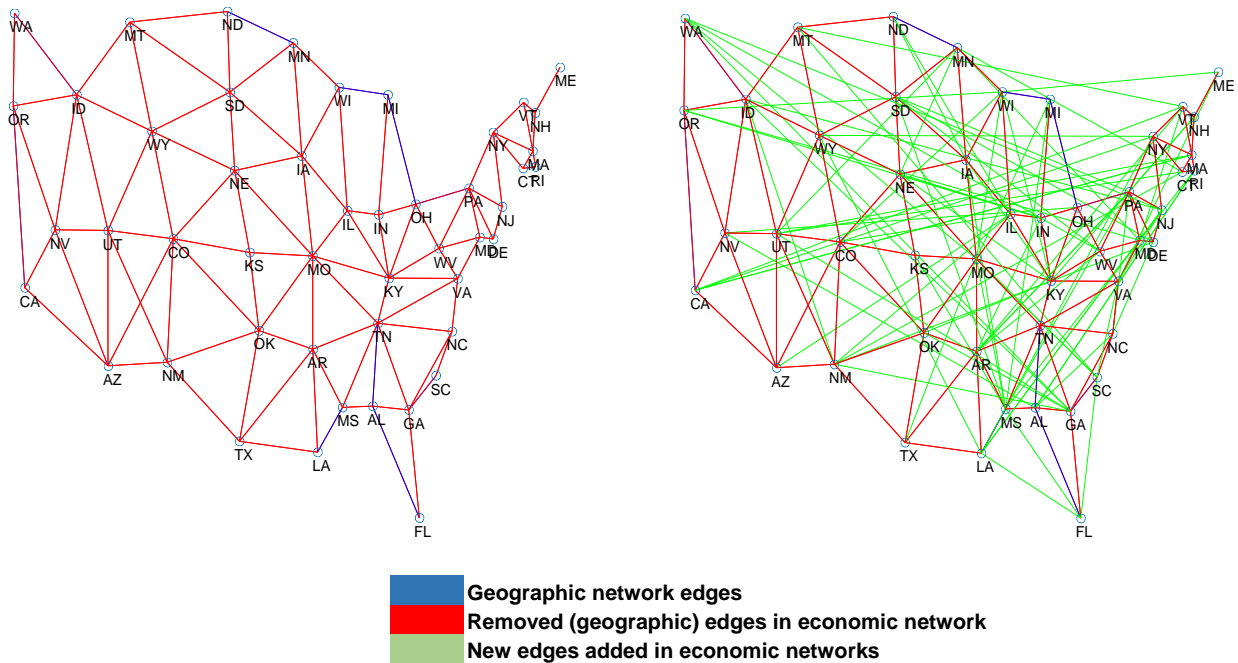
Notes: Figure 1B represents the continental United States (N=48). The economic network is derived from our preferred specification, where we penalize geographic neighbors to states, and allow for exogenous social effects. A blue edge is drawn between a pair of states if they are geographic neighbors and were estimated as connected. A red edge is drawn between a pair of states if they are geographic neighbors but were not estimated as connected. A green edge is drawn between a pair of states if they are not geographic neighbors and were estimated connected. The left hand side graph just shows red and blue edges. The right hand side shows all three types of edges. State abbreviations are as used by US Post Office (http://about.usps.com/who-we-are/postal-history/state-abbreviations.pdf).

Figure 2: Out-degree Distribution
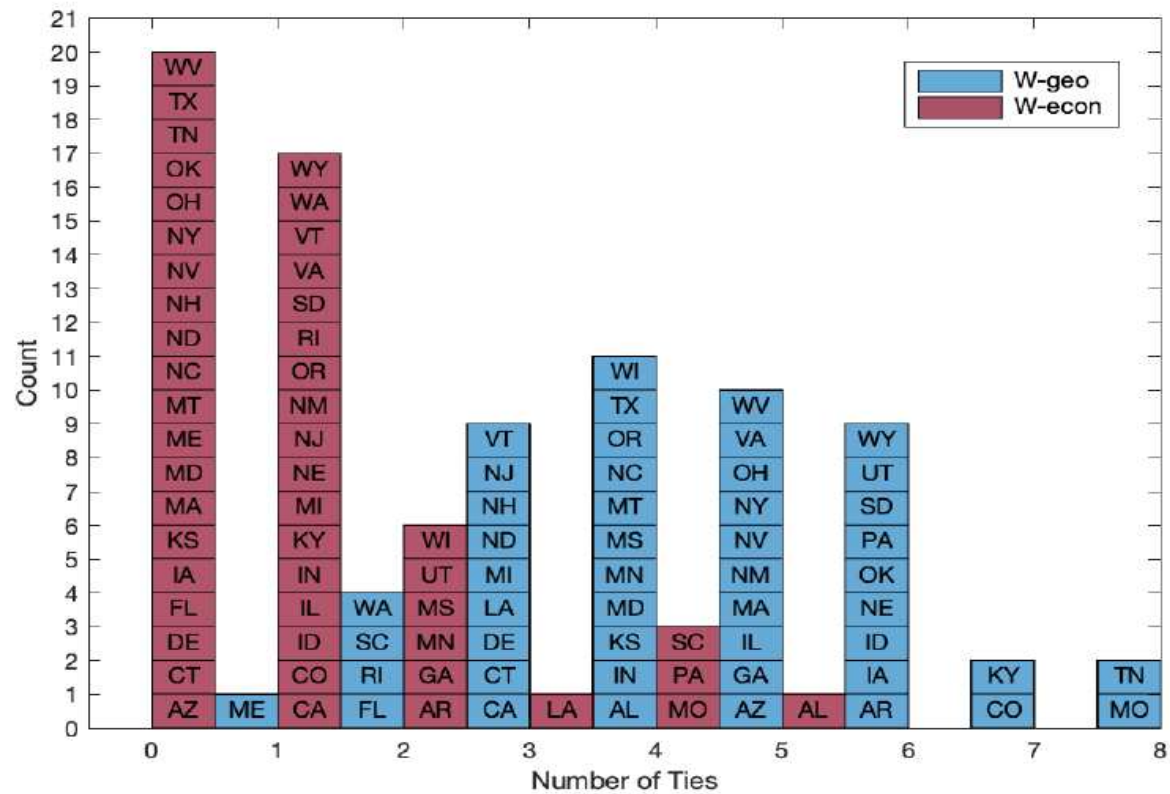
Notes: The out-degree distribution calculated from geographic neighbor's network (W-geo) is shown in blue. The distribution calculated from economic neighbor's network in (W-econ) is shown in red. State abbreviations are as used by US Post Office (http://about.usps.com/who-we-are/postal-history/state-abbreviations.pdf).

Figure 3: Dynamic Endogenous Social Effects (rho)

A. OLS
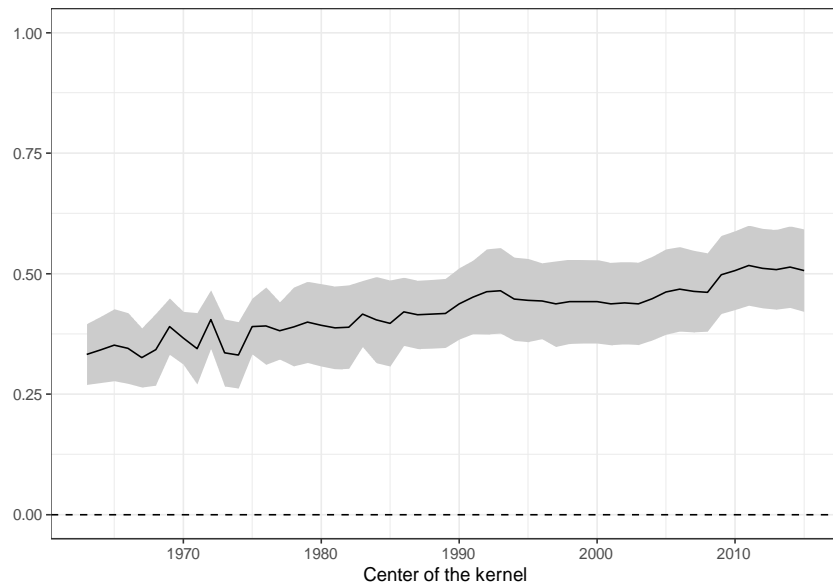
B. GMM
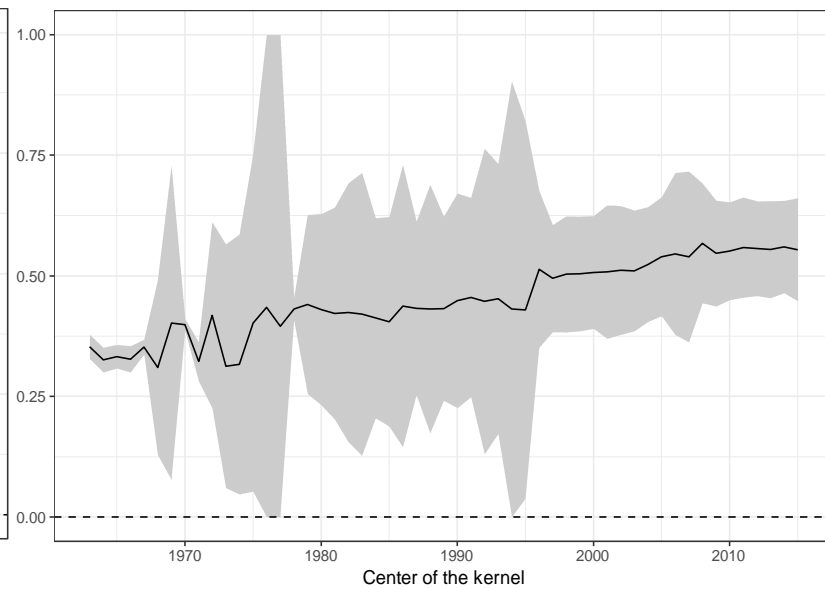
Notes: Panel A shows the OLS estimates of the endogenous social effects estimate (rho) with a Gaussian kernel with center varying period-by-period from 1962 to 2015. The variance of the kernel is set such that 75% of the weight is given to the first half of the data (i.e. pre-1988) with the kernel centered at 1962. Panel B shows the GMM estimates. Shaded areas are the 95% confidence intervals of the period-by-period estimates. Robust standard errors are shown in Panel A and standard errors based on the Caner and Zhang (2014) procedure are shown in Panel B.

Figure 4: Dynamic Network Graph of US States, Identified Economic Neighbors

Centered in 1965
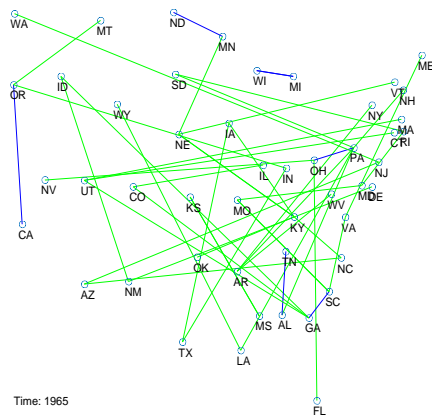
Centered in 1975
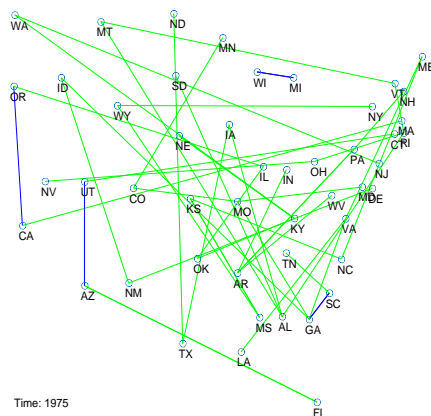
Centered in 1985
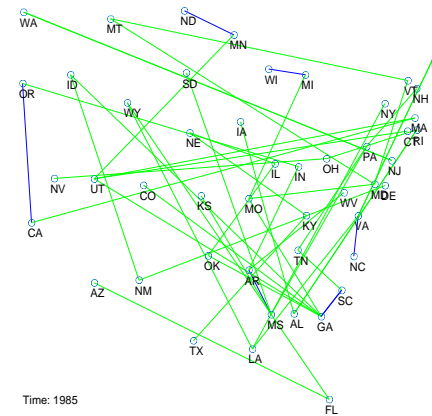
Centered in 1995
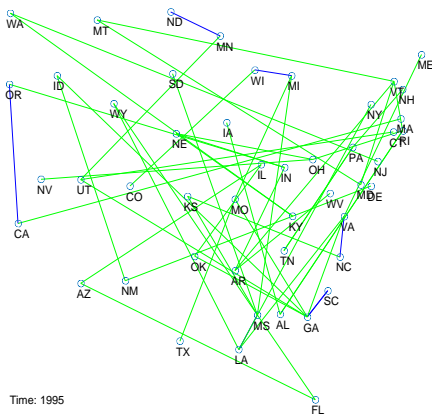
Centered in 2005

Centered in 2015

Geographic network edges
New edges added in economic networks
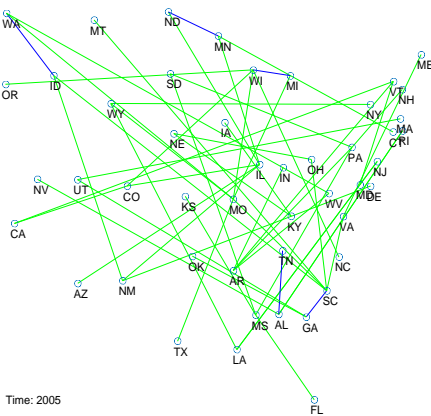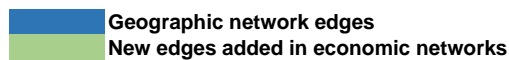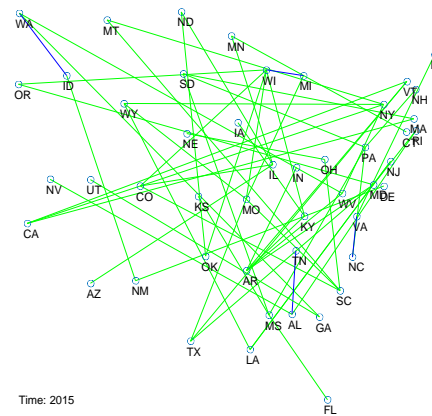
Notes: Each Figure represents the continental United States (N=48). The economic network is derived from our preferred specification, where we allow for exogenous social effects. A blue edge is drawn between a pair of states if they are geographic neighbors and were estimated as connected. A green edge is drawn between a pair of states if they are not geographic neighbors and were estimated connected. State abbreviations are as used by US Post Office (http://about.usps.com/who-we-are/postal-history/state-abbreviations.pdf).

Figure 5: Dynamic Network Graph of US States, Identified Economic Neighbors

A. Share of edges kept from previous network
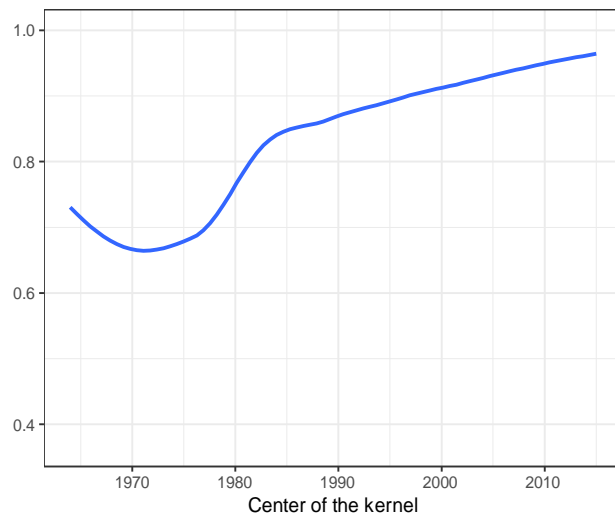
B. Share of edges in W-econ only
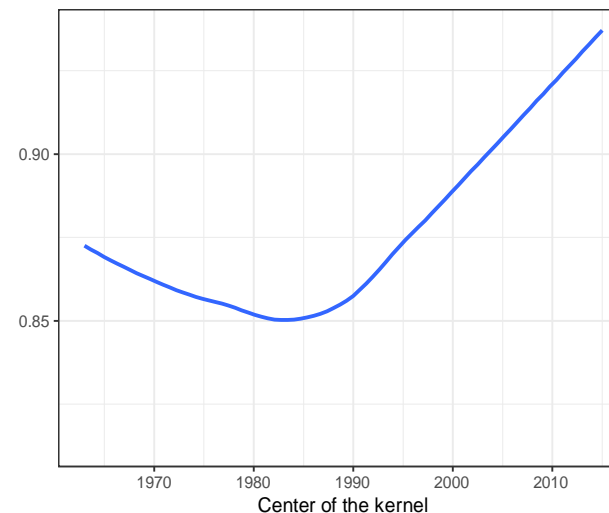
C. Clustering
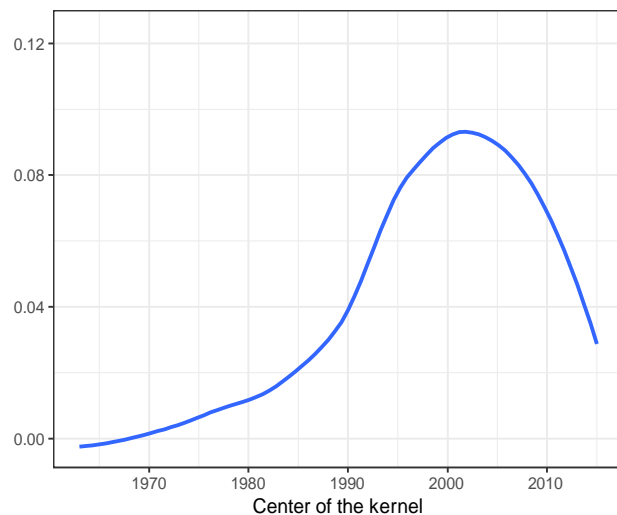
D. Reciprocity
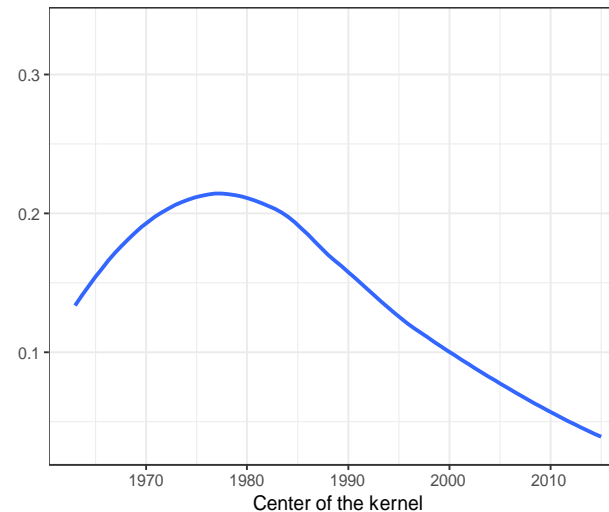
Notes: The panels show various statistics of the estimated economic networks using a Gaussian kernel with its center varying period-by-period from 1962 to 2015. the variance of the kernel is set such that 75% of the weight is given to the first half of the data (i.e. pre-1988) with the kernel centered at 1962. Panel A shows the share of edges kept from the network in the previous period. Panel B shows the share of edges in W-econ only (compared to W-geo). Panel C shows the clustering coefficient of the estimated economic networks. Panel D shows the share of reciprocated edges in the economic network. In all networks, edges smaller than 1/47 are removed. This cutoff is chosen as, in theory, states can only link at maximum with 47 other states. The blue line shows the smoothed estimates across time periods.

Figure 6: General Equilibrium Impacts of South Carolina Tax Rises
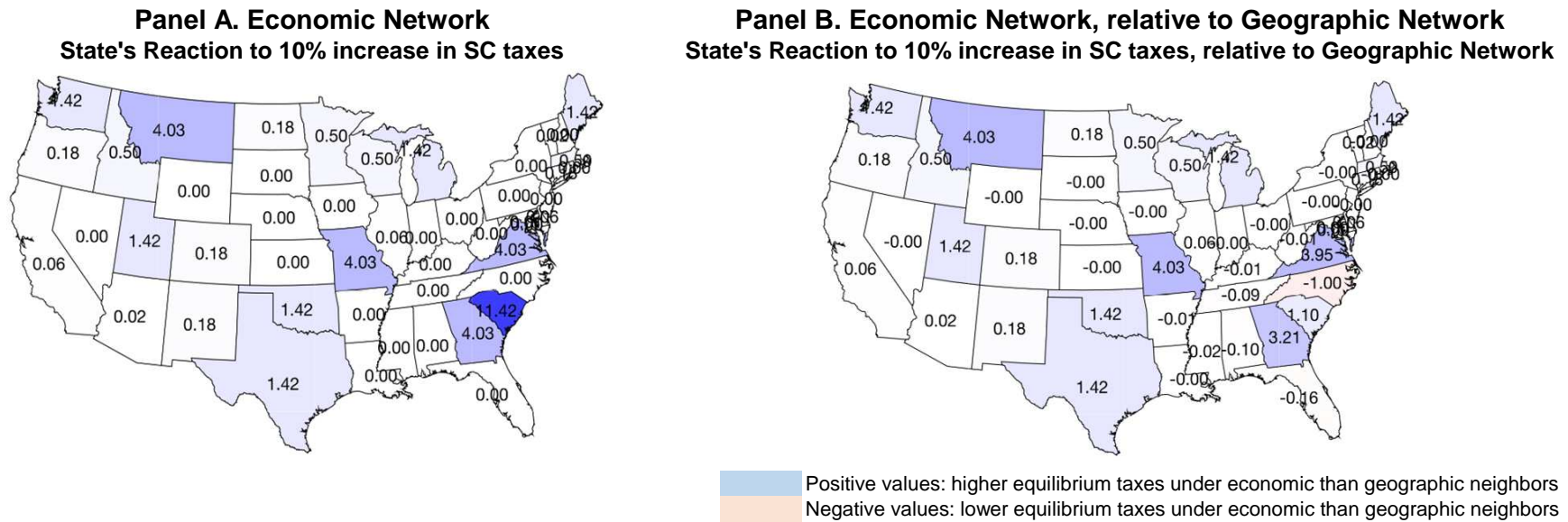
Panel A. Economic Network
State's Reaction to 10% increase in SC taxes

Panel B. Economic Network, relative to Geographic Network
State's Reaction to 10% increase in SC taxes, relative to Geographic Network

Positive values: higher equilibrium taxes under economic than geographic neighbors
Negative values: lower equilibrium taxes under economic than geographic neighbors

Notes: This shows the equilibrium impulse responses in taxes set in each state as a result of South Carolina increasing its tax change by 10%. We compare these derived tax changes under the identified economic network structure, relative to that assumed under a geographic neighbors structure. We graph the log change in equilibrium taxes under economic neighbors, minus the log change in equilibrium taxes under geographic neighbors. Positive values (red shaded) states indicate higher equilibrium taxes under economic neighbors than geographic neighbors, and negative values (blue shaded) states indicate lower equilibrium taxes under economic neighbors than geographic neighbors.

Figure 7: Dynamic General Equilibrium Impacts of SC Tax Rise Shocks
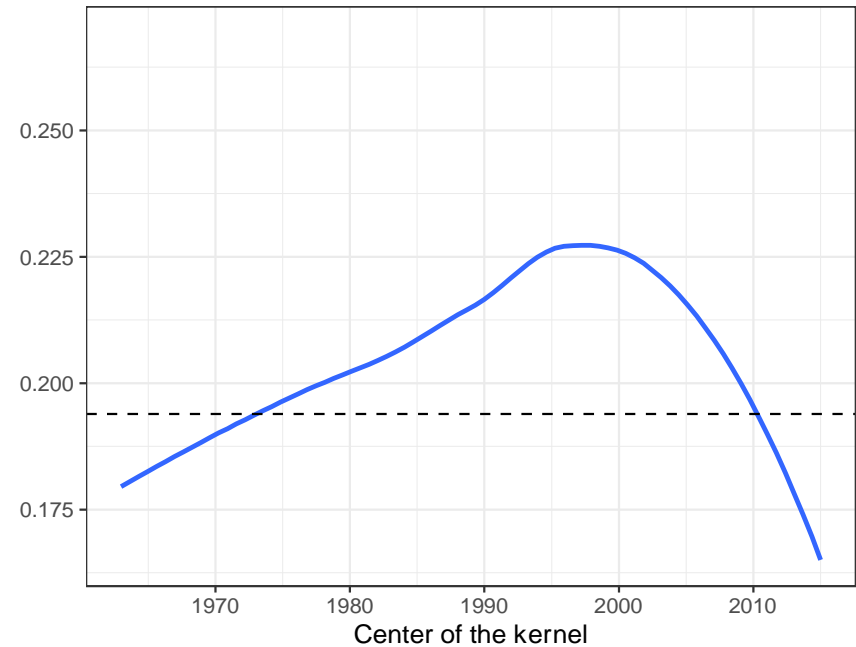
Notes: The panels show equilibrium impulse responses in taxes set in each state as a result of South Carolina increasing its tax change by 10%. These are based on estimated economic networks using a Gaussian kernel with its center varying period-by-period from 1962 to 2015. The variance of the kernel is set such that 75% of the weight is given to the first half of the data (i.e. pre-1988) with the kernel centered at 1962. Panel A shows the average tax increase for the kernel centered in each period (in gray dots) and the smoothed line (in blue). The horizontal dashed line corresponds to the average tax increase if the network was considered to be static. Panel B shows a similar construction for the variance of tax increase across states.

Table 1: Geographic Neighbors

Dependent variable: Change in per capita income and corporate taxes
Coefficient estimates, standard errors in parentheses

	Besley and Case (1995) Sample		Extended Sample	
	(1) OLS	(2) 2SLS: IVs are Characteristics of Geographic Neighbors	(3) OLS	(4) 2SLS: IVs are Characteristics of Geographic Neighbors
Geographic Neighbors' Tax Change (t - [t-2])	.375***	.868***	.271***	.642***
	(.080)	(.359)	(.050)	(.200)
Period	1962-1988	1962-1988	1962-2015	1962-2015
First Stage (F-stat)		14.2		24.2
Controls	Yes	Yes	Yes	Yes
State and Year Fixed Effects	Yes	Yes	Yes	Yes
Observations	1,296	1,248	2,544	2,544

Notes: *** denotes significance at 1%, ** at 5%, and * at 10%. In all specifications, a pair of states are considered neighbors if they share a geographic border. The sample covers 48 mainland US states. In Columns 1 and 2 the sample runs from 1962 to 1988 (as in Besley and Case (1995)). In Columns 3 and 4 the sample is extended to run from 1962 to 2015. The dependent variable is the change in state i's total taxes per capita in year t. OLS regressions estimates are shown in Columns 1 and 3. Columns 2 and 4 show 2SLS regressions where each geographic neighbor's tax change is instrumented by lagged neighbor's state income per capita and unemployment rate. All regressions control for state i's income per capita in 1982 US dollars, state i's unemployment rate, the proportion of young (aged 5-17) and elderly (aged 65+) in state i's population, and the state governor's age. All specifications include state and time fixed effects. With the exception of governor's age, all variables are differenced between period t and period t-2. Robust standard errors are reported in parentheses.

Table 2: Economic Neighbors

Dependent variable: Change in per capita income and corporate taxes
Coefficient estimates, standard errors in parentheses

	No Exogenous Social Effects		Exogenous Social Effects	
	(1) OLS	(2) GMM	(3) OLS	(4) GMM
Economic Neighbors' Tax Change (t - [t-2])	.649***	.709***	.402***	.452***
	(.047)	(.035)	(.044)	(.132)
Period	1962-2015		1962-2015	
Controls	Yes	Yes	Yes	Yes
State and Year Fixed Effects	Yes	Yes	Yes	Yes
Observations	2,544	2,544	2,544	2,544

Notes: *** denotes significance at 1%, ** at 5%, and * at 10%. The sample covers 48 mainland US states running from 1962 to 2015. The dependent variable is the change in state i's total taxes per capita in year t. We allow for exogenous social effects in Columns 3 and 4. OLS regressions estimates are shown in Columns 1 and 3. Columns 2 and 4 show the GMM estimates where each economic neighbors' tax change is instrumented by the characteristics of all states. All regressions control for state i's income per capita in 1982 US dollars, state i's unemployment rate, the proportion of young (aged 5-17) and elderly (aged 65+) in state i's population, and the state governor's age. All specifications include state and time fixed effects. With the exception of governor's age, all variables are differenced between period t and period t-2. Columns 1 and 3 report robust standard errors in parentheses. Columns 2 and 4 report standard errors adopting the procedure described in Caner and Zhang (2014).

Table 3: Geographic Versus Economic Networks

	Geographic Network	Economic Network
Number of Edges	214	49
Edges in Both Networks	9	9
Edges in W-geo only	205	
Edges in W-econ only		40
Clustering	.419	.042
Reciprocated Edges	100%	12.2%
Degree Distribution Across Nodes (states)		
out-degree	4.458 (1.597)	1.021 (0.144)
in-degree		1.021 (1.246)

Notes: This compares statistics derived from the geographic network of US states to those from the estimated economic network among US states. The number of edges, edges in both networks, edges in W-geo only, edges in W-econ only, counts the number of edges in those categories. Reciprocated edges is the frequency of in-edges that are reciprocated by out-edges (by construction, this is 100% for geographic networks). The clustering coefficient is the frequency of the number of fully connected triplets over the total number of triplets. The degree distribution across nodes counts the average number of connections (standard deviation in parentheses): we show this separately for in-degree and out-degree (by construction, these are identical for geographic networks).

Table 4: Predicting Links to Economic Neighbors

Linear Probability Model
Dependent variable = 1 if Economic Link Between States Identified, = 0 if geographically linked
Robust standard errors in parentheses

	Distance	Economic and Demographic Homophily	Labor Mobility	Yardstick Competition	Tax Havens	Fixed Effects
	(1)	(2)	(3)	(4)	(5)	(6)
Distance	.890***	.921***	.921***	.940***	.940***	1.287***
	(.081)	(.082)	(.082)	(.091)	(.091)	(.120)
Distance sq.	-.135***	-.139***	-.139***	-.144***	-.145***	-.255***
	(.025)	(.024)	(.025)	(.027)	(.027)	(.039)
GDP Homophily		-.063	-.063	-.083	-.092	-.219
		(.078)	(.079)	(.082)	(.085)	(.348)
Demographic Homophily		-1.745***	-1.745***	-1.047*	-.960	.579
		(.552)	(.554)	(.605)	(.604)	(1.240)
Net Migration			-.033	-.020	-.185	-.039
			(.603)	(.577)	(.612)	(1.48)
Political Homophily				-.337***	-.321***	-.287*
				(.120)	(.119)	(.155)
Tax Haven					-.093**	
					(.036)	
Origin and destination FE	No	No	No	No	No	Yes
Adjusted R-squared	.664	.664	.664	.651	.657	.831
Observations	254	254	254	212	212	212

Notes: *** denotes significance at 1%, ** at 5%, and * at 10%. The specifications in all Columns are cross-sectional linear probability models where the dependent variable is equal to 1 if an economic clink between states is identified, and zero if a geographic link exists between the states. A pair of states is considered a first-degree geographic neighbor if they share a border. Distance and distance squared are calculated from the centroids of states' capital cities. GDP homophily is the absolute difference of states' GDP per capita. Demographic homophily is the absolute difference of share of young (aged 5-17) plus the absolute difference of the share of elderly in states' population (aged 65+). Net migration (in millions) based on individuals tax returns (Source: Internal Revenue Service, https://www.irs.gov/statistics/soi-tax-stats-migration-data). Political homophily is equal to one if a pair of states have governors of same party at given year. Nevada, Delaware, Montana, South Dakota, Wyoming and New York are considered tax haven states. Time averages are taken for all explanatory variables. Robust standard errors are shown in parentheses.

Table 5: General Equilibrium Impacts of South Carolina Tax Rises

	Geographic Neighbor Network	Economic Neighbor Network	Ratio
Average tax increase	0.03	0.08	3.10
Variance tax increase	0.15	0.19	1.30
Tax dispersion	0.01	0.32	34.41
States with tax increase > 0.05%	12	26	2.17
States with tax increase > 0.5%	7	23	3.29
States with tax increase > 1%	4	20	5.00
States with tax increase > 2.5%	3	15	5.00
States with tax increase > 5%	3	15	5.00

Notes: This shows the equilibrium impulse responses in taxes set in each state as a result of South Carolina increasing its tax change by 10%. The rho coefficient is derived from our preferred specification to estimate the economic network where we allow for exogenous social effects (based on a sample of 48 mainland US states running from 1962 to 2015). We compare these derived tax changes under the identified economic network structure, relative to that assumed under a geographic neighbors structure. The final Column shows the ratio of the same statistic derived under each network.

Figure A1: Simulation Results, Adaptive Elastic Net GMM
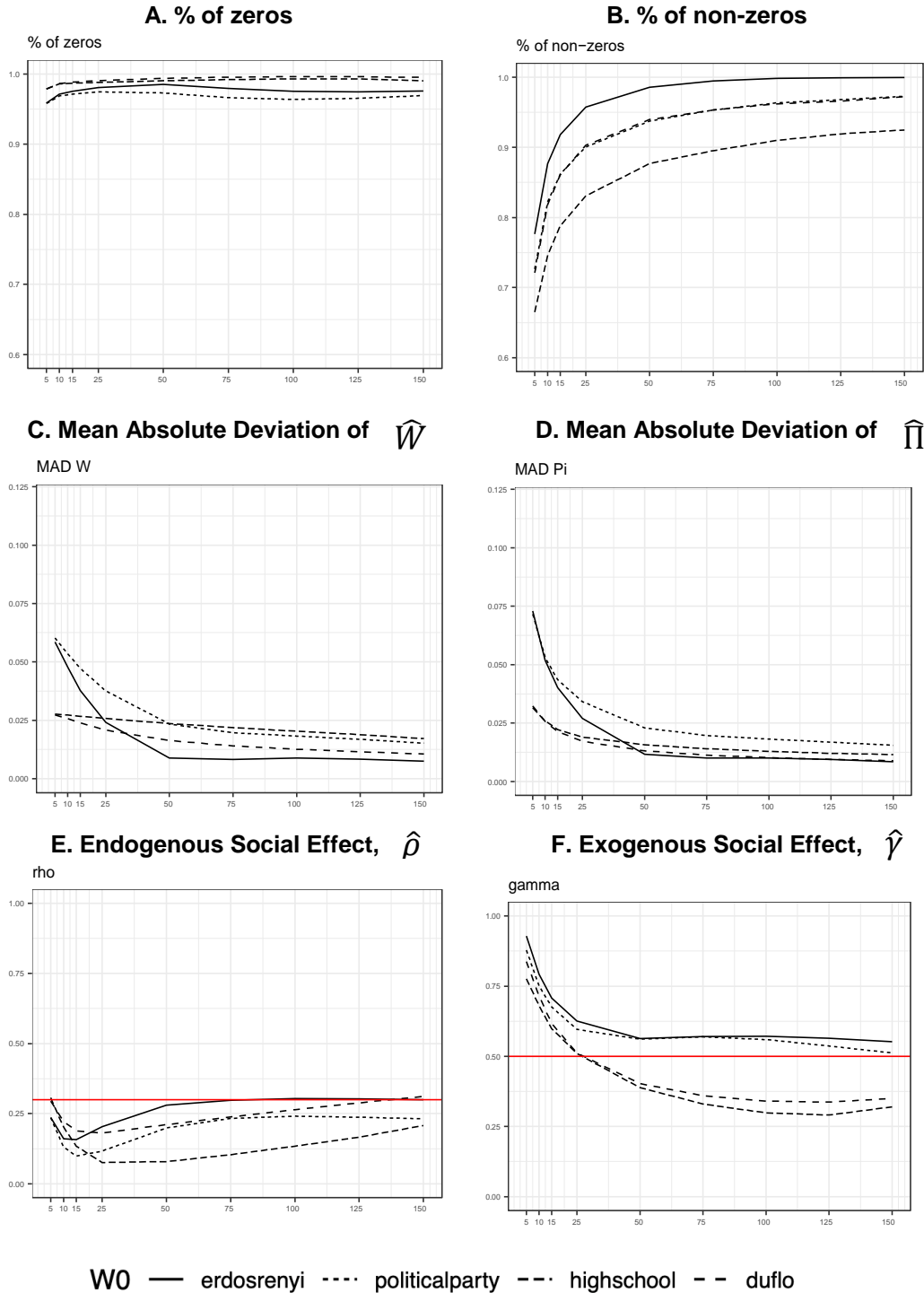
A. % of zeros

B. % of non-zeros

C. Mean Absolute Deviation of $\widehat{W}$

D. Mean Absolute Deviation of $\widehat{\Pi}$

E. Endogenous Social Effect, $\widehat{\rho}$

F. Exogenous Social Effect, $\widehat{\gamma}$

W0 —— erdosrenyi ···· politicalparty –·– highschool – – duflo

Notes: These simulation results are based on the Unpenalised GMM algorithm, with penalization parameters chosen by BIC, under various true networks and time periods T= 25, 50, 75, 100, 125 and 150. In all cases, 1000 Monte Carlo iterations were performed. The true parameters are rho-0=.3, beta-0=.4 and gamma-0=.5. In Panel A, the % of zeroes refers to the proportion of true zero elements in the social interaction matrix that are estimated as smaller than .05. In Panel B, the % of non-zeros refers to the proportion of true elements greater than .3 in the social interaction matrix that are estimated as non-zeros. In Panels C and D, the Mean Absolute Deviations are the mean absolute error of the estimated network compared to the true network for the social interaction matrix W and the reduced form matrix respectively. In Panels E and F, the true parameter values are marked in the horizontal red lines. The recovered parameter are the estimated parameters averaged across iterations. All specifications include time and node fixed effects.

Figure A2: Simulation Results, Adaptive Elastic Net GMM, Distribution of Main Estimates

High-School Friendship Network
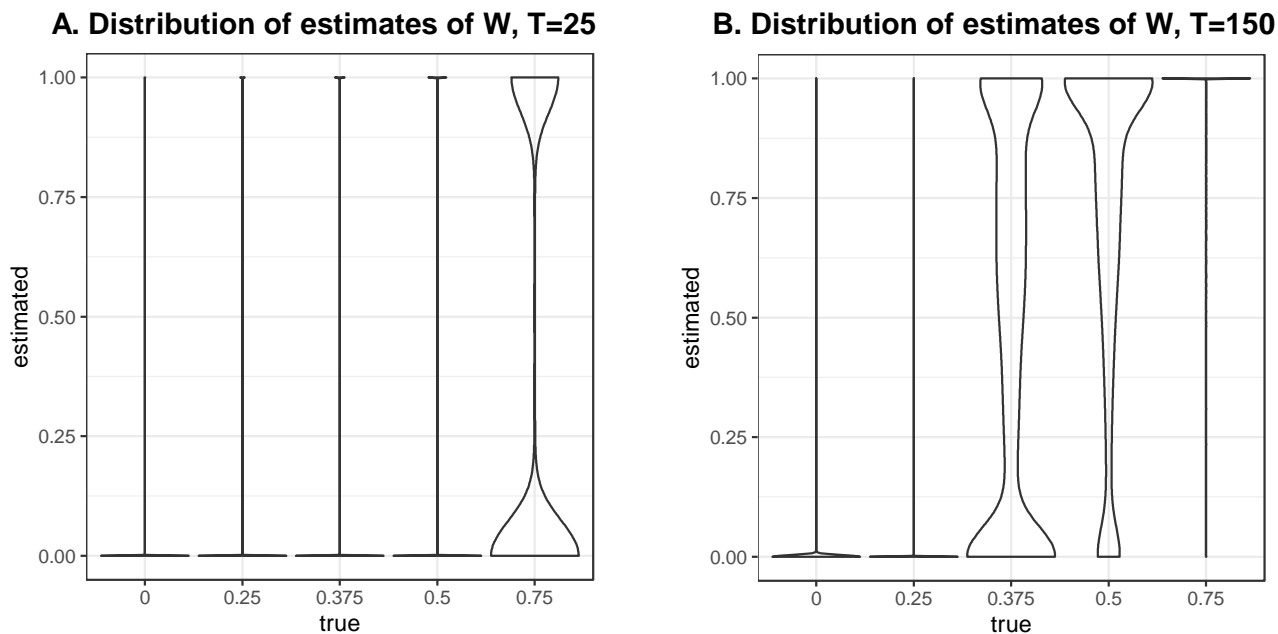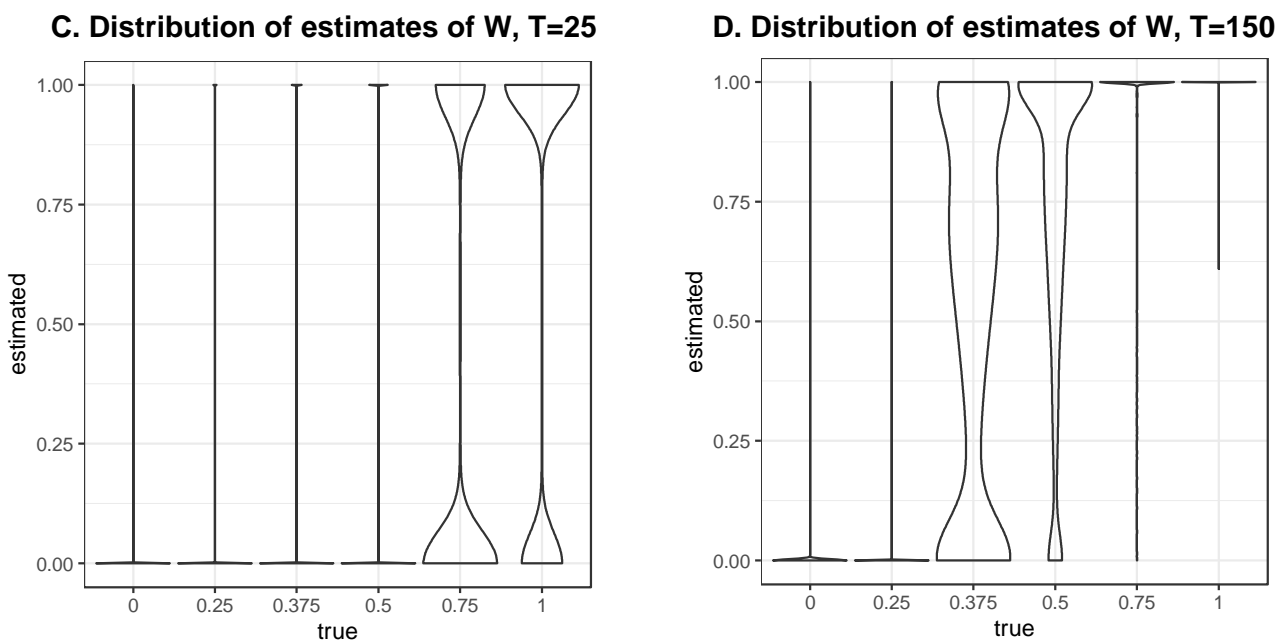
A. Distribution of estimates of W, T=25

B. Distribution of estimates of W, T=150

Village Network

C. Distribution of estimates of W, T=25

D. Distribution of estimates of W, T=150

Notes: These simulation results are based on the Unpenalised GMM algorithm, with penalization parameters chosen by BIC, under the high-school network. In all cases, 1000 Monte Carlo iterations were performed. The true parameters are rho-0=.3, beta-0=.4 and gamma-0=.5. Panels A and C shows the distribution of the estimates of W by their true value and T=25. We show the distribution of the estimated elements of W in five distinct values of W true values. Panels B and D shows the corresponding distribution for T=150. All specifications include time and node fixed effects.

Figure A3: Simulated and True Networks

A. Erdos-Renyi

Erdos-Renyi
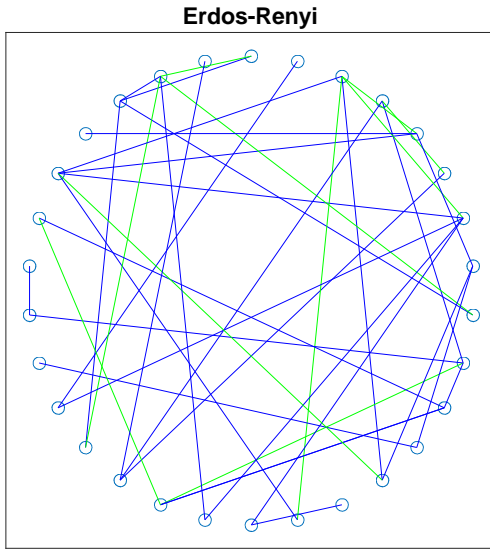
B. Political Party

Political party
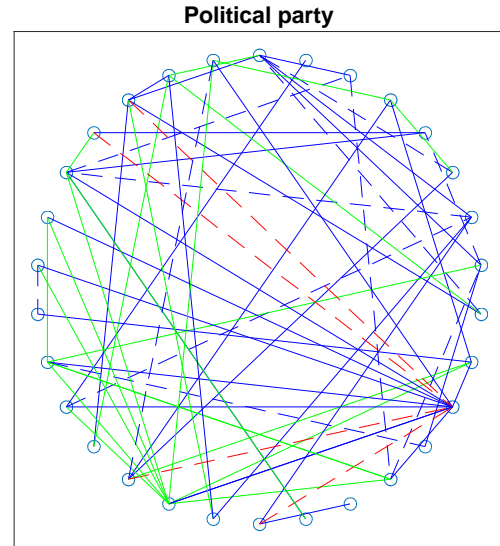
C. High-school

High school
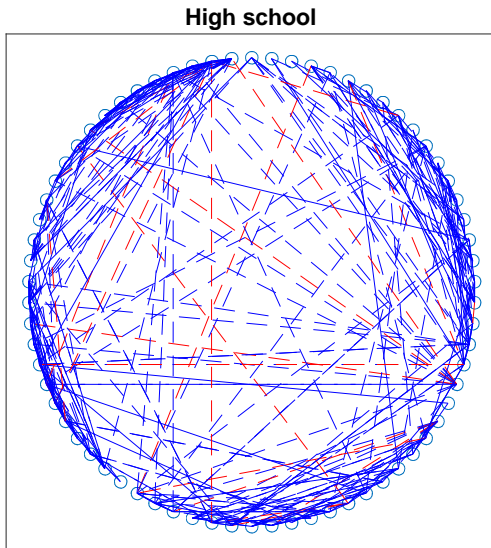
D. Village
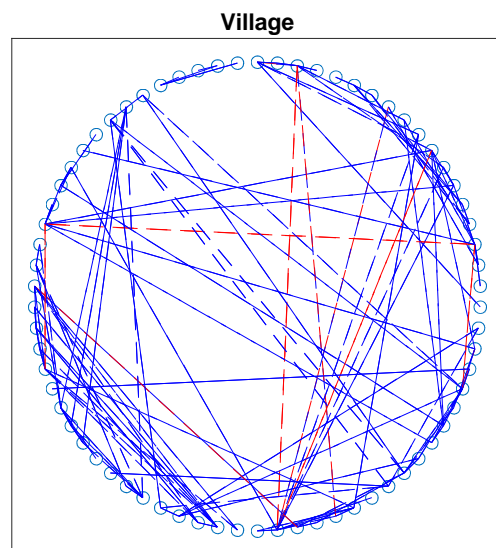
Village

Notes: These simulation results are based on the Unpenalised GMM algorithm, with penalization parameters chosen by BIC, under various true networks and time periods T=50, 100 and 150. In the two stylized networks (Erdos-Renyi and political party), we set N=30, and the real world networks, the high school friendship and village network are based on N=65 and 70 non-isolated nodes respectively. Party leaders in the political party network are marked in black in Panel B. In all cases, 1,000 Monte Carlo iterations were performed. The true parameters are rho-0=.3, beta-0=.4 and gamma-0=.5. All specifications include time and node fixed effects. Kept edges are depicted in blue: these links are estimated as non-zero in at least 5% of the iterations and are also non-zero in the true network. Added edges are depicted in green: these links are estimated as non-zero in at least 5% of the iterations but the edge is zero in the true network. Removed edges are depicted in red: these links are estimated as zero in at least 5% of the iterations but are non-zero in the true network. The figures further distinguish between strong and weak links: strong links are shown in solid edges (whose strength is greater than or equal to .3), and weak links are shown as dashed edges.

Figure A4: Kernel Used for Dynamic Specifications
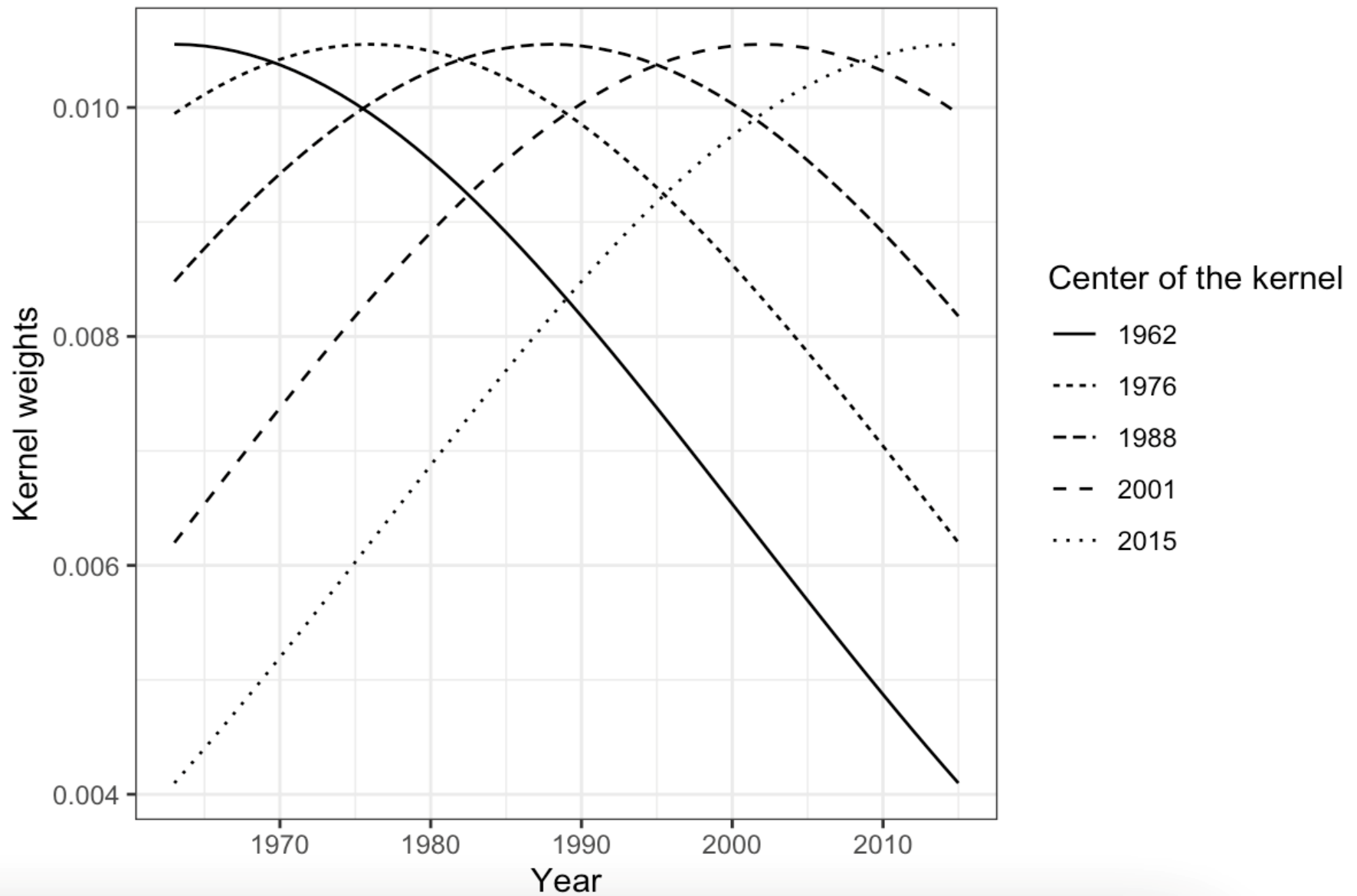
Figure A5: Simulation Results, Adaptive Elastic Net GMM
Partial Knowledge of W_0, Village Network

A. % of zeros

B. % of non-zeros

C. Mean Absolute Deviation of $\widehat{W}$

D. Mean Absolute Deviation of $\widehat{\Pi}$

E. Endogenous Social Effect, $\widehat{\rho}$

F. Exogenous Social Effect, $\widehat{\gamma}$

Known connections —— Top 5 ---- Top 10 –·–
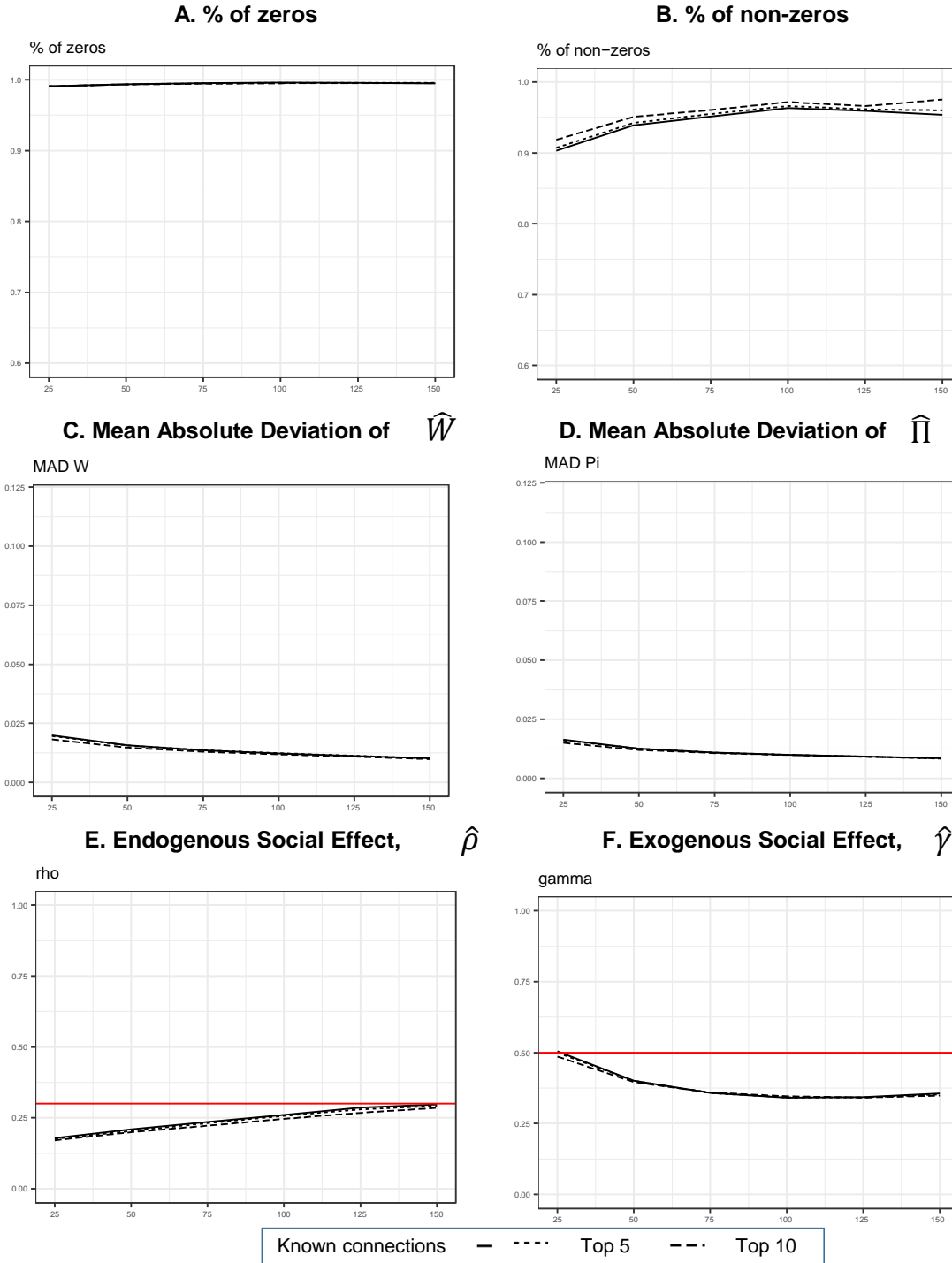
Notes: These simulation results are based on the Banerjee et al. (2013) village network, using the Adaptive Elastic Net GMM algorithm, with penalization parameters chosen by BIC, under various assumptions about knowledge of the true network and time periods T=25, 50, 100, 125 and 150. The "Village" case refers to the simulation implemented without knowledge about the true network. "Village (top 3)" refers to the case where all connections of the three households with highest out-degrees are assumed to be known. "Village (top 5)" and "Village (top 103)" are analogously defined. In all cases, 1000 Monte Carlo iterations were performed. The true parameters are rho-0=.3, beta-0=.4 and gamma-0=.5. In Panel A, the % of zeroes refers to the proportion of true zero elements in the social interaction matrix that are estimated as smaller than .05. In Panel B, the % of non-zeros refers to the proportion of true elements greater than .3 in the social interaction matrix that are estimated as non-zeros. In Panels C and D, the Mean Absolute Deviations are the mean absolute error of the estimated network compared to the true network for the social interaction matrix W and the reduced form matrix respectively. In Panels E and F, the true parameter values are marked in the horizontal red lines. The recovered parameter are the estimated parameters averaged across iterations. All specifications include time and node fixed effects.

Table A1: True and Recovered Networks

	Erdos-Renyi	Political Party	High school Coleman (1964)	Village Banerjee et al. (2013)
A. True Networks				
Number of nodes	**30**	**30**	**70**	**65**
(a) Network-wide statistics				
Number of edges	30	45	366	240
Number of strong edges	30	30	61	65
Number of weak edges	0	15	305	180
Number of reciprocated edges	2	2	184	242
Clustering coefficient	.000	.037	.404	.327
Number of components	2	1	1	4
Size of maximal component	20	30	70	51
Standard deviation of the diagonal of squared W	.254	.254	.084	.205
(b) Node-level statistics				
In-degree distribution	1.00 (1.05)	1.50 (2.49)	5.23 (3.64)	3.50 (2.39)
Out-degree distribution	1.00 (0.00)	1.50 (0.51)	5.23 (2.04)	3.50 (2.37)
Nodes with highest out-degree	{ 7, 11, 26 }	{ 1, 11, 28 }	{ 21, 22, 69 }	{ 16, 35, 57 }
B. Recovered Networks				
(a) Network-wide statistics				
Number of edges	30	41	113	124
Number of strong edges	30	41	113	124
Number of weak edges	0	0	0	0
Number of reciprocated edges	2	2	24	84
Clustering coefficient	.000	.027	.330	.441
Number of components	2	1	2	7
Size of maximal component	20	30	68	42
(b) Node-level statistics				
In-degree distribution	1.00 (1.05)	1.37 (1.88)	1.61 (1.44)	1.77 (1.37)
Out-degree distribution	1.00 (0.00)	1.37 (0.49)	1.61 (0.82)	1.77 (1.05)
Nodes with highest out-degree	{ 7, 11, 26 }	{ 1, 11, 28 }	{ 21, 22, 69 }	{ 16, 35, 57 }

Notes: Panel A refers to the true networks. Panel B refers to the recovered networks. In each Panel, the summary statistics are divided into network-wide and node-level statistics. Strong edges are defined as those with strength greater than or equal to .3. For the in-degree and out-degree distribution, the mean is shown and the standard deviation is in parentheses. The nodes with the highest out-degree are those with the greatest influence on others, and are calculated as the column-sum of the social interaction matrix. The recovered networks statistic are calculated over the average network across simulations with T=100.

Table A2: Simulation Results, Adaptive Elastic Net GMM, Alternative Network Sizes

	A. Erdos-Renyi									B. Political party								
	N = 15			N = 30			N = 50			N = 15			N = 30			N = 50		
	T=50	100	150	T=50	100	150	T=50	100	150	T=50	100	150	T=50	100	150	T=50	100	150
% True Zeroes	.945	.960	.974	.985	.975	.976	.997	.997	.991	.939	.958	.975	.973	.964	.969	.993	.993	.985
	(.016)	(.014)	(.011)	(.006)	(.006)	(.005)	(.001)	(.001)	(.003)	(.017)	(.015)	(.012)	(.007)	(.007)	(.006)	(.002)	(.002)	(.003)
% True Non-Zeroes	.973	.996	1.000	.986	.998	1.000	.993	.999	1.000	.949	.980	.993	.937	.964	.973	.974	.989	.995
	(.045)	(.017)	(.004)	(.023)	(.007)	(.004)	(.013)	(.004)	(.001)	(.063)	(.038)	(.022)	(.048)	(.037)	(.032)	(.025)	(.016)	(.012)
$MAD(\widehat{W})$	.027	.014	.008	.009	.009	.008	.004	.001	.003	.037	.024	.019	.023	.018	.015	.013	.007	.007
	(.009)	(.006)	(.004)	(.004)	(.002)	(.002)	(.002)	(.001)	(.001)	(.008)	(.005)	(.004)	(.004)	(.003)	(.002)	(.002)	(.001)	(.001)
$MAD(\widehat{\Pi})$	.030	.017	.011	.012	.010	.008	.005	.002	.003	.038	.026	.021	.023	.018	.016	.012	.007	.008
	(.008)	(.005)	(.003)	(.004)	(.002)	(.002)	(.002)	(.001)	(.001)	(.007)	(.005)	(.003)	(.004)	(.002)	(.002)	(.002)	(.001)	(.001)
$\widehat{\rho}$	.270	.281	.282	.280	.304	.300	.279	.298	.309	.242	.250	.246	.199	.241	.232	.205	.250	.272
	(.070)	(.046)	(.037)	(.039)	(.030)	(.025)	(.026)	(.018)	(.017)	(.082)	(.053)	(.043)	(.056)	(.042)	(.036)	(.033)	(.023)	(.022)
$\widehat{\beta}$	.409	.405	.403	.403	.402	.402	.402	.400	.400	.411	.404	.399	.404	.402	.401	.404	.400	.401
	(.043)	(.029)	(.024)	(.030)	(.020)	(.017)	(.024)	(.016)	(.013)	(.046)	(.030)	(.025)	(.031)	(.021)	(.017)	(.025)	(.016)	(.013)
$\widehat{\gamma}$	.618	.549	.518	.563	.572	.552	.519	.505	.529	.593	.508	.471	.561	.560	.512	.483	.469	.513
	(.071)	(.045)	(.031)	(.043)	(.034)	(.027)	(.025)	(.019)	(.019)	(.079)	(.051)	(.037)	(.057)	(.042)	(.037)	(.028)	(.023)	(.024)

Notes: These simulation results are based on the Unpenalised GMM algorithm, with penalization parameters chosen by BIC, under various true networks, network sizes and time periods T=50, 100 and 150. In all cases, 1000 Monte Carlo iterations were performed. The true parameters are rho-0=.3, beta-0=.4 and gamma-0=.5. The % of true zeroes refers to the proportion of true zero elements in the social interaction matrix that are estimated as smaller than .05. The % of true non-zeroes refers to the proportion of true elements greater than .3 in the social interaction matrix that are estimated as non-zeros. The Mean Absolute Deviations are the mean absolute error of the estimated network compared to the true network for the social interaction matrix W and the reduced form matrix respectively. The recovered parameter are the estimated parameters averaged across iterations. All specifications include time and node fixed effects. Standard errors across iterations are in parentheses.

Table A3: Simulation Results, Adaptive Elastic Net GMM, Alternative Parameters

A. Erdos-Renyi

	ρ_0				β_0		γ_0		q			
	.1	.5	.7	.9	.2	.6	.3	.7	.3	.5	.8	1.0
% True Zeroes	.967	.987	.995	.985	.993	.979	.964	.985	.981	.987	.998	1.000
	(.006)	(.004)	(.003)	(.006)	(.005)	(.006)	(.007)	(.004)	(.005)	(.004)	(.002)	.000
% True Non-Zeroes	.999	.998	.970	.437	.978	1.000	.989	1.000	1.000	1.000	1.000	1.000
	(.004)	(.008)	(.039)	(.131)	(.032)	.000	(.020)	.000	.000	.000	.000	.000
$MAD(\widehat{W})$	.012	.004	.003	.031	.004	.006	.015	.004	.005	.003	.000	.000
	(.002)	(.001)	(.003)	(.006)	(.003)	(.002)	(.003)	(.001)	(.002)	(.001)	(.000)	(.000)
$MAD(\widehat{\Pi})$	.008	.008	.015	.219	.005	.008	.011	.007	.006	.004	.002	.001
	(.001)	(.002)	(.009)	(.056)	(.003)	(.002)	(.002)	(.002)	(.001)	(.001)	(.001)	(.000)
$\widehat{\rho}$	.091	.496	.683	.811	.278	.302	.302	.296	.299	.297	.291	.292
	(.029)	(.020)	(.020)	(.108)	(.026)	(.023)	(.035)	(.020)	(.021)	(.018)	(.012)	(.006)
$\widehat{\beta}$	.403	.400	.398	.482	.208	.602	.404	.401	.401	.401	.400	.399
	(.017)	(.017)	(.017)	(.090)	(.016)	(.017)	(.017)	(.017)	(.014)	(.012)	(.007)	(.001)
$\widehat{\gamma}$	.589	.515	.487	.452	.506	.545	.395	.720	.530	.510	.485	.481
	(.030)	(.022)	(.022)	(.300)	(.025)	(.028)	(.035)	(.023)	(.021)	(.016)	(.010)	(.005)

B. Political party

	ρ_0				β_0		γ_0		q			
	.1	.5	.7	.9	.2	.6	.3	.7	.3	.5	.8	1.0
% True Zeroes	.963	.978	.986	.989	.990	.966	.959	.978	.971	.976	.991	.999
	(.007)	(.006)	(.005)	(.004)	(.005)	(.007)	(.007)	(.006)	(.006)	(.006)	(.004)	(.001)
% True Non-Zeroes	.966	.976	.969	.791	.901	.992	.910	.990	.991	.997	1.000	1.000
	(.037)	(.033)	(.042)	(.102)	(.071)	(.017)	(.058)	(.021)	(.020)	(.010)	.000	.000
$MAD(\widehat{W})$	.018	.013	.011	.020	.014	.014	.023	.011	.013	.011	.007	.005
	(.002)	(.002)	(.002)	(.005)	(.003)	(.002)	(.003)	(.002)	(.002)	(.001)	(.001)	(.001)
$MAD(\widehat{\Pi})$	.012	.022	.046	.232	.013	.016	.015	.017	.014	.012	.009	.008
	(.001)	(.003)	(.005)	(.014)	(.003)	(.002)	(.002)	(.002)	(.002)	(.001)	(.001)	(.001)
$\widehat{\rho}$	.052	.401	.555	.692	.203	.249	.222	.231	.240	.244	.239	.238
	(.035)	(.034)	(.033)	(.046)	(.033)	(.035)	(.047)	(.029)	(.033)	(.027)	(.020)	(.014)
$\widehat{\beta}$	.401	.399	.398	.406	.210	.601	.403	.399	.401	.400	.399	.398
	(.017)	(.017)	(.018)	(.027)	(.015)	(.017)	(.017)	(.017)	(.014)	(.012)	(.008)	(.003)
$\widehat{\gamma}$	.539	.476	.434	.362	.429	.538	.379	.656	.502	.486	.448	.436
	(.039)	(.032)	(.031)	(.065)	(.034)	(.037)	(.041)	(.034)	(.029)	(.023)	(.014)	(.010)

Notes: These simulation results are based on the Adaptive Elastic Net GMM algorithm, with penalization parameters chosen by BIC, under various true networks, network sizes, time periods T=100 and parameter values. In all cases, 1000 Monte Carlo iterations were performed. The % of true zeroes refers to the proportion of true zero elements in the social interaction matrix that are estimated as smaller than .05. The % of true non-zeroes refers to the proportion of true elements greater than .3 in the social interaction matrix that are estimated as non-zeros. The Mean Absolute Deviations are the mean absolute error of the estimated network compared to the true network for the social interaction matrix W and the reduced form matrix respectively. The recovered parameter are the estimated parameters averaged across iterations. All specifications include time and node fixed effects. Standard errors across iterations are in parentheses.

Table A4: Simulation Results, Adaptive Lasso

	A. Erdos-Renyi									B. Political party								
	N = 15			N = 30			N = 50			N = 15			N = 30			N = 50		
	T=500	1000	1500	T=500	1000	1500	T=500	1000	1500	T=500	1000	1500	T=500	1000	1500	T=500	1000	1500
% True Zeroes	.935	.959	.974	.975	.987	.991	.979	.988	.992	.957	.969	.974	.974	.983	.986	.982	.990	.992
	(.052)	(.043)	(.034)	(.009)	(.005)	(.005)	(.012)	(.007)	(.005)	(.015)	(.013)	(.013)	(.019)	(.011)	(.009)	(.010)	(.004)	(.003)
% True Non-Zeroes	1.000	1.000	1.000	1.000	1.000	1.000	1.000	1.000	1.000	1.000	1.000	1.000	1.000	1.000	1.000	1.000	1.000	1.000
	(.000)	(.000)	(.000)	(.000)	(.000)	(.000)	(.000)	(.000)	(.000)	(.000)	(.000)	(.000)	(.000)	(.000)	(.000)	(.000)	(.000)	(.000)
$MAD(\widehat{W})$	.073	.058	.040	.013	.010	.011	.009	.008	.007	.031	.031	.031	.020	.019	.018	.009	.007	.008
	(.108)	(.098)	(.075)	(.011)	(.003)	(.015)	(.023)	(.028)	(.026)	(.010)	(.008)	(.007)	(.029)	(.020)	(.016)	(.013)	(.002)	(.002)
$MAD(\widehat{\Pi})$	.250	.152	.079	.007	.006	.005	.008	.006	.003	.018	.015	.015	.017	.010	.008	.007	.004	.004
	(.451)	(.363)	(.263)	(.004)	(.001)	(.004)	(.029)	(.029)	(.006)	(.004)	(.003)	(.002)	(.060)	(.022)	(.010)	(.020)	(.000)	(.000)
$\widehat{\rho}$	.429	.379	.332	.225	.267	.277	.144	.208	.227	.272	.274	.277	.243	.259	.259	.109	.172	.200
	(.277)	(.224)	(.162)	(.097)	(.043)	(.037)	(.121)	(.100)	(.066)	(.064)	(.043)	(.033)	(.132)	(.077)	(.055)	(.111)	(.086)	(.069)
$\widehat{\beta}$	.358	.365	.370	.374	.378	.379	.379	.384	.385	.371	.374	.376	.370	.375	.377	.376	.381	.383
	(.190)	(.051)	(.045)	(.012)	(.008)	(.007)	(.012)	(.008)	(.006)	(.020)	(.014)	(.011)	(.013)	(.008)	(.007)	(.013)	(.007)	(.005)
$\widehat{\gamma}$	.373	.384	.404	.525	.462	.445	.625	.533	.501	.445	.422	.415	.465	.419	.411	.601	.507	.471
	(.438)	(.283)	(.139)	(.111)	(.049)	(.040)	(.113)	(.087)	(.069)	(.062)	(.040)	(.031)	(.115)	(.067)	(.052)	(.112)	(.090)	(.072)

Notes: These simulation results are based on the Adaptive Lasso algorithm, with penalization parameters chosen by BIC, under various true networks, network sizes and time periods T=50, 100 and 150. In all cases, 1000 Monte Carlo iterations were performed. The true parameters are rho-0=.3, beta-0=.4 and gamma-0=.5. The % of true zeroes refers to the proportion of true zero elements in the social interaction matrix that are estimated as smaller than .05. The % of true non-zeroes refers to the proportion of true elements greater than .3 in the social interaction matrix that are estimated as non-zeros. The Mean Absolute Deviations are the mean absolute error of the estimated network compared to the true network for the social interaction matrix W and the reduced form matrix respectively. The recovered parameter are the estimated parameters averaged across iterations. All specifications include time and node fixed effects. Standard errors across iterations are in parentheses.

Table A5: Simulation Results, OLS

	A. Erdos-Renyi									B. Political party								
	N = 15			N = 30			N = 50			N = 15			N = 30			N = 50		
	T=500	1000	1500	T=500	1000	1500	T=500	1000	1500	T=500	1000	1500	T=500	1000	1500	T=500	1000	1500
% True Zeroes	.748	.823	.873	.774	.841	.882	.796	.852	.892	.752	.828	.877	.775	.842	.883	.795	.854	.893
	(.050)	(.034)	(.023)	(.033)	(.020)	(.013)	(.044)	(.023)	(.012)	(.031)	(.023)	(.021)	(.031)	(.019)	(.022)	(.039)	(.025)	(.013)
% True Non-Zeroes	1.000	1.000	1.000	1.000	1.000	1.000	1.000	1.000	1.000	1.000	1.000	1.000	1.000	1.000	1.000	1.000	1.000	1.000
	(.000)	(.000)	(.000)	(.000)	(.000)	(.000)	(.000)	(.000)	(.000)	(.000)	(.000)	(.000)	(.000)	(.000)	(.000)	(.000)	(.000)	(.000)
$MAD(\widehat{W})$	.078	.049	.037	.059	.043	.035	.054	.041	.033	.062	.043	.035	.058	.042	.035	.053	.040	.033
	(.070)	(.037)	(.018)	(.023)	(.015)	(.002)	(.019)	(.016)	(.001)	(.039)	(.004)	(.003)	(.026)	(.011)	(.015)	(.023)	(.017)	(.001)
$MAD(\widehat{\Pi})$	.134	.051	.028	.054	.030	.024	.058	.030	.023	.054	.029	.023	.052	.031	.026	.051	.030	.023
	(.306)	(.157)	(.078)	(.080)	(.025)	(.025)	(.073)	(.023)	(.001)	(.124)	(.035)	(.002)	(.074)	(.035)	(.037)	(.055)	(.025)	(.001)
$\widehat{\rho}$	.342	.313	.303	.233	.249	.270	.269	.255	.263	.303	.302	.301	.218	.252	.284	.238	.247	.262
	(.223)	(.103)	(.057)	(.167)	(.109)	(.086)	(.191)	(.092)	(.063)	(.102)	(.048)	(.035)	(.172)	(.120)	(.088)	(.203)	(.112)	(.077)
$\widehat{\beta}$	.433	.402	.396	.401	.393	.396	.483	.392	.395	.389	.395	.396	.388	.393	.395	.427	.392	.395
	(.460)	(.183)	(.017)	(.240)	(.008)	(.007)	(.607)	(.010)	(.005)	(.028)	(.014)	(.010)	(.110)	(.008)	(.007)	(.440)	(.013)	(.005)
$\widehat{\gamma}$	.488	.507	.516	.687	.620	.574	.602	.641	.600	.568	.522	.518	.719	.618	.559	.719	.649	.602
	(.635)	(.267)	(.065)	(.405)	(.142)	(.106)	(.822)	(.156)	(.084)	(.231)	(.052)	(.042)	(.286)	(.150)	(.103)	(.555)	(.138)	(.103)

Notes: These simulation results are based on OLS estimates, under various true networks, network sizes and time periods T=500, 1000 and 1500. In all cases, 1000 Monte Carlo iterations were performed. The true parameters are rho-0=.3, beta-0=.4 and gamma-0=.5. The % of true zeroes refers to the proportion of true zero elements in the social interaction matrix that are estimated as smaller than .05. The % of true non-zeroes refers to the proportion of true elements greater than .3 in the social interaction matrix that are estimated as non-zeros. The Mean Absolute Deviations are the mean absolute error of the estimated network compared to the true network for the social interaction matrix W and the reduced form matrix respectively. The recovered parameter are the estimated parameters averaged across iterations. All specifications include time and node fixed effects. Standard errors across iterations are in parentheses.

Table A6: Summary Statistics, Tax Competition Application

	Obs	Mean	SD	Min	q25	Median	q75	Max
A. Besley and Case sample (1962-1988)								
State total tax per capita	1,248	0.371	0.266	0.036	0.145	0.300	0.530	1.345
State income per capita	1,248	10.617	2.248	4.452	9.120	10.587	12.141	19.409
Unemployment rate	1,248	5.868	2.209	1.800	4.200	5.500	7.000	17.800
Proportion of young	1,248	0.258	0.029	0.180	0.240	0.260	0.280	0.340
Proportion of elderly	1,248	0.106	0.020	0.050	0.090	0.110	0.120	0.180
State governor's age	1,248	51.088	7.441	33.000	45.000	50.000	56.000	73.000
B. Extended sample (1962-2015)								
State total tax per capita	2,544	1.016	0.798	0.036	0.300	0.858	1.579	4.298
State income per capita	2,544	13.394	3.850	4.452	10.564	13.025	15.866	27.974
Unemployment rate	2,544	5.754	2.037	1.800	4.300	5.400	6.800	17.800
Proportion of young	2,544	0.235	0.033	0.170	0.210	0.230	0.260	0.340
Proportion of elderly	2,544	0.118	0.023	0.050	0.100	0.120	0.130	0.190
State governor's age	2,544	53.538	8.049	33.000	47.000	53.000	59.000	78.000

Notes: Summary statistics of variables (in levels) used in subsequent regressions. Besley and Case sample runs from 1962 to 1988 and extended sample until 2015. State total tax per capita is the sum of sales, income and corporation tax in thousands of 1982 US dollars. State income per capita in thousands of 1982 US dollars. Proportion of young is the proportion of the population between 5 and 17 years. Proportion of elderly is the proportion of the population aged 65 or older. State governor's age in years. Data sources: State total tax per capita, Census of Governments (1972, 1977, 1982, 1987, 1992-2016) and Annual Survey of Government Finances (all other years); State income per capita, Bureau of Economic Analysis; Unemployment rate, Bureau of Labor Statistics; Proportion of young (aged 5-17) and elderly (aged 65+), Census Population & Housing Data; State governor's age and political variables manually sourced from individual governor's webpages on Wikipedia.

Table A7: Exogenous Social Effects

Dependent variable: Change in per capital income and corporate taxes
Coefficient estimates, standard errors in parentheses

	(1) OLS	(2) GMM
Economic Neighbors' tax change (t - [t-2])	.402***	.452***
	(.044)	(.132)
Economic Neighbors' income per capita	.041***	.043
	(.007)	(.066)
Economic Neighbors' unemployment rate	1.062	17.401***
	(1.826)	(.026)
Economic Neighbors' population aged 5-17	790.8***	3253.387***
	(303.5)	(.032)
Economic Neighbors' population aged 65+	-1155.7***	3712.6***
	(328.9)	(.022)
Economic Neighbors' governor age	-0.274	2.358***
	(.264)	(.035)
Period	1962-2015	
First Stage (F-stat)		10.5
Controls	Yes	Yes
State and Year Fixed Effects	Yes	Yes
Observations	2,544	2,544

Notes: *** denotes significance at 1%, ** at 5%, and * at 10%. The sample covers 48 mainland US states running from 1962 to 2015. The dependent variable is the change in state i's total taxes per capita in year t. In the OLS and GMM regressions, the economic neighbors' effect is calculated as the weighted average of economic neighbors-of-neighbors variables. Column 2 shows the GMM estimates where each economic neighbors' tax change is instrumented by the characteristics of all states. All regressions control for state i's income per capita in 1982 US dollars, state i's unemployment rate, the proportion of young (aged 5-17) and elderly (aged 65+) in state i's population, and the state governor's age. All specifications include state and time fixed effects. With the exception of governor's age, all variables are differenced between period t and period t-2. Column 1 reports robust standard errors in parentheses. Column 2 reports standard errors adopting the procedure described in Caner and Zhang (2014).